GSBS Dissertations and Theses   Graduate School of Biomedical Sciences

2018-11-30

Identification of Deubiquitinating Enzymes that Control the Cell Cycle in Saccharomyces cerevisiae

Claudine E. Mapa
University of Massachusetts Medical School

Let us know how access to this document benefits you.

Repository Citation

IDENTIFICATION OF DEUBIQUITINATING ENZYMES THAT CONTROL

THE CELL CYCLE IN SACCHAROMYCES CEREVISIAE

A Dissertation Presented

By

CLAUDINE ESTACIO MAPA

Submitted to the Faculty of the
University of Massachusetts Graduate School of Biomedical Sciences, Worcester
In partial fulfillment of the requirements for the degree of

DOCTOR OF PHILOSOPHY

November 30, 2018

CANCER BIOLOGY

IDENTIFICATION OF DEUBIQUITINATING ENZYMES THAT CONTROL

THE CELL CYCLE IN SACCHAROMYCES CEREVISIAE

A Dissertation Presented
By

CLAUDINE ESTACIO MAPA

This work was undertaken in the Graduate School of Biomedical Sciences

Program in Cancer Biology

Under the mentorship of

Jennifer Benanti, Ph.D., Thesis Advisor

Daniel Bolon, Ph.D., Member of Committee

Dannel McCollum, Ph.D., Member of Committee

Eduardo Torres, Ph.D., Member of Committee

Eric Streiter, Ph.D., External Member of Committee

Albertha J. M. Walhout, Ph.D., Chair of Committee

Mary Ellen Lane, Ph.D.,
Dean of the Graduate School of Biomedical Sciences

November 30, 2018

Abstract

A large fraction of the proteome displays cell cycle-dependent expression, which is important for cells to accurately grow and divide. Cyclical protein expression requires protein degradation via the ubiquitin proteasome system (UPS), and several ubiquitin ligases (E3) have established roles in this regulation. Less is understood about the roles of deubiquitinating enzymes (DUB), which antagonize E3 activity. A few DUBs have been shown to interact with and deubiquitinate cell cycle-regulatory E3s and their protein substrates, suggesting DUBs play key roles in cell cycle control. However, in vitro studies and characterization of individual DUB deletion strains in yeast suggest that these enzymes are highly redundant, making it difficult to identify their in vivo substrates and therefore fully understand their functions in the cell. To determine if DUBs play a role in the cell cycle, I performed a screen to identify specific DUB targets in vivo and then explored how these interactions contribute to cell cycle control.

I conducted an in vivo overexpression screen to identify specific substrates of DUBs from a sample of UPS-regulated proteins and I determined that DUBs regulate different subsets of targets, confirming they display specificity in vivo. Five DUBs regulated the largest number of substrates, with Ubp10 stabilizing 40% of the proteins tested. Deletion of Ubp10 delayed the G1-S transition and reduced expression of Dbf4, a regulatory subunit of Cdc7 kinase, demonstrating Ubp10 is important for progression into S-phase. We hypothesized that compound deletion strains of these five DUBs would be deficient in key cellular processes because they

regulated the largest number of cell cycle proteins from our screen. I performed genetic analysis to determine if redundancies exist between these DUBs. Our results indicate that most individual and combination deletion strains do not have impaired proliferation, with the exception of cells lacking *UBP10*. However, I observed negative interactions in some combinations when cells were challenged by different stressors. This implies the DUB network may activate redundant pathways only upon certain environmental conditions. While deletion of *UBP10* impaired proliferation under standard growth conditions, I discovered that deletion of the proteasome-regulatory DUBs Ubp6 or Ubp14 rescues the cell cycle defect in *ubp10Δ* cells. This suggests in the absence of Ubp10 substrates such as Dbf4 are rapidly degraded by the proteasome, but deletion of proteasome-associated DUBs restores cell cycle progression. Our work demonstrates that in unperturbed cells DUBs display specificity for their substrates in vivo and that a coordination of DUB activities promotes cell cycle progression.

List of Tables

List of Figures

List of Abbreviations and Nomenclature

APC: Anaphase promoting complex

DUB: deubiquitinating enzyme

E3: ubiquitin ligase

IDR: intrinsically disordered region

Rhod: rhodanese homology domain

SCF: Skp, Cullin, F-box containing complex

UPS: ubiquitin-proteasome system

Table of Contents

Chapter I: Introduction

The Eukaryotic Cell Cycle

In order for all cells to accurately grow and divide they must undergo a tightly regulated series of events. These events include Gap Phase 1 (G1), DNA Synthesis Phase (S), Gap Phase 2 (G2), and Mitosis (M) and together comprise the cell cycle (Fig 1.1) [1]. There are several controls in place that ensure cells proceed through these stages in a unidirectional manner. The disruption of any of these regulatory processes can lead to defects in the cell's ability to copy its genetic information and divide its contents to create two daughter cells; these errors can manifest as diseases, notably human cancers [2, 3].
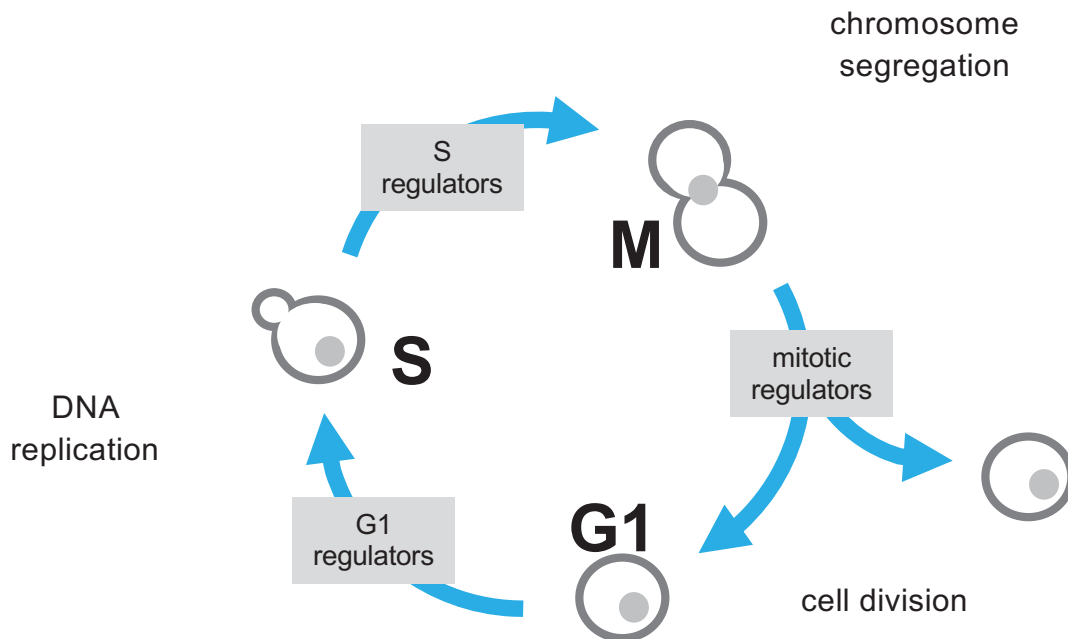
Figure 1.1 The budding yeast cell cycle.

In eukaryotes cell cycle control is driven by periodic protein expression, which entails coordinated gene expression and protein degradation. This periodic gene expression pattern has been demonstrated in the budding yeast Saccharomyces cerevisiae [4-7] and in human cells [8]. In these experiments, cells were synchronized and released cells from various stages of the cell cycle and genes with oscillating transcripts were identified. These studies have identified 800-1000 yeast and 1800 human genes whose transcripts cycle (including many known cell cycle regulators), generating clusters of genes defined by the cell cycle stage of their peak transcription.

The Ubiquitin-Proteasome System

Of the nearly 6,000 protein coding genes in budding yeast only about 15% of proteins are turned over. Many of these proteins have been identified as cell cycle regulators [9-11]. The primary mechanism for achieving timely and specific protein degradation in eukaryotes is the Ubiquitin Proteasome System (UPS). Within the UPS, a cascade of enzymes facilitates the marking of proteins intended for degradation by the proteasome: the ubiquitin activating enzyme (E1), the ubiquitin conjugating enzyme (E2), the ubiquitin ligase (E3) (Fig 1.2). An E1 "activates" ubiquitin through the ATP-dependent step of forming a thiol ester linkage with the ubiquitin C-terminus. Ubiquitin is then transferred to an E2, which interacts with an E3 responsible for catalyzing the attachment of ubiquitin to a lysine residue on a specific target protein. The ubiquitin signal can be reversed with the aid of

deubiquitinating enzymes (DUBs) (Fig. 1.2), which will be discussed in detail in the following sections.

E1= ubiquitin-activating enzyme
E2 = ubiquitin-conjugating enzyme
E3 = ubiquitin ligase
DUB = deubiquitinating enzyme
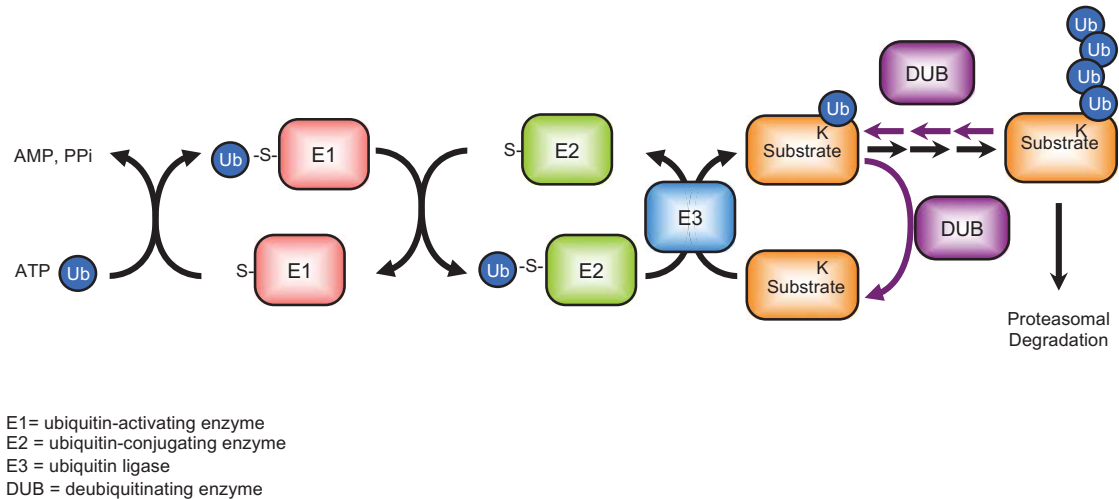
Figure 1.2 The Ubiquitin Proteasome System. A cascade of enzymes facilitates the attachment of ubiquitin onto proteins intended for degradation by the proteasome. Deubiquitinating enzymes reverse the E3-mediated ligation of ubiquitin.

Proteins can be ubiquitinated on a single residue (monoubiquitination), with monomeric ubiquitin on several residues (multi-monoubiquitination), and/or by chains of ubiquitin (polyubiquitination). Polyubiquitin chains are formed when ubiquitin molecules are linked by any of seven lysines (K6, K11, K27, K29, K33, K48, K63) or the N-terminal methionine. They can be constructed from the same linkage type or from multiple linkages that form "branched" chains. The complexity of the ubiquitin code allows these post-translational modifications to alter a protein's localization, function, activity, and half-life. Different types of ubiquitination are associated with different cellular processes; the roles of K48 and K63 ubiquitination have been studied extensively, with K48 signaling proteasomal degradation [12, 13]

and K63 functioning in DNA repair and membrane trafficking [14, 15]. A protein may be ubiquitinated for proteasome degradation for various reasons – for example if it is misfolded, there is an excess of the protein, or its function is only required for a specific time frame. Much like protein phosphorylation, protein ubiquitination offers cells an additional method to fine-tune cellular processes and responses to environmental stimuli.

The most regulated step of protein ubiquitination is at the level of E3s, which mediate substrate specificity. Consistent with their important role in the UPS there are a large number of E3s in both yeast (>60) and humans (>600). E3s are classified into two classes: catalytic HECT (homologous to the E6AP carboxyl terminus) and non-catalytic E3s. HECT E3s bind E2s with their N-terminus and form a thioester-linked intermediate between their C-terminal catalytic domain and ubiquitin transferred from an E2 [16]. The largest family of non-catalytic E3s is the RING-finger (Really interesting new gene) ligases, which serve as a scaffold for the interaction between a substrate and ubiquitin conjugated to an E2 [17]. This family can be further subdivided into RING E3s that function as monomers, dimers, or multi-subunit complexes. Among the multi-subunit E3s the SCF (Skp1-Cullin-F-box) and APC (anaphase-promoting complex) are two examples of mechanistically similar cullin-based E3s, and both SCF and APC are essential for cell cycle progression in all eukaryotes [1]. SCF complexes employ modular subunits called F-box proteins that provide specificity for different targets. The best-characterized include the yeast proteins Cdc4 and Grr1, which recognize different sets of phosphorylated substrates through distinct protein binding domains: Cdc4 through a

WD40 repeat domain and Grr1 though a leucine-rich repeat (LRR) domain [18]. On the other hand, APC can bind either of two co-activators, Cdh1 and Cdc20, which contain binding sites that recognize short linear sequence motifs, called degrons, on substrates [19].

Deubiquitinating Enzymes

DUBs are a superfamily of proteases that regulate the UPS by cleaving isopeptide bonds between ubiquitin molecules or between ubiquitin and a protein target. In doing so, DUBs synthesize mature ubiquitin from precursors, reverse the conjugation of ubiquitin by E3 ligases, and recycle ubiquitin molecules for continual use in the UPS [20] (Fig. 1.2). They have been found in all cellular compartments and have been implicated in most intracellular processes including protein degradation, signal transduction, endocytosis, and the DNA damage response [21, 22]. Similar to E3s, DUBs play important roles in regulating the UPS, and as such there is a large number of them in both yeast (21) and humans (100).

The 21 DUBs in budding yeast fall into 5 families based on their distinct domains: Ubiquitin specific proteases (USP), ovarian tumor proteases (OTU), JAB1/MPN/MOV34 (JAMM), ubiquitin C-terminal hydrolases (UCH), and MINDY (MIU) [23, 24]. USP, OTU, UCH, and MIU fall into the category of cysteine proteases while the JAMM DUB, Rpn11, is a zinc metalloprotease. The large USP family contains 16 DUBs that are mostly linkage non-specific [25], while one of the most recently discovered DUB families, MINDY, displays high specificity for K48 chains [24, 25]. OTU DUBs generally prefer one or a few chain types [26, 27]. Most JAMM

DUBs are K63-specific and UCH DUBs have displayed weak or no activity towards diubiquitin [25]. However, yeast proteasome-associated DUBs Rpn11 and Yuh1, which fall into the JAMM and UCH families, have been reported to deubiquitinate multiple ubiquitin chain types [28, 29].

Identifying DUB Substrates in Vivo

While many other proteins in the UPS have established roles, the specific functions, binding partners, and specificity of many yeast and human DUBs remain unknown because it has been challenging to identify in vivo substrates. However, in the past 15 years studies in multiple model systems have uncovered a great deal of information about the complexity of the ubiquitin code and how DUBs process these signals. In vitro studies using synthetic di-ubiquitin molecules suggest that mammalian USP family DUBs display little chain specificity [30]. In vitro deubiquitination assays with budding yeast DUBs suggest they do not display high activity on tetra-ubiquitin-labelled substrates but they remove mono and diubiquitin at similarly high rates [27]. Together these data suggest more analysis of physiological substrates may be necessary for an accurate assessment of DUB specificity.

A key to understanding DUB function and regulation is the identification of their protein partners [31]. Several groups have conducted systematic analyses of DUBs in *H. sapiens*, *S. pombe*, and *S. cerevisiae* that have helped fill some gaps in the DUB field.

In 2009, Sowa and colleagues were the first to assay the DUB interactome by performing a global proteomic analysis in human cells [32]. They expressed N-terminal Flag-HA fusion DUBs purified by anti-HA IP and detected interaction partners by LC-MS/MS. They developed a software that identified 744 unique high-confidence candidate interacting proteins associated with 80% of DUBs, which increased the number of known and candidate DUB interactions [31]. Using Gene Ontology (GO), they identified 1/3 of the DUBs interact with proteins involved with protein turnover, transcription, RNA processing, or the DNA damage checkpoint, which is consistent with previous findings that DUBs are important for essential cellular activities. They also found 26/75 DUBs associate with proteins that contain domains involved in ubiquitin conjugation, hinting that DUB regulation may depend on ubiquitin conjugation machinery. Interactions with a small number of DUBs could not be identified, perhaps because of the transient nature of DUB-substrate interactions and/or the low steady-state levels of these proteins [32, 33]. Because of these challenges, the need for techniques to stabilize UPS proteins and the use of catalytically inactive DUBs to improve detection of these interactions has been highlighted in many studies [34-37].

Shortly after the DUB interactome was assayed in human cells it was assayed by Kouranti and colleagues using confocal microscopy, proteomics, and enzymatic activity assays to investigate the 20 DUBs in fission yeast [22]. Localization data revealed yeast DUBs in log phase cells are present in almost all cellular compartments (although there is a possibility these localizations may be altered under different growth or stress conditions). Similar to Sowa et al. they

performed a comprehensive proteomic analysis to determine how these proteins are targeted to, and regulated at, their subcellular localizations. They identified nine DUBs that interact with protein complexes, and seven of these DUBs were found to interact with homologous complexes in human cells [22]. These data lend more evidence to the conclusion that some DUBs are involved in many intricate processes and their functions may be regulated by interactions with protein complexes [38].

While interacting partners of DUBs can be identified by mass spectrometry, these proteins may be involved in regulating DUB activity, localization, or function. So far, it has been challenging to identify substrates DUBs. To circumvent this, other groups have conducted in vitro assessments of DUB activity, which have demonstrated that eukaryotic DUBs display similar protease activities towards the same substrates [27, 39]. These findings contribute to the uncertainty of DUB specificity in vivo.

As an alternative to screening for DUB interactors, studying the effects on the proteome in the absence of DUBs can provide a deeper understanding of the DUB network. Poulsen et al. performed the first global proteome study aimed at the effects of DUB deletion on protein levels in eukaryotic cells [40], and this was followed by a similar profiling study on a subset of nine yeast DUBs from Isasa et al. [41]. Both groups found deletion of individual DUBs exerts widely different effects on protein abundance in cells, which suggests loss of these DUBs affects the levels of different subsets of the proteome. For example, deletion of *UBP7* resulted in significant alterations to 5% of the proteome while deletion of *UBP3* resulted in changes to 30% of the proteome. Poulsen et al. found levels of several transcription

factors changed in many DUB deletion strains including *ubp10Δ* and *ubp8Δ*, suggesting large proteomic changes may be an indirect effect of changes in gene expression. From these proteomics data they independently identified novel functions and putative targets for several DUBs, in particular Ubp3's roles in vesicle transport between the ER and Golgi and the cytochrome oxidase C complex. These two studies suggest DUBs have both a direct and indirect role in regulating the expression of different groups of substrates and these substrates are likely involved in distinct pathways, however, further validation of putative substrates is required to determine DUB substrate specificity.

In all, these DUB profiling studies support the ideas that DUBs 1) are involved in essential cellular functions, 2) may have some overlapping functions, 3) appear to regulate the abundance of different subsets of the proteome, and 4) the functions of several DUBs may be coupled to their interaction with macromolecular complexes. Because of the growing knowledge of DUB roles in essential cellular processes, it is unsurprising that human DUBs have been implicated in several cancers and autoimmune and neurodegenerative diseases, and that their human counterparts are being targeted for drug design [42, 43]. However, in order to treat human diseases we must to determine which DUBs might be good candidates to develop inhibitors against.

The Interplay Between DUBs and E3s

DUBs and E3 ligases perform opposing functions in the cell, and studies on the DUB interactome suggest DUBs and E3s interact [22, 32, 38], so it is

conceivable that these interactions may mediate their activities and substrate specificity. These interactions can modulate the stabilities and activities of E3s, DUBs, and/or their substrates (Figure 1.3). Some DUBs facilitate the activation of E3s and in doing so promote the destruction of E3 substrate levels (Figure 1.3a). One example is human USP44, which deubiquitinates the APC activator CDC20 to prevent its premature dissociation from its inhibitor MAD2 [44]. Once ubiquitinated and freed from MAD2, CDC20 activates the APC, which degrades securin to initiate anaphase [1], thus USP44 deubiquitination plays a role in activating a cell cycle regulatory E3.

Some data indicate that DUBs and E3s can regulate one another's stabilities. This is seen with the mammalian DUB USP8 and the E3 NRDP1, which promotes cell proliferation through the ubiquitination of receptor-tyrosine kinases, such as ERBB [45] (Figure 1.3b). NRDP1 was found to be intrinsically unstable due to its auto-ubiquitination [46], but in response to serum stimulation USP8 binds to and stabilizes NRDP1 to promote cell growth (and when uncontrolled, this leads to tumor formation) [47, 48]. In starved human fibroblasts NRDP1 ubiquitinates itself as well as USP8, reducing proliferation signals and eventually leading to cell death [46, 47].

Alternatively, DUB-E3 cross-regulation can serve to modify the activity, rather than stability, of each protein (Figure 1.3c). The mammalian E3 TRAF2 ubiquitinates both itself and its substrates with K63 chains to initiate NF-κB signaling, which promotes cell survival and upregulates the expression of many proteins including the DUB CYLD [49, 50]. CYLD deubiquitinates TRAF2, contributing to the deactivation

of the NF-κB pathway and generating a negative-feedback loop that subsequently downregulates its own expression [51-53].

DUBs and E3s can also interact to fine-tune the ubiquitination of a common substrate. The DUB USP7 can interact with the MDM2 ligase and its substrate p53 in a mutually-exclusive manner to control the stability of p53 [54] (Figure 1.3d). In unstressed cells, MDM2 ubiquitinates p53 to prevent the induction of p53-mediated cell cycle arrest and apoptosis [55]. MDM2 also undergoes auto-ubiquitination [56], but this is counteracted by the DUB USP7 [54]. Upon genotoxic stress, USP7 gains increased affinity for p53 over MDM2 (leading to MDM2 auto-ubiquitination and degradation), and USP7 stabilizes p53 so it can induce the expression of genes to launch a stress response [57].

Lastly, DUB-E3 interactions can regulate chain composition on common substrates (Figure 1.3e). For example, budding yeast DUBs Ubp2 and Ubp3 can form a complex with Rsp5 and its substrates under heat stress [58, 59]. In unstressed cells, Rsp5 has been implicated in regulating the trafficking of plasma membrane proteins through its addition of K63 ubiquitin tags [58, 60]. Upon heat stress, Ubp2 and Ubp3 bind to Rsp5 and trim K63 chains on Rsp5 substrates that have become misfolded, allowing Rsp5 to replace them with K48 chains that promote the degradation of those substrates [59]. In a similar situation, some proteins contain both E3 and DUB activities.
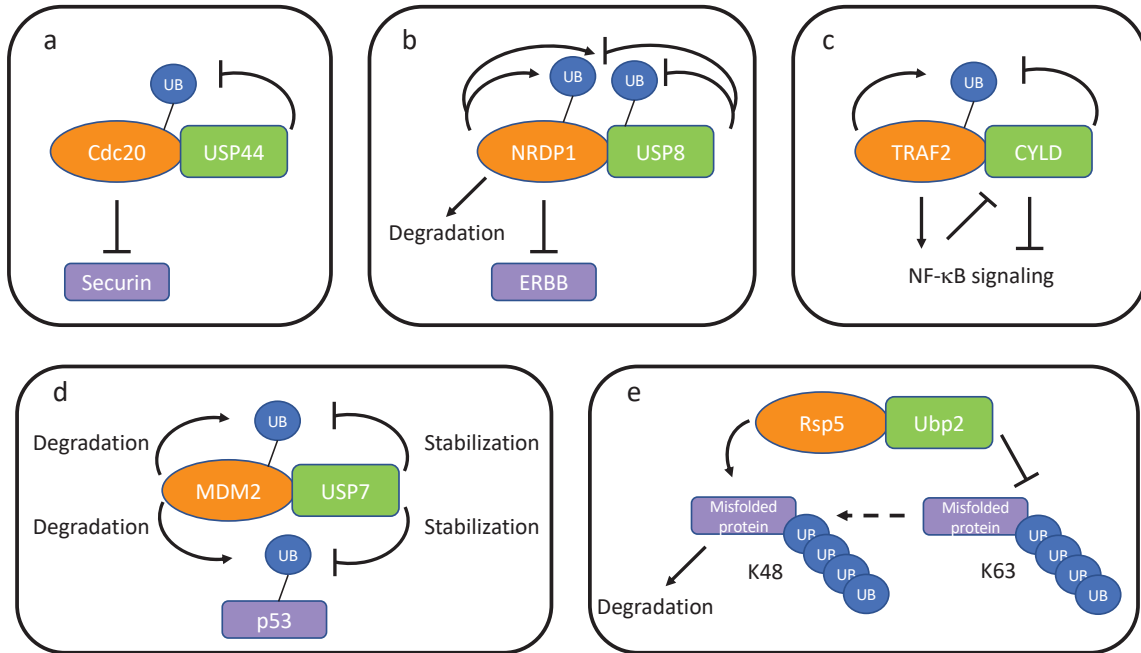
Figure 1.3. Types of DUB-E3 interactions. DUB = green, E3 = orange, substrate = purple. a) A DUB can promote the activity of an E3: USP44 deubiquitinates an APC activator Cdc20, in turn activating it and the APC complex, which stabilizes substrate such as securin. b) A DUB and E3 can regulate one another's protein stability. c) A DUB and E3 can regulate one another's activity: CYLD deubiquitinates TRAF2 to activate it, while TRAF2 induces NF-κB signaling, which turns off CYLD expression. d) A DUB and E3 can fine-tune the ubiquitination status of a common substrate: MDM2 ubiquitinates p53, promoting its degradation, while USP7 deubiquitinates p53, promoting its stabilization. e) A DUB and E3 can edit chains on a common substrate: Ubp2 deubiquitinates existing K63-linked ubiquitin on a misfolded protein, allowing Rsp5 to build K48 chains to target the protein for degradation.

The Proteasome is a Bottleneck for Ubiquitin Homeostasis

As previously described, proteins intended for degradation are ubiquitinated by E3s for recognition by the 26S proteasome. Within the UPS, the proteasome and its associated DUBs facilitate the critical processes of protein degradation and recycling of ubiquitin chains into the free ubiquitin pool; as such, the proteasome can be considered a bottleneck for ubiquitin homeostasis [61]. Since the proteasome drives recycling of ubiquitin chains into free ubiquitin it is likely that insufficient ubiquitin levels negatively impact cells. This has been observed in yeast, where decreased free ubiquitin production (due to deletion of *UBI4*, the stress-induced polyubiquitin precursor) results in sensitivity of cells to stresses such as temperature, starvation, and amino acid analogs [62]. Knockout of either of two polyubiquitin precursor genes, UBC and UBCC, leads to embryonic lethality in *Ubc*-/- and infertility and neurodegeneration in *Ubcc*-/- mice [63-65]. These data suggest that ubiquitin homeostasis is essential for cell survival and proper development.

In cells with wild type ubiquitin genes, free ubiquitin depletion can occur when the proteasome is overloaded with ubiquitinated conjugates; this is similar to the accumulation of ubiquitinated proteins that occurs during proteotoxicity. To determine the effects of this proteasome bottleneck on ubiquitin homeostasis in yeast, London et al. measured ubiquitin levels in yeast strains with the deletion of 20S proteasome subunits *PRE1* and *PRE3*, *UBI4*, or the ubiquitin recycling and endosomal trafficking DUB *UBP4*, all of which display proteotoxicity [66]. This study identified an increase in high molecular weight ubiquitin conjugates (in all instances except *ubi4Δ*) and a decrease in free ubiquitin. The free ubiquitin pool was

16

presumably depleted because only degradation and ubiquitin recycling, but not

ubiquitin conjugation, was impaired in these strains. In response to proteotoxicity,

they found the cell downregulates expression of ubiquitin precursor gene *UBI4*, as

increased free ubiquitin was detrimental to cells under stress because it allows E3s

to generate more ubiquitin conjugates that would overload the proteasome.

Additionally, expression of Rpn4, the transcription factor responsible for maintaining

proteasome levels, is upregulated to help clear the misfolded proteins and ubiquitin

conjugates that accumulate during stress. However, the high volume of ubiquitin

conjugates in these cells suggests increased proteasome production is not enough

to reduce high-molecular weight ubiquitin species to wild type levels. In cases where

proteins form insoluble aggregates that cannot be cleared by upregulation of the

proteasome, the cell may induce autophagy to clear toxic proteins [67].

While little has been published about the fate of different ubiquitin chain types

upon proteotoxic stress, K48 chains have been shown to increase after inhibition of

the proteasome or proteasome-associated DUBs [68]; this was expected due to the

role of K48 chains in targeting substrates for degradation by the proteasome. A

closer look at the composition of K48-containing chains under these conditions

discovered that it is specifically branched K11/K48 chains that are conjugated to

proteasomal substrates [69]. This study demonstrated that E3s UBR4 and UBR5 are

responsible for constructing K11/K48 branched chains upon proteasome inhibition

and subsequent proteotoxic stress. These K11/K48 branched chains had a much

higher affinity for adaptors of the proteasome and its associated segregase,

p97/VCP, than did homotypic K48 chains. Additionally, analysis of multiple human

cell types demonstrated that proteasomal substrates decorated with these branched chains formed aggregates when proteasome activity was impaired. This suggests a conserved mechanism for coping with proteasomal stress: proteins awaiting proteasomal degradation aggregate and are marked with heterotypic ubiquitin chains that serve as a more efficient signal to the proteasome than homotypic chains. As proteotoxic stress has been characterized by a depletion of free ubiquitin and DUBs are involved in maintaining this pool, it is possible that some DUBs may also be tasked with removing or editing existing K48 chains on proteasomal substrates so that UBR4/UBR5 can ligate K11/K48 branched chains that are preferentially recognized by the proteasome. To determine what role(s) DUBs may play in the cellular response to the build-up of ubiquitinated proteins it will be important to better understand how different DUBs contribute to recycling and processing of ubiquitin. To this end, this thesis will explore how one of the proteasome-associated DUBs, Ubp6, mediates the balance of proteasomal substrates in yeast.

The Role of the E3s and DUBs in Cell Cycle Regulation

The UPS has been shown to be important for many cellular processes, including the maintenance of cell cycle regulation. Known as the primary cell-cycle regulatory E3s, SCF and APC complexes orchestrate the orderly ubiquitination of proteins that is essential for cell cycle phase transitions. These activities are conserved in all eukaryotes, but were first described in the budding yeast model system. SCF is active throughout the cell cycle, however it's best-characterized cell

cycle role is in controlling the G1/S transition by promoting the activation of Cyclin-dependent kinase (Cdk), which is required for entry into S phase. In early G1, the transcription inhibitor Whi5 is recruited to promoters of the G1/S genes that are activated by SCB-binding transcription factor (SBF) [70]. The G1 cyclin Cln3 binds Cdk1 and coordinates the phosphorylation and inactivation of Whi5, which enables SBF/MBF to induce expression of G1/S cyclins Cln1 and Cln2 and commits cells through the G1/S checkpoint known as Start [71]. SCF[Cdc4] and SCF[Grr1] then rapidly target Cln3 for degradation [72, 73]. After accumulating in G1, Cln1 and Cln2 phosphorylate the Cdk1 inhibitor Sic1 [74], and SCF[Cdc4] is recruited to these phosphorylation sites and facilitates Sic1 ubiquitination and degradation. Sic1 degradation relieves its inhibition on Clb5 and Clb6, both of which can then initiate origin firing [1, 75]. Cln1 and Cln2 are eventually phosphorylated by Cdk1 and ubiquitinated by SCF[Grr1] [76, 77], engaging a positive feedback loop for their own expression [78].

The primary functions of the APC occur later in the cell cycle during the transitions from metaphase to anaphase and from mitosis to G1. In metaphase, APC[Cdc20] initiates the ubiquitination of Clb2 and securin [79, 80]. Sister chromatids held together by cohesin must be cleaved by separase in order for chromosomes to properly segregate during anaphase. Securin inhibits separase until APC[Cdc20] ubiquitinates securin, relieving the hold on separase and allowing cells to complete mitosis. APC[Cdh1] promotes the degradation of proteins from mitotic exit to early G1, including Cdc5 [81], Cdc20 [82], and components of the replication initiation machinery (Cdc6, Cdc7-Dbf4, Geminin) [83-85]. Together these APC activities

ensure chromosomes are properly segregated, cells successfully exit mitosis, and origins are primed for another round of replication in daughter cells.

While the contributions of SCF and APC ligases to cell cycle control are well-understood, only a few DUBs in yeast have known roles in the cell cycle. Ubp15 deubiquitinates Clb5 during G1/S to protect it from APC[Cdc20]-mediated degradation [86]. The subsequent increase in Clb5 levels and Cdk activation initiates origin firing and promotes timely S-phase entry [1]. In S-phase Ubp10 rapidly deubiquitinates PCNA after repair from MMS- and hydroxyurea-induced damage to allow PCNA to recruit replicative DNA polymerases and restore S-phase progression [87]. And Ubp7, which was originally characterized as a DUB in the endosomal sorting complex [88], has also been implicated in S-phase progression [89]. Although the mechanism of Ubp7's contribution to the DNA damage response (DDR) is still unknown, Bohm and colleagues report that loss of *UBP7* leads to sensitivity to hydroxyurea – an inhibitor of the enzyme ribonucleotide reductase and DNA replication. This is potentially due to Ubp7's interaction with Mrc1, which is required for intra-S-phase checkpoint signaling, or to loss of UBP7-mediated H2B stability [89, 90].

In order to develop a better understanding of DUB function we must be able to identify their in vivo substrates. Proteomic approaches in deletion strains suggest functional redundancy as they have not identified many specific substrates of DUBs. While in vitro experiments may help simplify our understanding of DUB functions, few specific substrates have been confirmed due to redundancy in the network and/or insufficiency of current techniques to detect substrate specificity [27, 30]. In

Chapter II I discuss an overexpression approach to screen all 21 budding yeast DUBs to determine if they can regulate specific targets among an array of UPS substrates and the follow-up experiments to examine the effect of these putative DUB-substrate interactions on cell cycle progression.

In several profiling studies DUBs have been associated with components of macromolecular complexes, however few provide data that test these interactions. In addition, the low concentrations of many UPS proteins and the presumed transient nature of DUB-substrate interactions make it challenging to capture specific DUB targets in vivo [33]. In Chapter III I discuss how I have applied the method of Bimolecular-Fluorescence Complementation (BiFC) to detect a stabilized complex between the E3 ligase SCF^{Grr1}, its substrate Hof1, and the DUB Ubp5 [35], and how I determined the F-box protein Grr1 may be required for this interaction.

Reported redundancies among DUBs and the variable phenotypes in multiple DUB deletion strains have made it challenging to model the DUB network. In Chapter IV I discuss genetic analysis in deletion strains of five DUBs that I identified as regulators of a number of cell cycle UPS targets. Surprisingly, I did not detect proliferation defects in the five DUB deletion strain in normal growth conditions. However, I observed impaired growth when testing these DUB deletion strains under certain stressors. These data allow me to develop a model for how DUB functions may coordinate to maintain the cell cycle under stress.

Chapter II: A balance of deubiquitinating enzymes controls cell cycle entry

Preface

Data presented in this chapter are from the following publication:

Mapa, C.E., et al., *A balance of deubiquitinating enzymes controls cell cycle entry.* Mol Biol Cell, 2018: p. mbcE18070425.

Introduction

Progression through the eukaryotic cell cycle is controlled by the periodic expression of regulatory proteins that are expressed precisely at the times their functions are needed [1]. This pattern of cyclical protein expression is dependent upon the ubiquitin proteasome system (UPS), which is the primary mechanism of regulated protein degradation. Within the UPS, E3 ubiquitin ligases recognize specific protein targets and attach chains of ubiquitin to direct those proteins to the proteasome for destruction. The actions of E3s can be opposed by deubiquitinating enzymes (DUBs) that remove ubiquitin chains.

Although many E3s have established roles in targeting cell cycle-regulatory proteins for degradation [91, 92], the roles of DUBs in cell cycle control are just beginning to be understood. In some instances, DUBs affect the cell cycle indirectly. For example, in fission yeast Ubp8 has been shown to indirectly antagonize the function of the essential mitotic-regulatory E3, the Anaphase Promoting Complex (APC) [93] . In mammalian cells, multiple DUBs have been identified that impact the cell cycle through deubiquitination of individual cell cycle regulators [94]. In budding yeast, only a few DUBs of 21 in total have been found to have cell cycle-regulatory roles. Ubp15 has been shown to control the cell cycle directly, by deubiquitinating the B-type cyclin Clb5 and promoting S-phase entry [86] . Two other DUBs, Ubp7 and Ubp10, are implicated in cell cycle control following DNA damage. Cells lacking *UBP7* are sensitive to replication stress, however the substrate(s) responsible for this role of Ubp7 is not known [89] . Ubp10 also plays a role in the DNA damage response, by removing ubiquitin from PCNA after DNA repair to promote recovery

from S-phase arrest [87]. Beyond these few examples, the roles of DUBs in regulation of the yeast cell-cycle proteome remain to be identified.

One reason that identifying DUB substrates has been challenging is that several lines of evidence suggest that DUBs may have overlapping or redundant functions. This possibility is supported by in vitro studies. Although DUBs form stable complexes with distinct interacting proteins that regulate their functions [22, 32, 95-97], assays of DUB complexes purified from budding yeast demonstrate that most DUB complexes have some ability to deubiquitinate the same ubiquitinated proteins in vitro [27]. Redundancy presents a technical hurdle for identifying DUB substrates using loss-of-function approaches, since mutations in multiple DUBs are necessary to impact levels of target proteins. For example, in fission yeast simultaneous deletion of five DUBs is required to disrupt ubiquitin-regulated membrane trafficking [22, 98]. To get around these problems, proteomics of ubiquitinated proteins has been used to identify specific DUB substrates involved in membrane trafficking [98]. However, this approach has not yet been applied to identifying DUB substrates whose ubiquitination leads to their degradation by the UPS. In general, UPS substrates that are rapidly degraded are expressed at low levels, making them difficult to detect by proteomic approaches. Indeed, quantitative whole cell proteomics of budding yeast strains with deletions of individual DUBs have not detected many UPS targets [40, 41]. Therefore, additional approaches to identify DUB targets in vivo are necessary.

Here we take an alternative approach to identify substrates by testing whether elevated levels of individual DUBs can stabilize cell cycle proteins in vivo. We

determined which of the 21 yeast DUBs, upon overexpression, can stabilize each of 37 cell cycle-regulatory proteins that are degraded by the UPS. We find that overexpression of the majority of DUBs leads to an increase in the levels of one or more cell cycle-regulatory proteins. Overexpression of Ubp10 increased the levels of 15 cell cycle proteins (40%), suggesting it plays a central role in regulating the cell cycle proteome. Indeed, either overexpression or deletion of *UBP10* impaired cell cycle progression, demonstrating that precisely tuned levels of Ubp10 are critical for normal proliferation. Interestingly, deletion of the proteasome-associated DUB Ubp6 rescued the cell-cycle defects and restored the stability of Ubp10 targets in *ubp10Δ* cells. Deletion of an alternate proteasome-regulatory DUB, *UBP14*, also rescued the proliferation defect in *ubp10Δ* cells, suggesting that partial proteasome inhibition can counteract the accelerated degradation of proteins that occurs in the absence of Ubp10. These studies uncover new roles for these DUBs in cell cycle control and demonstrate that DUBs must act in concert to facilitate accurate progression through the cell cycle.

Results

A gain of function screen to examine DUB specificity

　　Since evidence suggests that DUBs act redundantly [27, 40, 41], potentially masking the effects of mutations in individual DUBs, we sought to design an overexpression/gain of function screen to identify DUBs that can regulate cell-cycle protein levels. Budding yeast express 21 DUBs that can be classified into five families based on their catalytic domains (Table 2.1). We first tested whether

overexpression of any of these 21 DUBs resulted in a cell cycle defect, or broadly and non-specifically affected ubiquitinated proteins. We overexpressed each DUB from a plasmid under the control of the galactose-inducible *GAL1* promoter. In agreement with previous reports, constitutive overexpression of no individual DUB resulted in a permanent growth arrest [87, 99], however seven strains overexpressing individual DUBs (*UBP1*, *UBP3*, *UBP10*, *UBP11*, *UBP12*, *UBP14*, *UBP15*) exhibited reduced growth after induction (Fig. 2.1A). We next examined the consequences of a 4-hour DUB induction, which was the amount of time it took to induce maximum expression of DUBs from the *GAL1* promoter (Figure 2.1B). Importantly, no cell cycle arrest was observed following overexpression of any DUB for four hours (Figure 2.2A). In addition, there was no evident decrease in long ubiquitin chains, which might be observed if a particular DUB could non-specifically target all ubiquitinated proteins in the cell (Figure 2.2B). Based on these results, a 4-hour induction time was selected to perform the screen for the stabilization of any of the selected proteins upon DUB overexpression.

DUB	systematic name	domains[a]	localization[b]	regulatory partners	references
Ubp1	YDL122W	USP	C, ER, CoP, CP, B		[100]
Ubp2	YOR124C	USP	C	Rsp5	[58, 100]
Ubp3	YER151C	USP	C	Bre5	[100, 101]
Ubp4, Doa4	YDR069C	USP, Rhod	C, E, M, SP	Bro1	[100, 102, 103]
Ubp5	YER144C	USP, Rhod	C, BN, N		[102]
Ubp6	YFR010W	USP, UBL	C, N, M, V	proteasome	[100, 104]
Ubp7	YIL156W	USP, Rhod	C, M		[100]
Ubp8	YMR223W	USP, ZnF	N, M	SAGA	[100, 105]
Ubp9	YER098W	USP	C		[100]
Ubp10, Dot4	YNL186W	USP, IDR	N, No, M	Sir4, Dhr2, Utp22	[100] [97, 106]
Ubp11	YKR098C	USP			
Ubp12	YJL197W	USP, DUSP	C, M, V	Rad23, Cdc48	[100, 107]
Ubp13	YBL067C	USP	C		[100]
Ubp14	YBR058C	USP, ZnF	C, N, V, M		[100]
Ubp15	YMR304W	USP, MATH	C, E, ER	Pex1/Pex6, Cdh1	[86, 100, 108]
Ubp16	YPL072W	USP	M, C, E		[100] [109]
Otu1	YFL044C	OTU, ZnF	C, N, V, M	Cdc48	[100] [110]
Otu2	YHL013C	OTU	C		[100]
Rpn11	YFR004W	JAMM	N, V	proteasome	[100] [104]
Yuh1	YJR099W	UCH			
Miy1	YPL191C	MINDY	C		[100]

[a]DUB catalytic domains: USP, ubiquitin-specific protease; UCH, ubiquitin C-terminal hydrolase; OTU, ovarian tumor; JAMM, JAB1/MPN/Mov34 Metalloenzyme; MINDY, motif interacting with Ub-containing novel DUB family. DUB accessory domains: Rhod, rhodanese-like; UBL, ubiquitin-like; ZnF, zinc finger; IDR, intrinsically-disordered region; DUSP, domain in ubiquitin specific proteases; MATH, Merpin and traf homology domain.
[b]C, cytoplasm; N, nucleus; No, nucleolus; ER, endoplasmic reticulum; CoP, cortical patches; CP, cell periphery; B, bud; BN, bud-neck; E, endosome; M, mitochondria; SP, spindle pole; V, vacuole

Table 2.1. Summary of *S. cerevisiae* DUBs.
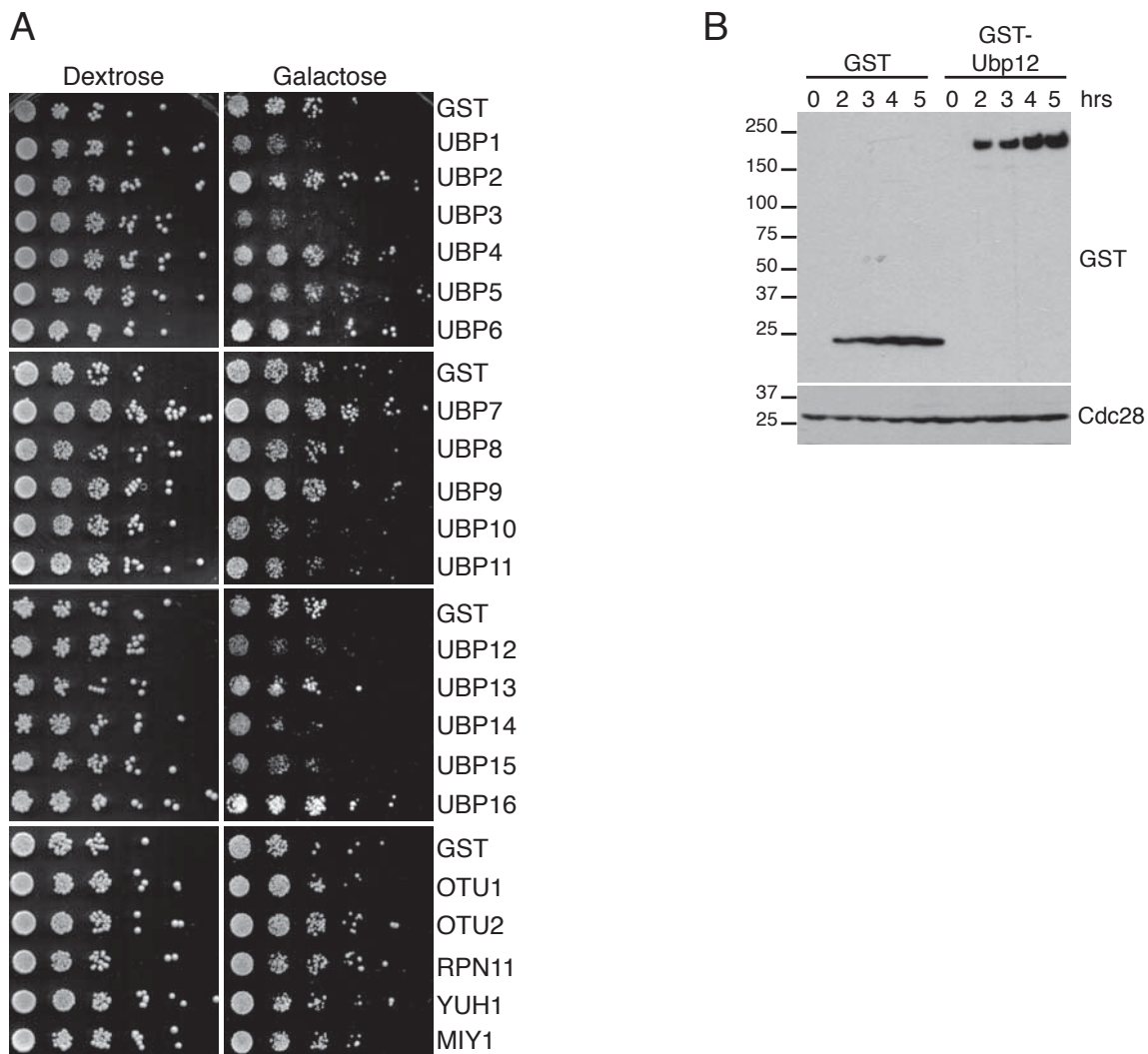
Figure 2.1 Controls for DUB overexpression. (A) 5-fold dilutions of cells containing plasmids that express GST or GST-tagged DUBs from the *GAL1* promoter were plated on media lacking uracil and containing either dextrose (expression off) or galactose (expression on). Although overexpression of no DUB is lethal, overexpression of *UBP1*, *UBP3*, *UBP10*, *UBP11*, *UBP12*, *UBP14*, or *UBP15* leads to smaller colony size, consistent with slower proliferation. (B) Time course of GST-DUB induction. Strains containing plasmids that express GST or GST-Ubp12 from the *GAL1* promoter were induced with 2% galactose for the indicated number of hours and levels analyzed by GST Western blot. Levels of Cdc28 are shown as a loading control.
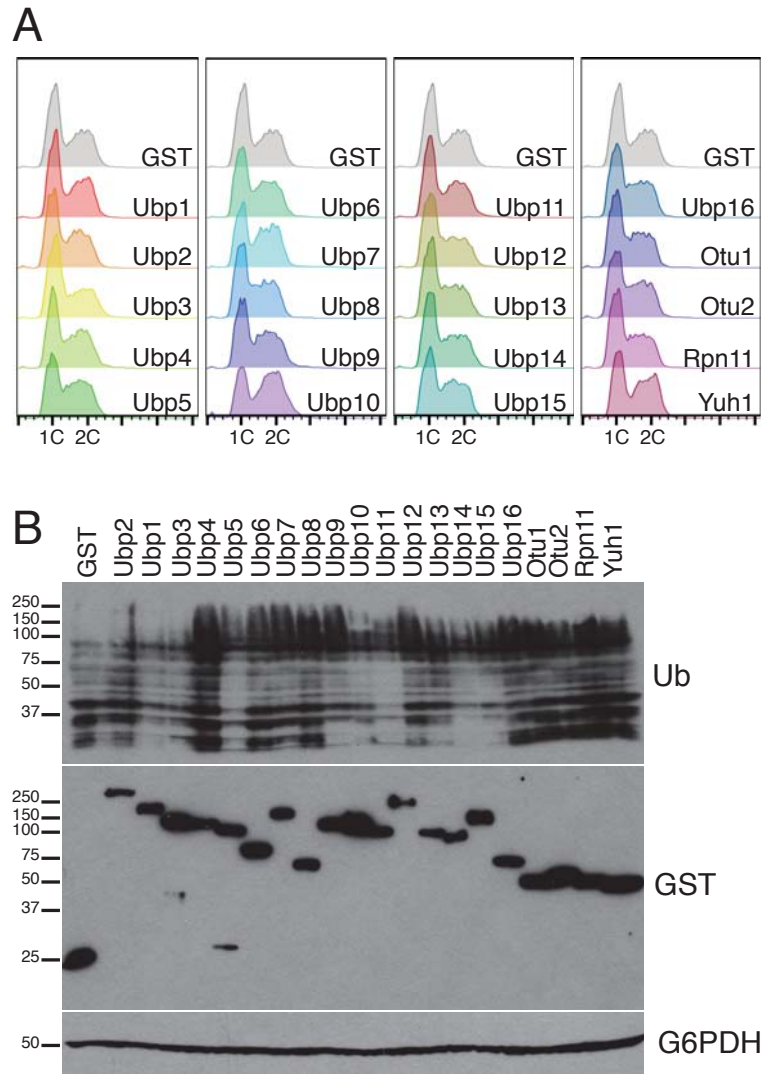
Figure 2.2. Acute overexpression of DUBs does not arrest the cell cycle. (A) Cell-cycle analysis following DUB overexpression. Expression of GST-tagged DUBs was induced from the *GAL1* promoter for four hours and DNA content quantified by flow cytometry. (B) Western blots for ubiquitin chains (Ub) and GST-DUB proteins following a 4-hour induction. G6PDH is shown as a loading control.

To identify DUBs that can regulate the degradation of specific cell cycle proteins, we tested a matrix of 777 pairs and asked whether overexpression of each of the 21 DUBs could upregulate any of 37 TAP-tagged cell-cycle proteins (Figure 2.3A). The 37 target proteins that were selected fit three criteria: (i) the target has been shown to be upregulated upon inactivation of an E3 or inhibition of the proteasome, (ii) expression of the target is cell cycle-regulated, and (iii) TAP-tagged alleles are included in a previously constructed TAP-tag strain collection [111] (Figure 2.1, Supplemental Data S1 [112]). Pilot experiments indicated that overexpression of Ubp2 did not significantly increase levels of any cell cycle protein compared to overexpression of GST alone (Figure 2.4A), so Ubp2 was used as a negative control for the screen. To perform the screen, expression of either the control (Ubp2) or the test DUB were induced in each TAP-tagged strain for four hours. Western blotting was performed with anti-TAP tag antibodies to quantify cell-cycle proteins and G6PDH was used as a loading control (Figure 2.3B). Proteins that changed at least 2-fold in two replicates of the screen were considered high-confidence changes (Figure 2.4, Supplemental Data S2[112]).

Among the 777 DUB-target pairs tested, 50 increases (6.9% of all pairs) and 9 decreases (1.2%) in protein levels were identified (Figure 2.3C). 27 of 37 targets were upregulated by overexpression of at least one DUB, and overexpression of 12 of 20 DUBs resulted in the upregulation of at least one target protein. The fact that more proteins exhibited increased levels than decreased levels is consistent with the prediction that overexpression of DUBs leads to ubiquitin chain removal, stabilization, and increased levels of their targets. Another notable result is that each

DUB regulated a different subset of cell-cycle proteins, demonstrating that DUBs

exhibit specificity for subsets of ubiquitinated proteins in vivo, even in an

overexpression setting.
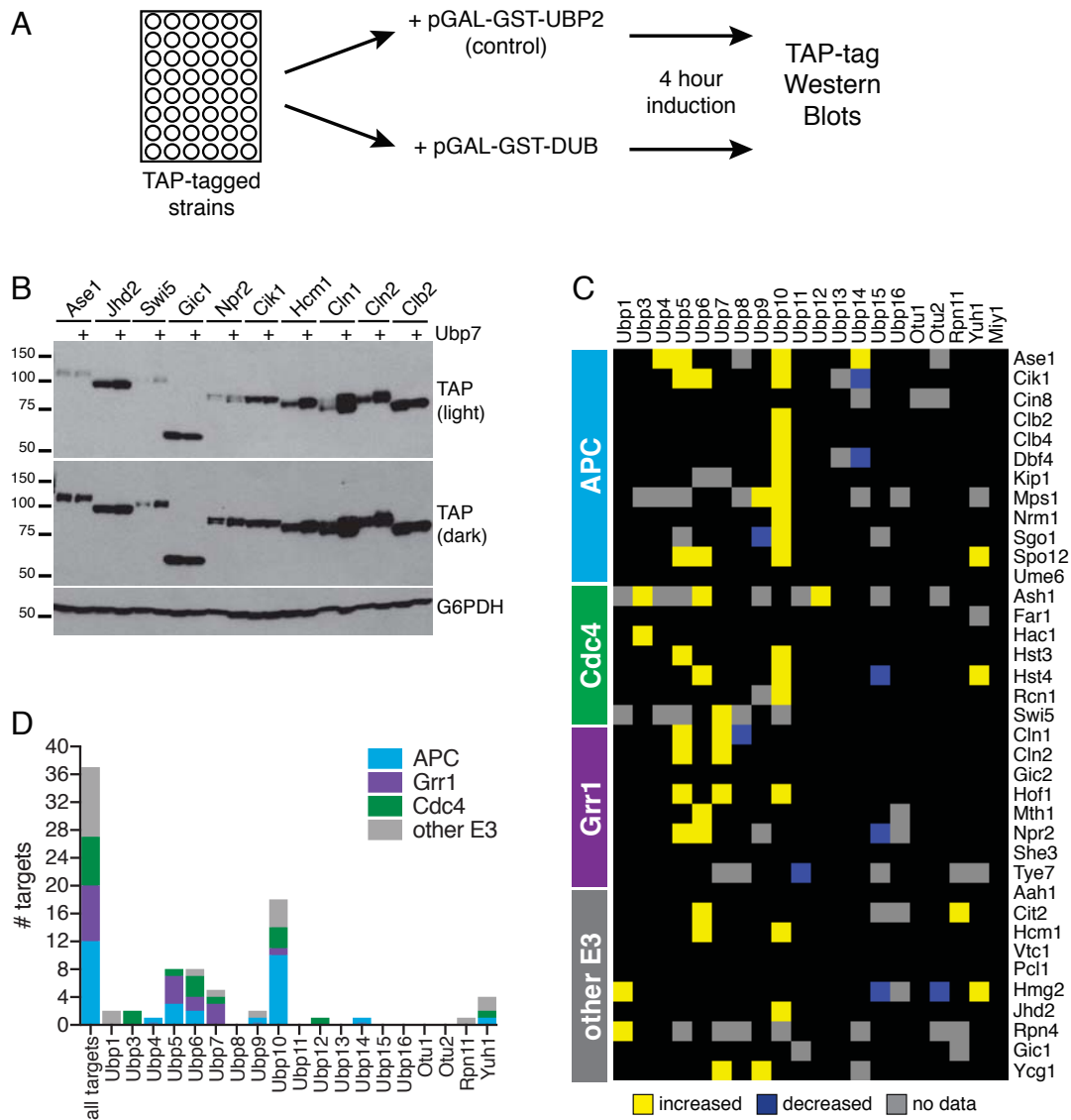
Figure 2.3. DUBs upregulate specific subsets of cell cycle proteins. (A) Design of overexpression screen to identify DUBs that target specific cell cycle regulators for degradation. (B) Representative data from DUB overexpression screen. Western blots show levels of 10 TAP-tagged target proteins (light and dark exposures are shown) and G6PDH following four hours of induction of a control (Ubp2) or Ubp7. (C) Summary heat map of DUB overexpression screen. DUBs are in columns, targets in rows. Targets are grouped by their corresponding E3 ubiquitin ligase (left). Yellow indicates the target increased at least 2-fold in two replicates of the screen, blue indicates the target decreased at least 2-fold in two replicates. Grey indicates no data. All primary data is reported in Supplemental Data S2. (D) Comparison of the number of targets upregulated by each DUB. Bars are color-coded to group targets by their regulatory E3.

A   Ubp2/GST   B   Ubp2/Ubp2

C   Ubp5/Ubp2   D   Ubp6/Ubp2

E   Ubp7/Ubp2   F   Ubp10/Ubp2

G   Yuh1/Ubp2
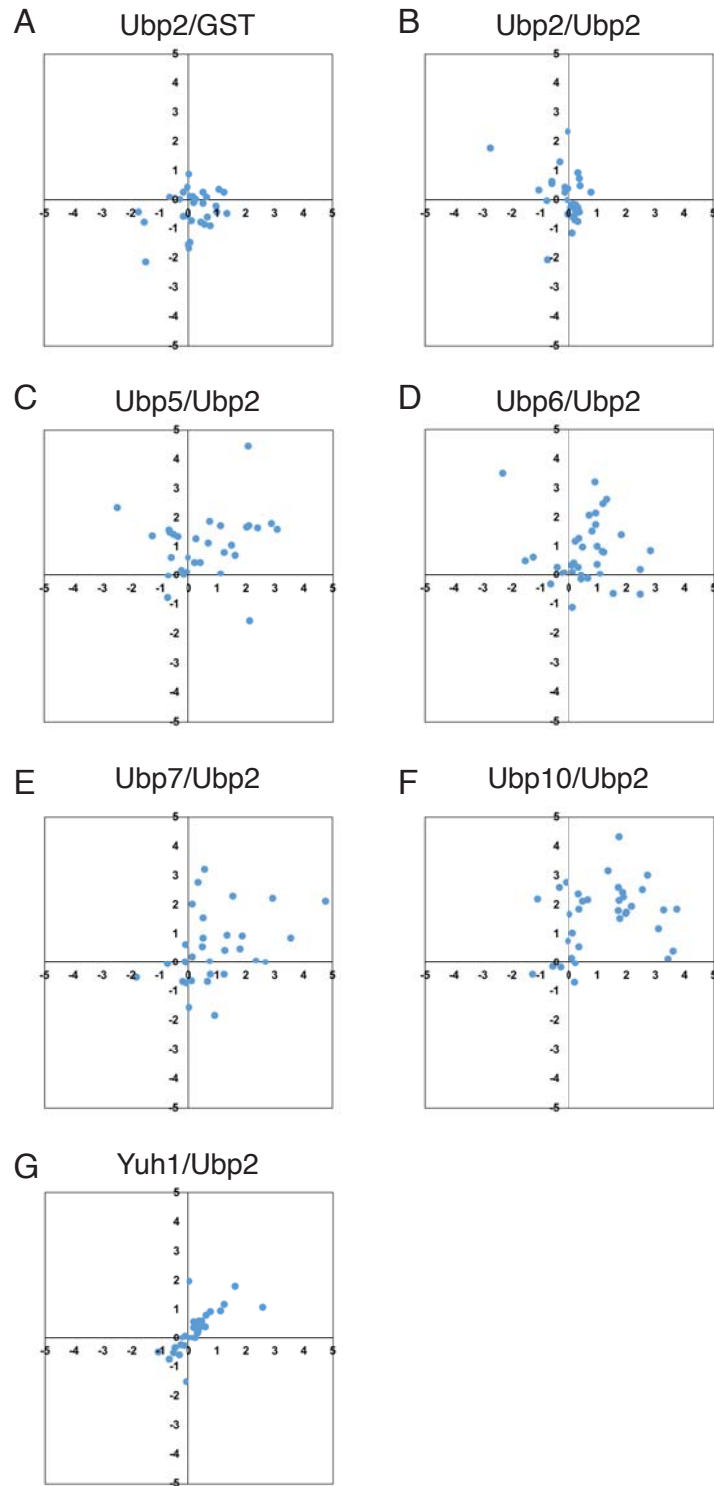
Figure 2.4 Scatter plots of DUB screen data. Shown are plots comparing replicate experiments quantifying log2 fold change of all target proteins after expression of a test DUB compared to a control. (A) Validation of Ubp2 as a control for the screen. Overexpression of Ubp2 does not lead to greater than a 2-fold increase (log2 fold change = 1) in any targets compared to GST overexpression. (B) Analysis of variability in the overexpression assay. Ubp2 was overexpressed in duplicate sets of strains and log2 fold changes calculated. These data were used to determine the cutoff for scoring high-confidence changes. Only changes greater than log2 fold change = 1 in both replicates of the screen are included in Figure 2. (C-G) Scatter plots comparing log2 fold change in replicate experiments following overexpression of the indicated DUBs compared to Ubp2.

How do DUBs achieve substrate specificity? One simple explanation might be that DUBs and ubiquitinated proteins only need to be co-localized in the same subcellular compartment to facilitate their interaction. To address this possibility, the localization of all targets and DUBs were examined in the Collection of Yeast Cells and Localization Patterns (CYCLoPs) database [100], which reports high confidence localization data for the majority of yeast proteins. With the exception of two DUBs whose localizations are unknown (Ubp11, Yuh1), all DUBs localize to the nucleus, the cytoplasm, or both (Table 2.1). Among the target proteins, 31 of 37 are localized to some extent in both the nucleus and the cytoplasm, which would make these proteins accessible to all DUBs tested (Supplemental Data S3 [112]). Of the six targets that are not reported to be nuclear or cytoplasmic, two (Hst3 and Swi5) are inferred to be nuclear based on their established functions, one (Hmg2) is membrane localized, and the localization of three is not known. However, the extent of overlap in localization patterns between the majority of targets and DUBs argues that localization cannot explain most DUB specificity observed in the screen.

Several DUBs have been found to interact with E3 ubiquitin ligases in cells [32, 60, 110], and in some instances an E3 has been shown to function as an adaptor to recruit the DUB to its substrates [60, 113, 114]. Since the identities of the E3s that ubiquitinate most of the cell cycle proteins in our screen are known, we examined whether any DUB regulated all substrates of a given E3, which would suggest this type of recruitment mechanism. We found that Ubp10 upregulated most of the APC substrates in our screen, whereas Ubp5 and Ubp7 upregulated many SCF^{Cdc4} and SCF^{Grr1} substrates (Figure 2.3D). However, each of these DUBs also

upregulated targets ubiquitinated by other E3s, and no DUB regulated all substrates of any particular E3, suggesting that additional mechanisms contribute to DUB-substrate specificity.

Although DUBs are predicted to stabilize targets by removing ubiquitin chains and blocking their degradation, it is possible that upregulation may be indirect, for instance if a transcriptional activator of cell cycle proteins is stabilized by a DUB. To determine if DUBs regulate the stability of candidate target proteins, eight targets were investigated further, to determine if DUB overexpression impaired their degradation. Cycloheximide-chase assays were performed to examine the stability of these targets following overexpression of each of the five DUBs that regulated the most targets in our screen (Ubp5, Ubp6, Ubp7, Ubp10, Yuh1), and GST as a control. Stabilization of substrates correlated well with upregulation of target proteins by specific DUBs (Figure 2.5, Figure 2.6). Moreover, DUBs differentially stabilized target proteins. For example, the G1 cyclins Cln1 and Cln2 were stabilized most strongly by Ubp7. In contrast the stabilities of Hst3 and Spo12 were not significantly affected by Ubp7 but were strongly stabilized by Ubp10. Thus, DUBs differentially stabilize proteasomal targets, which supports the conclusion that DUBs exhibit substrate specificity in vivo.
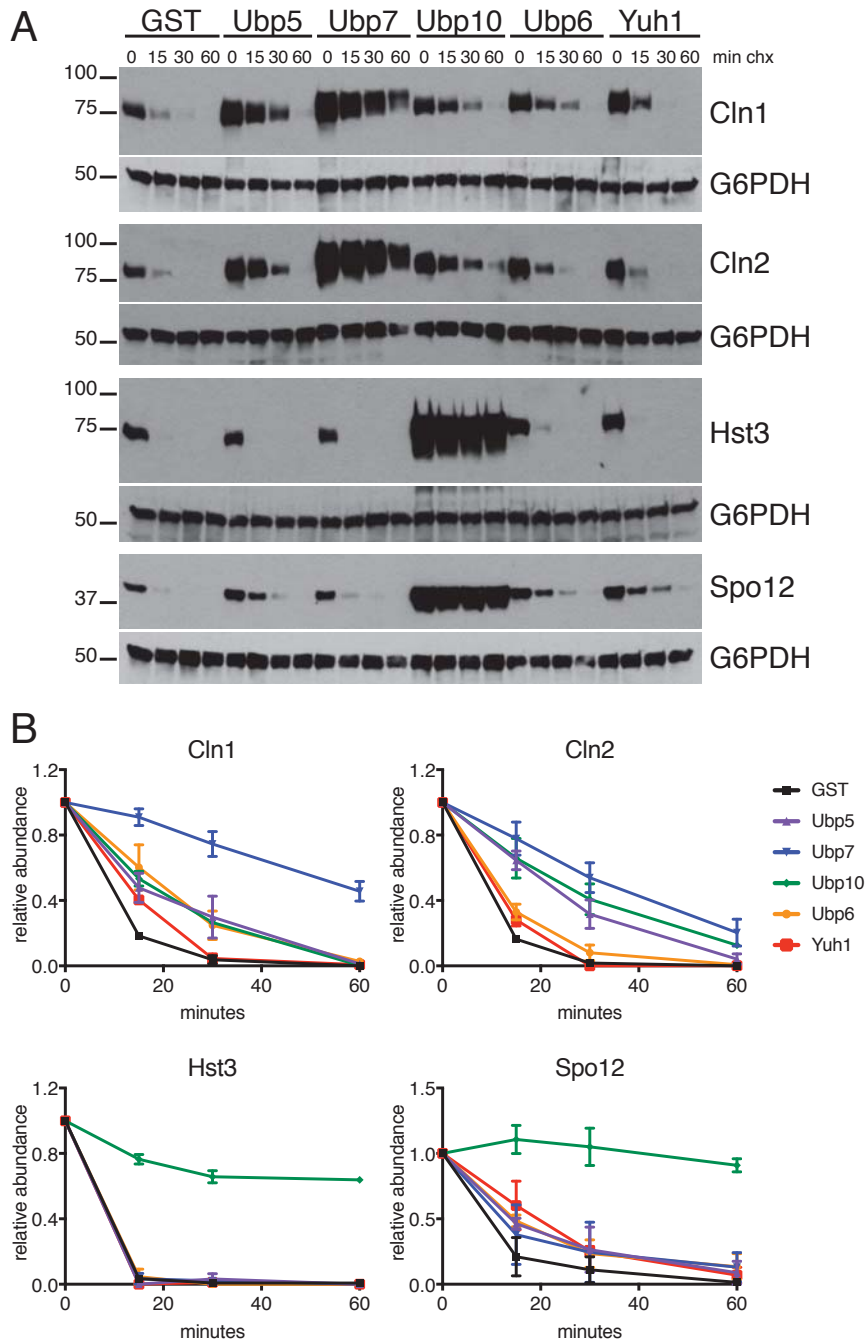
Figure 2.5. DUBs differentially stabilize substrates. (A) Cycloheximide-chase assays of the indicated targets following four hours of overexpression of GST, Ubp5, Ubp7, Ubp10, Ubp6, or Yuh1. Western blots of TAP-tagged targets and G6PDH (loading control) are shown. (B) Quantitation of cycloheximide-chase assays from (A). Shown are the average of n=2 experiments, errors bars represent the standard error of the mean.

38
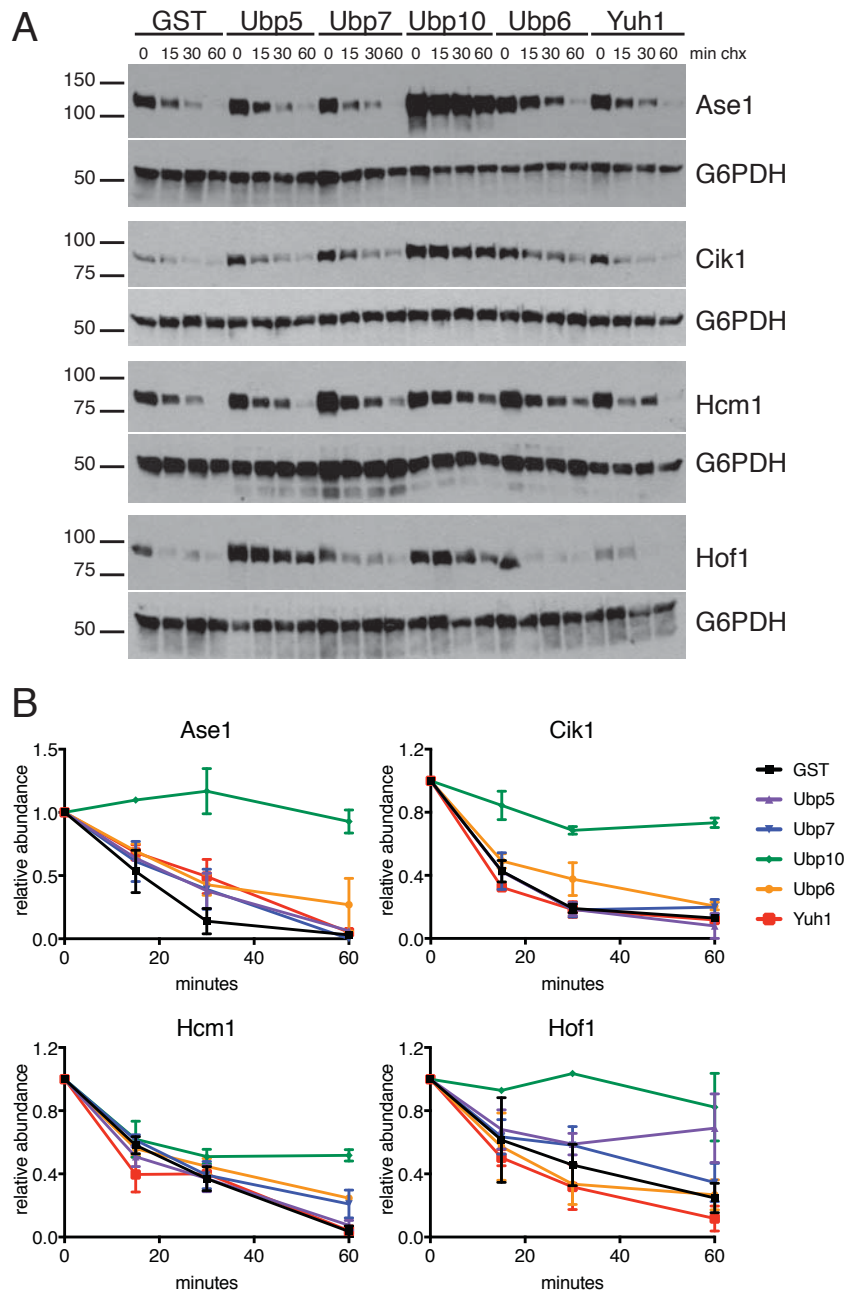
Figure 2.6. DUBs differentially stabilize target proteins. Experiments were performed as in Figure 3 examining additional target proteins. (A) Cycloheximide-chase assays of the indicated targets following four hours overexpression of GST, Ubp5, Ubp7, Ubp10, Ubp6, or Yuh1. Western blots of TAP-tagged targets and G6PDH (loading control) are shown. (B) Quantitation of cycloheximide-chase assays from (A). Shown are the average of n=2 experiments, errors bars represent the standard error of the mean.

Ubp10 regulates the cell cycle

Ubp10 is a USP family DUB (Table 1, Figure 2.7A) that has established roles in gene silencing, ribosome biogenesis and recovery from DNA damage [87, 97, 106, 115]. Interestingly, Ubp10 upregulated the greatest number of cell cycle proteins in our screen and we confirmed that 15 of 16 candidate targets were upregulated by Ubp10 compared to GST (Figure 2.7B). Mutation of the catalytic cysteine residue of Ubp10 to serine was previously shown to eliminate its deubiquitinase activity [106]. We tested whether the deubiquitinase activity of Ubp10 is necessary for its ability to stabilize its targets, and for all four targets that were tested, the catalytic activity of Ubp10 contributed to their upregulation (Figure 2.7C). Ubp10 has a unique N-terminus containing an intrinsically disordered region (IDR) that is required for its interaction with several established binding partners [116]. To determine if this domain is also required to stabilize the targets that we identified, a mutant of Ubp10 that lacks the IDR (Ubp10ΔN) was tested in an overexpression assay. Although Ubp10 and Ubp10ΔN were not induced to equal levels in all experiments, stabilization of nine of 15 targets was reproducibly dependent upon the N-terminal IDR, whereas five others showed intermediate effects and one was unaffected (Figure 2.7B). To confirm that changes in protein levels reflected changes in protein stability, the half-life of one target whose upregulation was completely dependent upon the IDR (Hst3), and one target that showed intermediate regulation by Ubp10ΔN (Dbf4) were assayed (Figure 2.7D). For both targets, stabilization by Ubp10ΔN correlated with the extent of upregulation that was observed. These data

strongly suggest that Ubp10 is recruited to its targets via its N-terminal IDR to remove ubiquitin and stabilize these proteins.

The fact that Ubp10 regulated expression of 40% of cell cycle proteins tested suggested that it controls progression through the cell cycle. Consistent with this possibility, asynchronous populations of cells overexpressing Ubp10 showed a reduced fraction of cells in G1 and an increased fraction of mitotic cells, with Ubp10ΔN overexpression having an intermediate effect (Figure 2.7E, Figure 2.8). Moreover, deletion of *UBP10* had the opposite effect, resulting in an increased fraction of G1 cells in an asynchronous population (Figure 2.9A). These data suggest that Ubp10 regulates entry into S phase. To test this, cells were arrested in G1, released, and DNA content was monitored at 15-minute intervals. Compared to wild type cells, *ubp10Δ* cells exhibited an approximately 15-minute delay in initiating DNA replication when grown in rich medium (Figure 2.9B-C). We next examined the levels of four representative target proteins that are stabilized by Ubp10 overexpression, to determine if their expression was altered in *ubp10Δ* cells. The expression of two proteins expressed in G2/M-phase, Hst3 and Spo12, was delayed approximately 15 minutes in *ubp10Δ* cells, in accordance with the requirement for Ubp10 to enter S-phase on time. Although the expression of these proteins was delayed in *ubp10Δ* cells, the peak levels of each protein were comparable to peak levels in wild type cells (Figure 2.9D). In contrast, Dbf4 and Mps1 protein levels increased with similar timing in wild type and *ubp10Δ* cells, however peak expression levels of both proteins were decreased in the absence of Ubp10. In

addition, Dbf4 was less stable in *ubp10Δ* cells, whereas Mps1, Spo12, and Hst3

half-lives were relatively unchanged (Figure 2.9E-F). These results suggest that

Dbf4 is deubiquitinated and stabilized by Ubp10 during an unperturbed cell cycle.
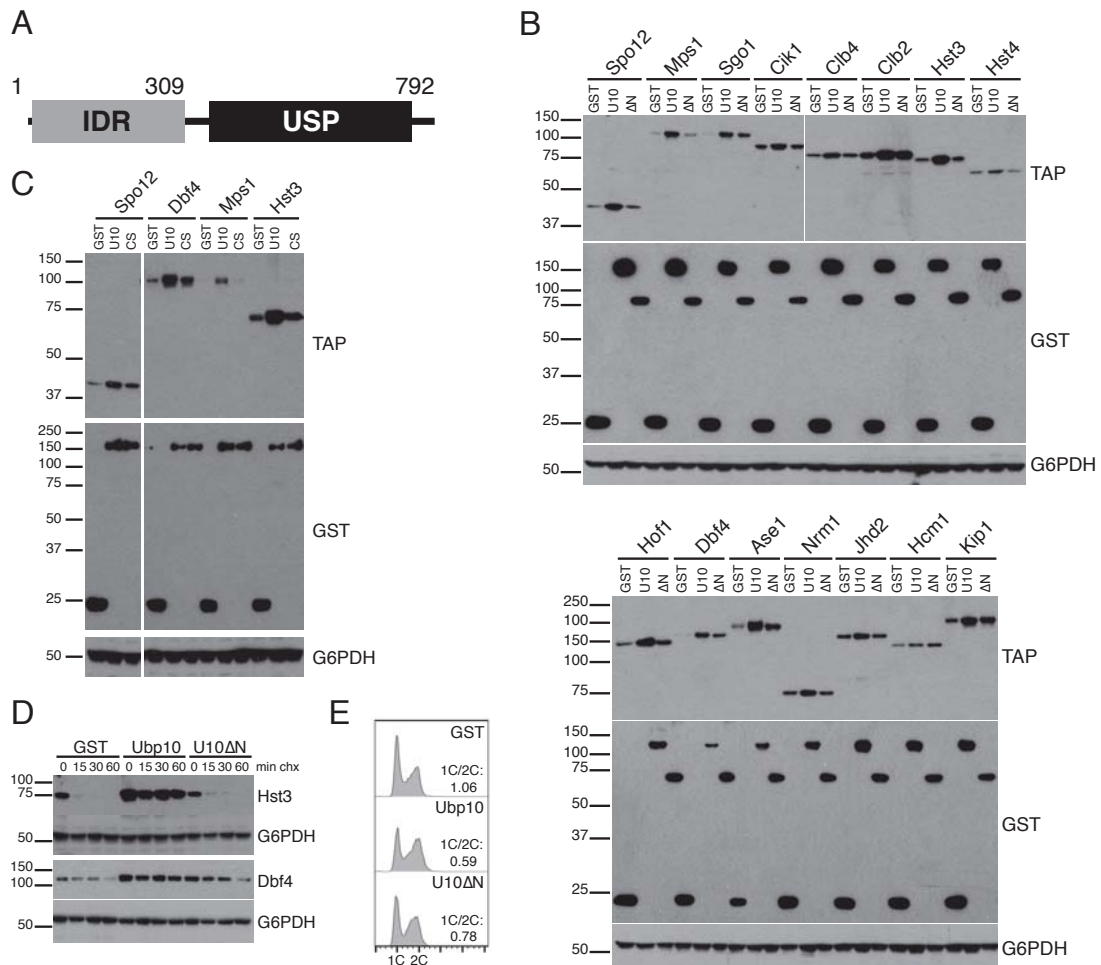
Figure 2.7. The catalytic activity and N-terminal IDR of Ubp10 contribute to target stabilization. (A) Diagram of domains in Ubp10. (B) Validation of Ubp10 candidate targets and analysis of the contribution of the IDR. Western blots showing levels of the indicated TAP-tagged candidate targets following 2-hour induction of GST, Ubp10, or Ubp10Δ2-309 (ΔN) proteins with 0.5% galactose. GST blots show similar expression of GST and DUBs, G6PDH blots confirm equal loading. (C) Ubp10 catalytic function is important for stabilization of substrates. Western blot showing levels of the indicated TAP-tagged candidate targets following overexpression of GST, Ubp10, or Ubp10-C371S (CS) as in (B). GST and G6PDH blots are shown as controls. (D) Cycloheximide-chase assays of Hst3 and Dbf4 following overexpression of GST, Ubp10 or Ubp10Δ2-309 (ΔN) as in (B). Western blots of TAP-tagged Dbf4 and Hst3 are shown. G6PDH blot confirms equal loading. (E) FACS profiles showing DNA content of cells overexpressing GST, Ubp10 or Ubp10Δ2-309 (U10ΔN) as in (B). 1C:2C ratio is shown to highlight the increased 2C population upon Ubp10 overexpression.
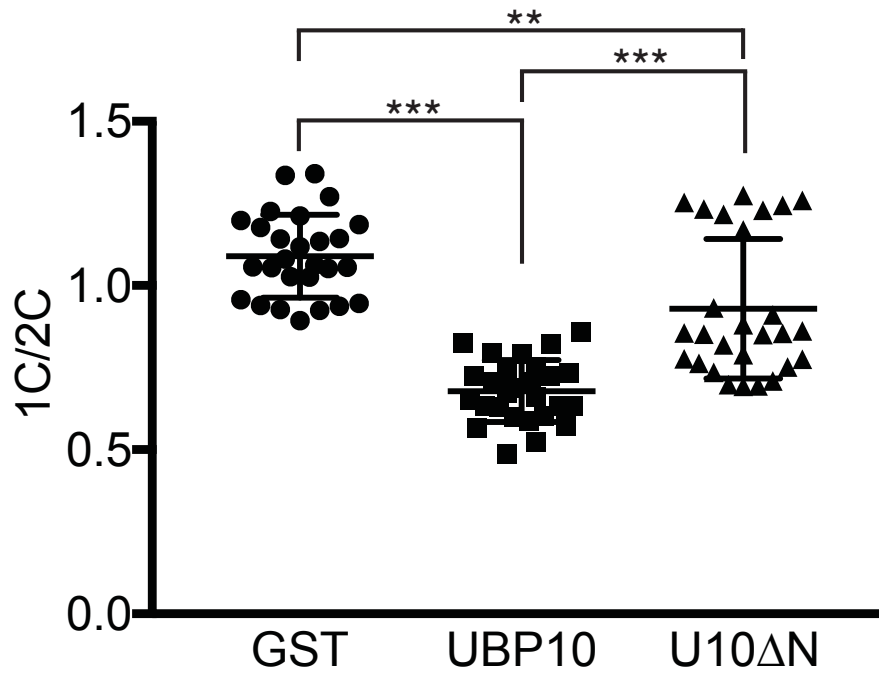
Figure 2.8. Overexpression of Ubp10 and Ubp10ΔN alter cell cycle distributions. Shown are mean 1C:2C DNA content values from 27 replicate experiments in which GST, Ubp10 and Ubp10 N were overexpressed. Note that replicates include overexpression experiments performed in wild type strains expressing different TAP-tagged target proteins (from Figure 4B). Black lines depict mean and standard deviation. Significance was calculated using a paired t-test, **p<0.005, ***p<0.0001.

A

WT
1C/2C: 0.54
ubp10Δ
1C/2C: 0.93

1C 2C

B

WT   *ubp10Δ*

0   0
15   15
30   30
45   45
60   60
75   75
90   90
105   105
120   120

1C 2C   1C 2C

C

D

WT   *ubp10Δ*
0 15 30 45 60 75 90 105 120   0 15 30 45 60 75 90 105 120 minutes

100 — Dbf4
50 — G6PDH
100 — Mps1
50 — G6PDH
75 — Hst3
50 — G6PDH
37 — Spo12
50 — G6PDH

E

WT   *ubp10Δ*
0 10 20 30   0 10 20 30 min chx

100 — Dbf4
50 — G6PDH
100 — Mps1
50 — G6PDH
75 — Hst3
50 — G6PDH
50 — Spo12
50 — G6PDH

F

Dbf4   Mps1
Hst3   Spo12

45
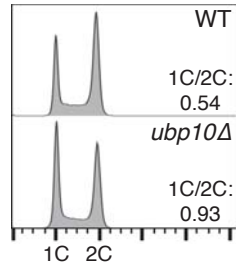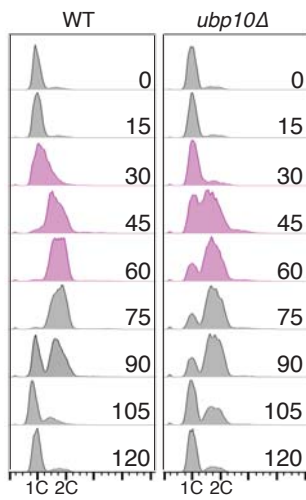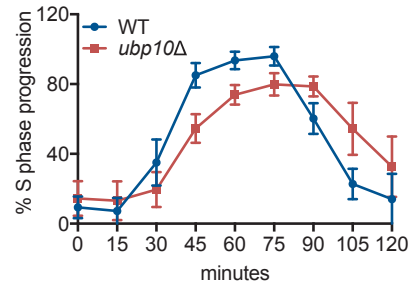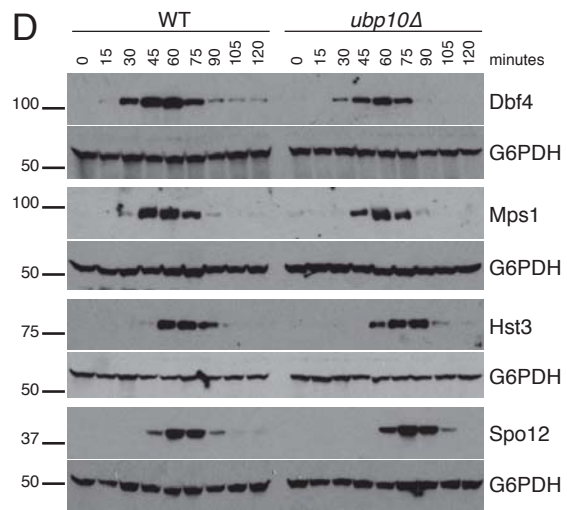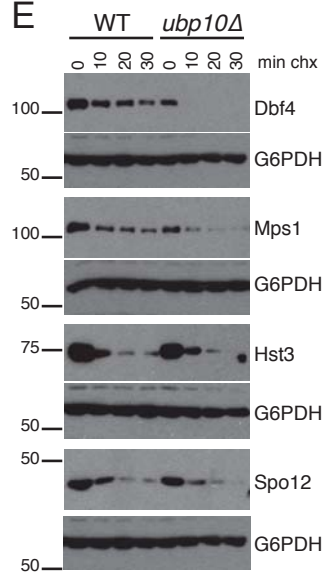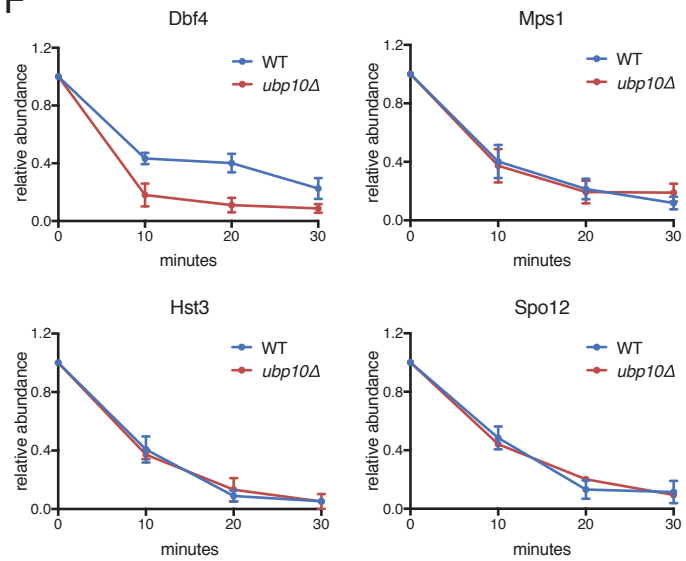
Figure 2.9 Ubp10 regulates entry into the cell cycle. (A) FACS profiles showing DNA content of asynchronous wild type (WT) and *ubp10Δ* cells growing in rich medium. 1C:2C ratio is shown to highlight increased 1C population upon deletion of *UBP10*. (B) S phase is delayed in *ubp10Δ* cells. Wild type (WT) and *ubp10Δ* cells growing in rich medium were arrested in G1 with alpha-factor and released into the cell cycle. Additional alpha-factor was added back after 30 minutes to arrest cells in the subsequent G1 phase. Representative FACS plots are shown, S phase time points are highlighted in purple. (C) Progression through S-phase was calculated as described in the Materials and Methods. An average of n=8 experiments is shown. Error bars represent standard deviations. The eight replicates include two experiments each performed in WT and *ubp10Δ* strains with the four different TAP-tagged candidates shown in part (D). (D) Expression of Ubp10 candidate targets are reduced and/or delayed in *ubp10Δ* cells. Strains expressing TAP-tagged candidate targets were followed over the cell cycle, as in (B). TAP and G6PDH Western blots are shown. (E) Cycloheximide-chase assays showing the half-life of candidate targets in WT and *ubp10Δ* cells. Western blots for TAP-tagged targets and G6PDH are shown. (F) Quantitation of cycloheximide-chase assays from (E). Shown are the average of n=8 (Dbf4), n=5 (Mps1), or n=3 (Spo12, Hst3) experiments, errors bars represent the standard error of the mean.

A previous study found that the slow growth phenotype of *ubp10Δ* cells growing on solid medium could be reversed by overexpression of Rpa190, a Ubp10 target that regulates ribosome biogenesis [97]. To determine if reduced Rpa190 expression in *ubp10Δ* cells contributes to the G1/S delay that we observed, arrest-release experiments were performed in wild type and *ubp10Δ* cells that overexpressed Rpa190. Surprisingly, although overexpression of Rpa190 did increase the colony size of *ubp10Δ* strains growing on plates (Figure 2.10A-B), it did not restore the timing of DNA replication following release from a G1 arrest to wild type (Figure 2.10C). Therefore, other pathways must be altered in *ubp10Δ* cells that result in delayed DNA replication.
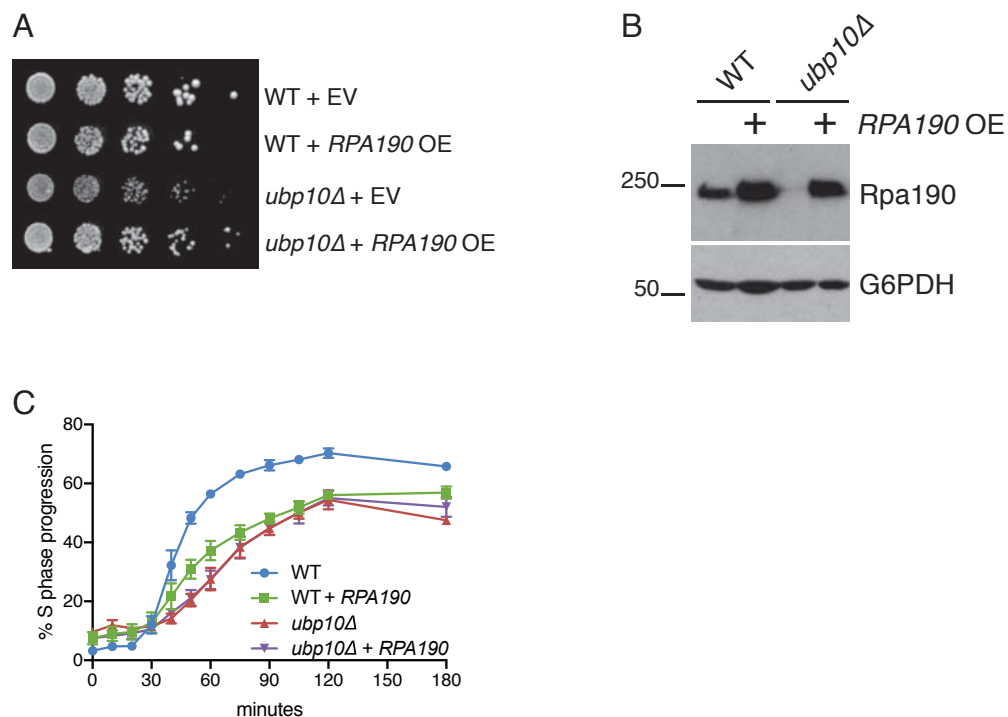
Figure 2.10. Overexpression of Rpa190 in *ubp10Δ* cells. (A) 5-fold dilutions of wild type (WT) or *ubp10Δ* strains overexpressing *RPA190* from its own promoter in a 2-micron plasmid (*RPA190* OE), or an empty vector control (EV), were plated on media lacking uracil. (B) Western blot of GFP-tagged Rpa190 in cells from (A). G6PDH is shown as a loading control. (C) Rpa190 overexpression does not restore S-phase timing in *ubp10Δ* cells. Strains from (A) were grown in synthetic medium lacking uracil, arrested in G1 with alpha-factor for three hours and then released into media without alpha-factor. Nocodazole was added to the cultures after 30 minutes to arrest cells in the following mitosis. Samples were taken for FACS at 10-30-minute intervals. Progression through S phase was calculated as described in the Materials and Methods. Shown is an average of n=3 experiments. Error bars represent standard deviations.

Among the candidate Ubp10 targets identified in our screen, the target most likely to impact DNA replication timing is Dbf4. Dbf4 is the activating subunit of the kinase Cdc7, which together phosphorylate subunits of the Mcm helicase to initiate DNA replication [117]. We found that Dbf4 was less stable and expressed at lower levels in *ubp10Δ* cells (Figure 2.9D-E), which could be the cause of the delay in DNA replication. To test this possibility, Dbf4 was overexpressed from a plasmid in *ubp10Δ* cells. Notably, *ubp10Δ* cells showed a greater delay in G1/S entry when growing in synthetic medium compared to rich medium (Figure 2.9B, 2.11A), and this delay was partially reversed upon Dbf4 overexpression (Figure 2.11). This result supports the possibility that regulation of Dbf4 by Ubp10 is important for timely cell cycle progression. However, since Dbf4 overexpression only partially restored the timing of S-phase entry, the deubiquitination of additional proteins by Ubp10 must also contribute to its cell cycle-regulatory role.
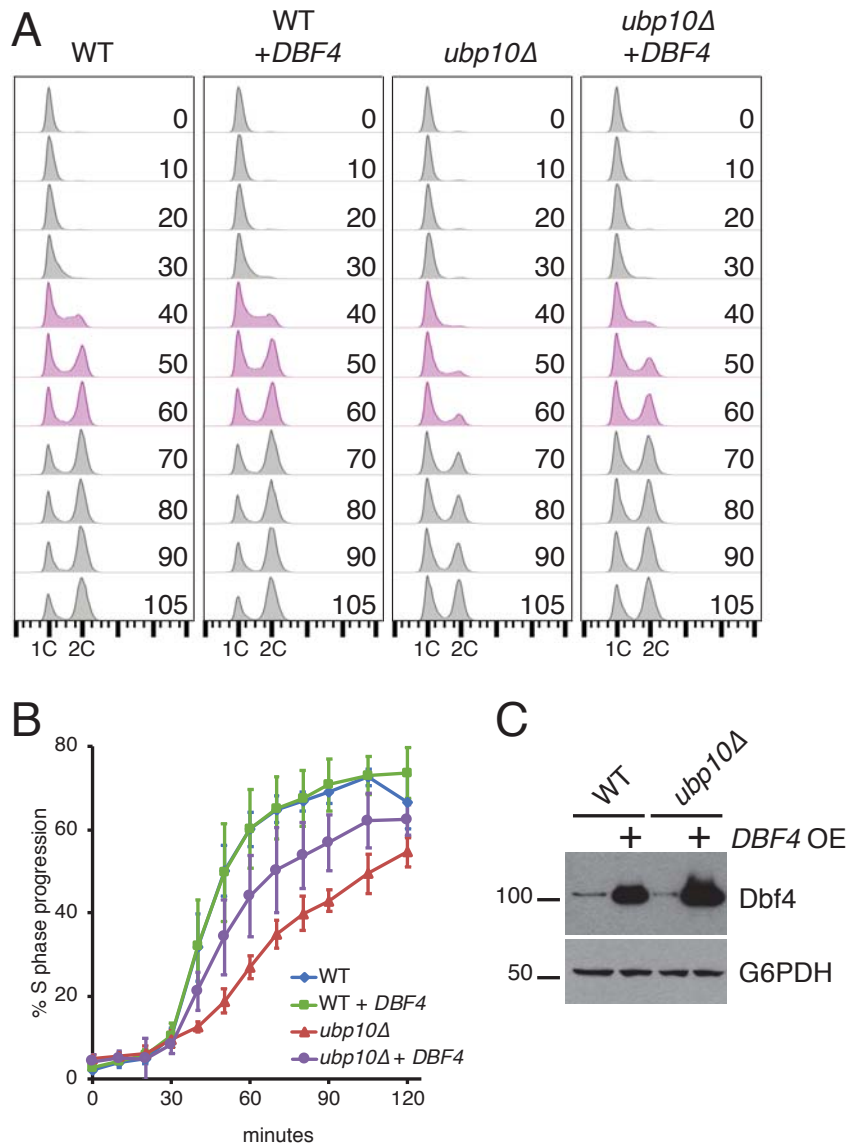
Figure 2.11. Dbf4 overexpression partially restores S-phase timing in *ubp10Δ* cells. (A) Strains expressing *DBF4* from its own promoter in a 2-micron plasmid (*DBF4* OE) or an empty vector control, were grown in synthetic medium lacking uracil, arrested in G1 with alpha-factor for three hours, and then released into medium without alpha-factor. Nocodazole was added to the cultures after 30 minutes to arrest cells in the following mitosis. Samples were taken for FACS at 10-30-minute intervals. A representative experiment is shown, time points that exhibit the greatest differences between strains are highlighted in purple. (B) Progression through S phase was calculated as described in the Materials and Methods. Shown is an average of n=5 experiments. Error bars represent standard deviations. (C) Western blot of TAP-tagged Dbf4 in cells from (A). G6PDH is shown as a loading control.

Genetic analysis of the DUB network

The modest phenotypes that have been reported for most DUB deletion strains suggest that there may be redundancies within the DUB network. However, most pairwise DUB deletions that have been examined do not exhibit negative genetic interactions, which would be expected if two DUBs redundantly regulate a critical process [118]. To explore potential higher order redundancies, we focused on the 5 DUBs that were able to stabilize the greatest number of cell cycle proteins upon overexpression (Ubp5, Ubp6, Ubp7, Ubp10, Yuh1), and constructed strains carrying all possible combinations of these deletions. All strains were viable, including the five DUB deletion strain, indicating that these DUBs are not redundantly required for any essential process.

To assay for potential combinatorial effects on proliferation, the doubling times of strains with each of the 32 genotypes (all possible combinations of deletions in the five selected DUBs) were measured. Among the single mutant strains, the only strain with a significant proliferation defect was *ubp10Δ* (Figure 2.12A). The average doubling time of *ubp10Δ* strains was 157 minutes in rich medium, compared to 118 minutes for wild type strains. None of the other four single deletion strains, or most combinations of mutations that included just these four DUBs had doubling times that were significantly different from wild type (Figure 2.12A). The one exception was *ubp6Δ ubp7Δ yuh1Δ*, which displayed a relatively small increase in doubling time. These results indicate that there are no strong negative genetic interactions among these five DUBs, indicating a lack of redundancy at least for cell cycle progression. Strikingly, however, we did discover a novel positive genetic

51

interaction: deletion of *UBP6* rescued the proliferation defect observed in *ubp10Δ* strains. All strains that included both *ubp10Δ* and *ubp6Δ* had doubling times that are decreased significantly compared to the *ubp10Δ* single mutant (Figure 2.12A, Table 2.2).

Since deletion of *UBP10* slows proliferation by delaying entry into the cell cycle (Figure 2.9B-C), we tested whether deletion of *UBP6* reversed the G1/S delay in *ubp10Δ* cells by comparing the timing of S-phase entry in wild type, *ubp6Δ*, *ubp10Δ*, and *ubp6Δ ubp10Δ* strains in G1 arrest-release experiments. Although deletion of *UBP6* had no effect on the cell cycle on its own, *ubp6Δ* in combination with *ubp10Δ* restored the timing of DNA replication to wild type (Figure 2.12B-C). This result suggests that Ubp6 activity may counteract Ubp10 function in cells and that the balance of their activities is important for cell cycle timing.

Ubp6 is one of two DUBs that associate with the proteasome, where it removes ubiquitin from proteasomal substrates and protects ubiquitin from degradation [95, 119]. Several studies have shown that Ubp6 inhibits the proteasome and that cells lacking Ubp6 display increased proteasomal activity [120, 121]. In contrast, another report showed that loss of Ubp6 impairs proteasomal function by preventing maximal opening of the gate to the substrate translocation channel [122]. Although the precise effect of Ubp6 on the proteasome remains unclear, these studies raise the possibility that altered proteasomal activity upon *UBP6* deletion might reverse the accelerated degradation of Ubp10 substrates in *ubp10Δ* cells. To test this possibility, we assayed the half-life of Dbf4 and Rpa190 in

ubp6Δ ubp10Δ strains. As previously observed, Dbf4 was degraded more quickly in *ubp10Δ* cells compared to wild type (Figure 2.9, Figure 2.12D-E). In addition, Rpa190 was stable in wild type cells, but was destabilized in the absence of Ubp10 (Figure 7D-E), consistent with a previous report [97]. Interestingly, the levels and stabilities of both proteins were restored to wild type in *ubp6Δ ubp10Δ* cells compared to the *ubp10Δ* single mutant. The effect of *UBP6* deletion on Dbf4 that was overexpressed from a plasmid (as in Figure 2.11) was greater than its effect on endogenous Dbf4, and overexpressed Dbf4 was significantly stabilized in both *ubp6Δ* and *ubp6Δ ubp10Δ* cells compared to wild type (Figure 2.12D-E). These data suggest that deletion of *UBP6* impairs degradation of these substrates by the UPS and reverses the accelerated degradation that occurs in *ubp10Δ* cells.
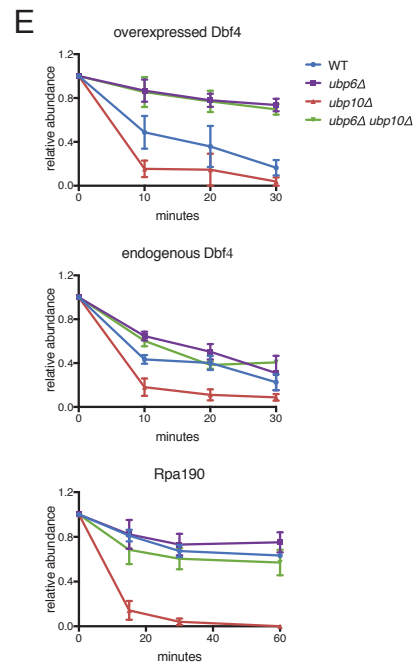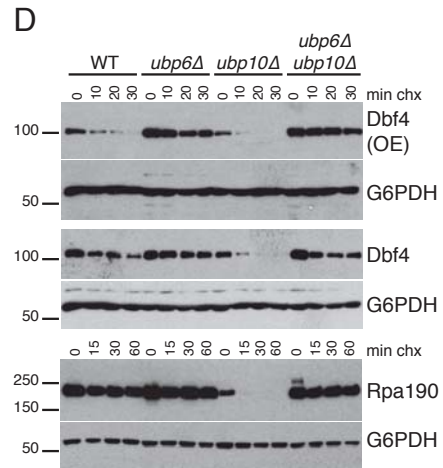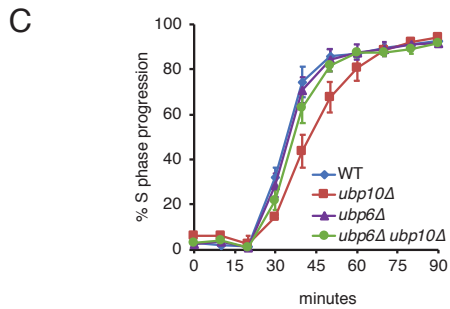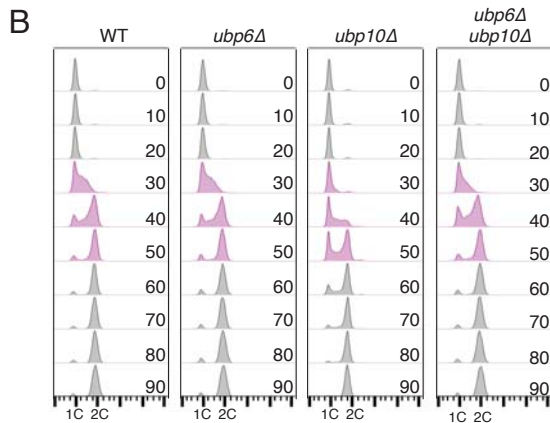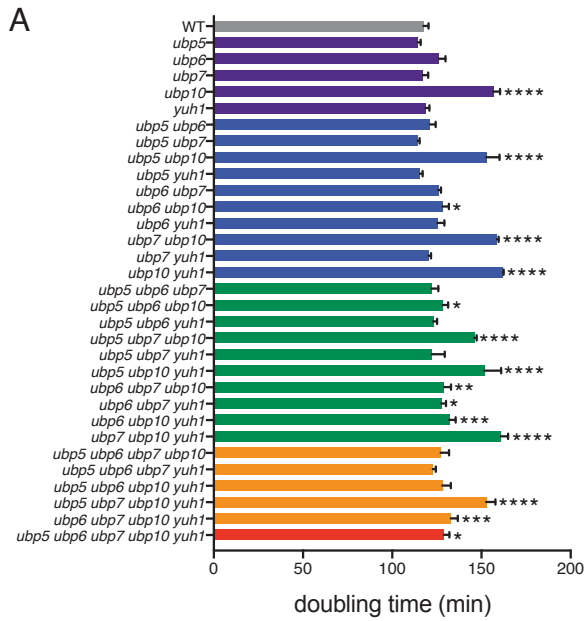
Figure 2.12. Deletion of *UBP6* restores cell cycle timing in *ubp10Δ* strains. (A) Doubling times of strains with deletions of the indicated DUBs. Colors represent number of deletions: single mutants, purple; double mutants, blue; triple mutants, green; quadruple mutants, orange; quintuple mutant, red. Shown are average doubling times for n=2-6 independently derived strains of each genotype. Error bars represent standard deviation. Asterisks indicate strains that are significantly different from wild type (WT) as measured by one-way ANOVA (*$p<0.05$, **$p<0.005$, ***$p<0.0005$, ****$p<0.0001$). All data is included in Supplemental Table S1 [112]. (B) G1 arrest-release of strains with the indicated genotypes, growing in rich medium. Representative FACS plots are shown, time points that exhibit the greatest differences between strains are highlighted in purple. (C) Progression through S phase was calculated as described in the Materials and Methods. Averages of n=3 biological replicates are shown. Error bars represent standard deviation. (D) Cycloheximide-chase assay of Dbf4-TAP and Rpa190-TAP in the indicated strains. In the top panels Dbf4 was overexpressed from a 2-micron plasmid (as in Figure 6); the middle and lower panels represent Dbf4 and Rpa190 expressed from their genomic loci. TAP and G6PDH (loading control) Western blots are shown. (E) Quantitation of cycloheximide-chase assays from (A). Shown are average of n=3 (Dbf4 OE), n=8 (endogenous Dbf4 in WT and *ubp10Δ*), or n=4 (endogenous Dbf4 in ubp6Δ and *ubp6Δ ubp10Δ*, Rpa190) experiments, error bars represent standard error of the mean.

genotype	number of isolates	mean doubling time	standard deviation	sig dif from WT[#]	adj p value	sig dif from ubp10[#]	adj p value
WT	3	117.5	2.925			****	<0.0001
ubp5	3	114.4	1.553	ns	0.9946	****	<0.0001
ubp6	2	126.2	3.642	ns	0.271	****	<0.0001
ubp7	3	117	3.168	ns	0.9999	****	<0.0001
ubp10	2	156.7	3.771	****	<0.0001		
yuh1	3	118.7	2.101	ns	0.9995	****	<0.0001
ubp5 ubp6	3	121.3	3.128	ns	0.9853	****	<0.0001
ubp5 ubp7	3	114.3	1.042	ns	0.9942	****	<0.0001
ubp5 ubp10	3	152.6	7.495	****	<0.0001	ns	0.9927
ubp5 yuh1	3	115.6	1.453	ns	0.9992	****	<0.0001
ubp6 ubp7	3	125.8	1.539	ns	0.2016	****	<0.0001
ubp6 ubp10	4	128.2	3.597	*	0.0204	****	<0.0001
ubp6 yuh1	3	125.3	3.977	ns	0.2708	****	<0.0001
ubp7 ubp10	4	158.7	0.9206	****	<0.0001	ns	0.9992
ubp7 yuh1	3	120.2	1.537	ns	0.9987	****	<0.0001
ubp10 yuh1	3	162.1	0.3686	****	<0.0001	ns	0.8901
ubp5 ubp6 ubp7	3	122.1	3.726	ns	0.9212	****	<0.0001
ubp5 ubp6 ubp10	3	128.4	2.988	*	0.0313	****	<0.0001
ubp5 ubp6 yuh1	3	123	2.186	ns	0.7634	****	<0.0001
ubp5 ubp7 ubp10	2	146.1	1.273	****	<0.0001	ns	0.1651
ubp5 ubp7 yuh1	3	122.2	7.23	ns	0.9071	****	<0.0001
ubp5 ubp10 yuh1	5	151.7	9.374	****	<0.0001	ns	0.8898
ubp6 ubp7 ubp10	5	129	3.893	**	0.0052	****	<0.0001
ubp6 ubp7 yuh1	5	127.6	2.581	*	0.0225	****	<0.0001
ubp6 ubp10 yuh1	4	131.9	3.575	***	0.0004	****	<0.0001
ubp7 ubp10 yuh1	6	160.9	3.992	****	<0.0001	ns	0.9632
ubp5 ubp6 ubp7 ubp10	3	127.1	4.693	ns	0.0824	****	<0.0001
ubp5 ubp6 ubp7 yuh1	3	122.7	1.758	ns	0.8093	****	<0.0001
ubp5 ubp6 ubp10 yuh1	2	128	4.879	ns	0.0983	****	<0.0001
ubp5 ubp7 ubp10 yuh1	4	152.7	5.128	****	<0.0001	ns	0.9857
ubp6 ubp7 ubp10 yuh1	4	132.9	3.873	***	0.0001	****	<0.0001
ubp5 ubp6 ubp7 ubp10 yuh1	3	129.1	2.96	*	0.0172	****	<0.0001

[#]Significance calculated by one-way ANOVA; ns, not significant

Table 2.2. Doubling time of DUB deletion strains.

Loss of *UBP6* results in accelerated degradation of ubiquitin itself, and as a result, decreases the pool of free ubiquitin in the cell that is available to be conjugated to substrates [95, 119, 123, 124]. We therefore considered that possibility that Ubp10 substrates may be stabilized in *ubp6Δ* cells because ubiquitin levels are reduced. To explore this possibility, we quantified free ubiquitin levels in DUB deletion strains. Consistent with previous studies, there was less free ubiquitin in *ubp6Δ* cells. However, free ubiquitin levels were also reduced in *ubp10Δ* and *ubp6Δ ubp10Δ* delete strains, and there was no correlation between increased levels of Dbf4 and decreased levels of ubiquitin (Figure 2.13A-B). This result suggests that ubiquitin levels are not limiting for Dbf4 degradation, and that Ubp6 does not affect the stability of Ubp10 substrates by reducing the amount of available ubiquitin in the cell.

Previous studies have also found that *UBP6* deletion alters the stability of proteasome substrates. However, not all substrates appear to be affected by *UBP6* deletion in the same way. N-end rule reporter substrates and the transcription factor Gcn4 are destabilized in *ubp6Δ* strains [120], whereas the model proteasomal substrates Ub-Pro-β-gal and Ub-Leu-β-gal are more stable upon *UBP6* deletion [95]. Together with our findings on Dbf4 and Rpa190, these results suggest that not all proteasomal substrates are affected by *UBP6* deletion in the same way. To determine whether Ubp6 regulates the stability of additional endogenous UPS substrates, we examined another four UPS targets to determine if their stabilities were altered in *ubp6Δ* cells. Notably, none of these proteins were destabilized upon

UBP6 deletion. Similar to Dbf4, Spo12, Hst3 and Cik1 were more stable in *ubp6Δ*

cells, whereas the stability of Cln2 was not changed (Figure 2.13C-D). These results

are consistent with the model that Ubp6 is required for the efficient degradation of

many proteasomal substrates in vivo and that *UBP6* deletion rescues cell cycle

defects in *ubp10Δ* cells by slowing the degradation of Ubp10 substrates.

If deletion of Ubp6 has a positive effect on *ubp10Δ* strains by impairing

proteasomal function, then other mutants that have compromised proteasomal

function should also rescue the defects in *ubp10Δ* strains. To test this possibility, we

combined deletion of an alternate DUB, *UBP14*, with *UBP10* deletion. Ubp14

degrades free ubiquitin chains in the cell [125]. Since free ubiquitin chains inhibit the

proteasome, *UBP14* deletion causes an accumulation of free ubiquitin chains and

impairs degradation of proteasomal substrates. As predicted by our model, deletion

of *UBP14* reduced the doubling time of *ubp10Δ* mutants to a near wild type level.

This result suggests that Ubp14 and Ubp6 act similarly to promote degradation of

UPS substrate in vivo. Moreover, it highlights the importance of maintaining the

appropriate balance of DUB activities in the cell, since deletion of either *UBP6* or

UBP14 can counteract the negative effects of losing Ubp10.
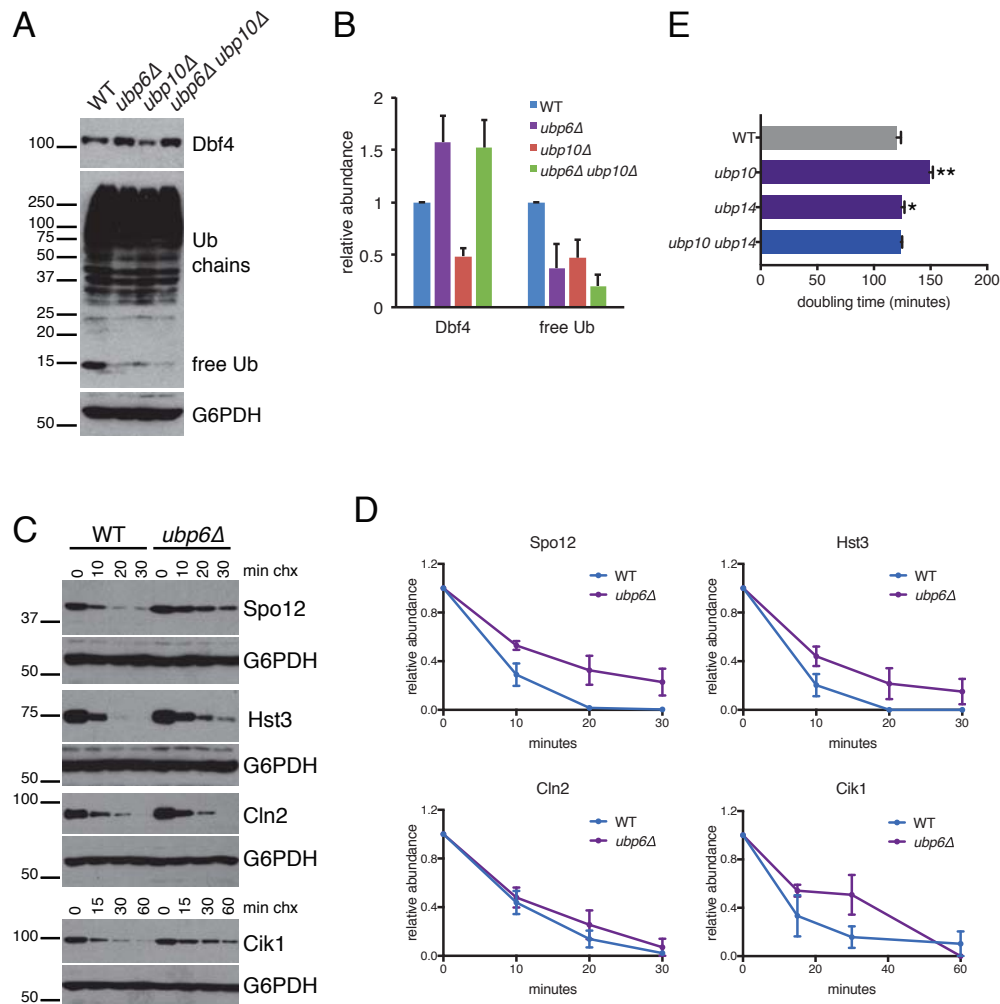
**Figure 2.13. Deletion of DUBs that promote proteasome function rescue
ubp10Δ phenotypes.** (A) Representative Western blot of Dbf4-TAP and ubiquitin in
asynchronous cells. G6PDH is shown as a loading control. (B) Quantitation of
Western blots in part (A). Dbf4-TAP and free ubiquitin levels were normalized to
G6PDH. Shown is an average of n=3 experiments, error bars represent standard
deviation. (C) Cycloheximide-chase assay of TAP-tagged UPS targets in wild type
(WT) and *ubp10Δ* cells as indicated. TAP and G6PDH blots are shown. (D)
Quantitation of cycloheximide-chase assays from (C). Shown is an average of n=3
experiments, error bars represent standard error of the mean. (E) Doubling time of
strains with deletions in the indicated DUBs. Shown is the average of n=4 replicates,
error bars represent standard deviation. Asterisks indicate strains that are
significantly different from wild type (WT) as measured by one-way ANOVA
(*$p<0.05$, **$p<0.005$).

Conclusions

Identifying the functions and substrates of DUBs has been challenging because the mechanisms by which most DUBs select and interact with their targets is not well understood. In yeast, single and double DUB deletion mutants display very minor phenotypes [23, 118] and only modest changes in their proteome in normal growth conditions [40]. Moreover, many DUBs are capable of deubiquitinating the same model substrates in vitro [27]. These findings all suggest that there is redundancy among the 21 DUBs in yeast. Here, we explored this possibility using both overexpression and deletion approaches. Our overexpression screen enabled us to identify proteasomal substrates that can be targeted by each DUB, even if redundancies exist. The data from the screen shows that more than half (12 of 21) of yeast DUBs are capable of upregulating expression of one or more UPS targets in the cell. Notably, each of these 12 DUBs upregulated a different subset of the 37 proteasomal substrates that were screened, demonstrating these DUBs exhibit specificity towards their targets in vivo.

In total, eight of 20 DUBs did not upregulate of any of the 37 UPS targets in our screen. This result was expected since several DUBs are known to regulate non-proteasomal functions of ubiquitin. For instance, Ubp8 is a component of the SAGA complex and removes monoubiquitin from histone H2B [105]. In addition, Ubp16 is a membrane protein that associates with mitochondria [109]. Another reason a DUB may not have regulated any UPS targets is if it needs to associate with other proteins to function. For example, Rpn11 is only active when it is incorporated into the proteasome [126], and therefore proteins regulated by Rpn11 may not have

been identified in our screen if the overexpressed protein is not proteasome-bound. Although we cannot draw conclusions about the specificity of the eight DUBs that did not upregulate any proteins in the screen, for each of the DUBs that did upregulate a subset of proteasomal targets we can conclude that they are active upon overexpression. In addition, these DUBs must display substrate specificity, since no two DUBs upregulated the same set of proteins.

In addition to the 20 yeast DUBs that fall into well-characterized DUB families, a recent study identified two additional yeast proteins belonging to a newly-discovered DUB family that exhibits specificity for K48-liked ubiquitin chains [24]. We tested one of these proteins, Miy1, in our screen but found it did not alter expression of any of the UPS targets tested. The homologous enzyme Miy2 was not screened since it does not display any activity towards ubiquitin chains in vitro [24].

Our data shows that many DUBs can recognize specific substrates in vivo, however we cannot rule out the possibility that some of the DUB-target interactions we identified do not normally occur when the DUB is expressed at endogenous levels. The best way to confirm that a candidate target is an endogenous substrate of a particular DUB is to show that the target is also less stable when that same DUB is deleted. However, in some instances we did not observe target destabilization in DUB delete cells (Figure 2.9E-F). There could be several reasons for this result. One possibility is that there is redundancy and that more than one DUB may need to be deleted for a target to be destabilized. Alternatively, the DUB in question may not be active during the context of an unperturbed cell cycle. 18 of 21 DUBs have been found to be phosphorylated in proteome-wide screens [127-129], which suggests

that their activities are subject to regulation. If future studies identify particular environmental conditions or states when specific DUBs are active, it will be interesting to reexamine many of these substrates to determine if they are regulated by those DUBs in those contexts. Although we cannot rule out that overexpression may drive interactions with some substrates in our screen, we have shown that one candidate target of Ubp10, Dbf4, is less stable in *ubp10Δ* cells (Figure 2.9E-F) and that the established protein interaction domain of Ubp10 and its catalytic activity contribute to Dbf4 stabilization by Ubp10 (Figure 2.7B-C). Therefore, many candidate targets identified here are likely to be endogenous substrates of the identified DUBs in some context.

Our dataset also identified DUBs with potential cell cycle-regulatory roles. Among the DUBs that regulated several targets in our screen, Yuh1 is a good candidate to regulate the cell cycle since it is required for Rub1-modification of the SCF subunit Cdc53 [130]. However, we and others have found that *yuh1Δ* cells proliferate as well as wild type cells (Figure 2.12A, [123]). This suggests that another enzyme can compensate for Yuh1 loss, or that blocking Rub1 modification of Cdc53 does not impair SCF activity enough to impact the cell cycle.

The DUB that had the greatest effect on the cell cycle was Ubp10. Notably, both overexpression and deletion of Ubp10 resulted in delays in different phases of the cell cycle. Previous studies have linked Ubp10 to regulation of diverse cellular processes through removal of both monoubiquitin and polyubiquitin chains. Ubp10 regulates non-proteasomal roles of ubiquitin by removing monoubiquitin from both PCNA and histone H2B [87, 131]. This role in H2B deubiquitination is partially

redundant with Ubp8 and regulates telomeric silencing [106, 115]. Ubp10 can also impact protein stability by removing polyubiquitin chains from proteasomal substrates. For example, Ubp10 deubiquitinates and stabilizes the largest subunit of RNA Polymerase I, Rpa190 [97]. Stabilization of Rpa190 by Ubp10 is critical for maximal rRNA synthesis and ribosome biogenesis.

Our data suggests that Ubp10 also controls the stabilities of many cell cycle proteins and regulates the timing of the G1/S transition (Figures 2.7, 2.9). Although our results suggest that stabilization of Dbf4 by Ubp10 contributes to proper S-phase timing (Figure 2.11), other functions of Ubp10 must also be involved. This delay does not appear to be the result of reduced Rpa190 expression (Figure 2.10), and it is also unlikely that other established Ubp10 targets are involved in this delay. The silencing defect resulting from increased H2B ubiquitination is not expected to affect the cell cycle, since other mutations that cause silencing defects do not alter cell cycle distribution [97]. Regulation of PCNA by Ubp10 is also unlikely to impact the cell cycle, since PCNA is not ubiquitinated during an unperturbed S phase in budding yeast, and it is only regulated by Ubp10 following exposure to DNA damage [87]. Additional Ubp10 substrates that control S-phase entry may be substrates that we have not yet identified. However, a more likely possibility is that the coordinate misregulation of several proteins in *ubp10Δ* cells results in the G1/S delay.

With the exception of Ubp10, no cell cycle changes were observed upon overexpression of any additional DUBs, and previous studies suggest DUB deletion strains proliferate at rates similar to wild type [23, 40]. For this reason, we attempted to uncover additional redundancies in the network by carrying out a comprehensive

genetic analysis of the 5 DUBs that our screen implicated in cell cycle regulation. The expectation was that if more than one of these DUBs redundantly regulates a critical cell cycle protein, combinations of those deletions might be lethal or slow proliferation. Remarkably, no strong negative genetic interactions were identified among these five DUBs, and even the *ubp5Δ ubp6Δ ubp7Δ ubp10Δ yuh1Δ* strain proliferated nearly as well as a wild type strain. It is possible that strains with combinations of DUB deletions have fitness defects in alternate environmental states, which will be of interest to examine in the future. Such studies may uncover context dependent redundancies between DUBs.

The surprising finding that our genetic analysis uncovered was that deletion of *UBP6* rescued the proliferation defect and cell cycle delay in *ubp10Δ* cells (Figure 2.12A-C). *UBP6* deletion also restored the stabilities of Ubp10 targets Dbf4 and Rpa190 in the absence of Ubp10 (Figure 2.13D-E). This rescue is most likely an indirect effect that is a result of the central role of Ubp6 in regulating proteasomal function. Ubp6 associates with the proteasome base and removes ubiquitin chains from substrates before they are translocated into the proteasomal channel [95, 121, 132]. Our results suggest that this deubiquitination by Ubp6 is important for efficient degradation of Ubp10 substrates, since they are stabilized its absence. This is a surprising result since previous studies suggest that cells lacking Ubp6 have increased proteasomal activity [120, 121]. However, not all studies agree [122] and we find that several endogenous UPS substrates are stabilized in the absence of Ubp6 (Figure 2.13C-D). Moreover, deletion of a second DUB that promotes proteasome function (Ubp14) also reversed the proliferation defect in *ubp10Δ* cells.

Together these findings suggest Ubp6 is normally required for efficient degradation of many UPS substrates.

The mechanism by which Ubp6 promotes degradation of proteasomal substrates is unclear. One possibility is that deletion of *UBP6* reduces the amount of free ubiquitin in the cell, limiting the amount of ubiquitin available for substrate degradation. However, *ubp10Δ* cells also have reduced free ubiquitin (Figure 2.13A), and Dbf4 and Rpa190 degradation is accelerated in these cells (Figure 2.12D-E), which suggests that ubiquitin levels are not limiting for their degradation. Moreover, not all proteasomal substrates are stabilized in *ubp6Δ* cells (Figure 2.13C-D). Therefore, Ubp6 does not affect all proteasomal substrates equally. A recent report found that Ubp6 (and the human homolog Usp14) only deubiquitinates substrates that have more than one ubiquitin chain [133], raising the possibility the Ubp6 only deubiquitinates substrates with particular ubiquitin chain configurations. In the future it will be of interest to elucidate how Ubp6 affects degradation of some substrates and not others. These experiments will also shed light on the cellular consequences of disrupting the balance of DUB activities.

Materials and Methods

Yeast strains and plasmids

All yeast strains are in the S288c background and were grown in rich (YM-1) or synthetic (C) medium at 30°C [134]. Strains from the TAP-tag collection were used for the DUB overexpression screen [111]. To generate the panel of DUB deletion strains used in Figure 6, DUB genes were deleted using standard methods [135]. Subsequently, a *ubp5Δ ubp6Δ ubp7Δ yuh1Δ* strain (YJB673) was crossed to a *ubp10Δ* strain (YCM313) and all possible combinations of genotypes were recovered. A complete list of strains is in Supplemental Table S2 [112].

DUB overexpression plasmids were obtained from the GST-tagged collection [99] and sequenced to verify the correct insert. Any GST-DUB plasmids that contained an incorrect sequence were reconstructed by cloning the gene from genomic DNA into the similar *URA3*-marked plasmid pYES2-GST [136]. Previously described *UBP10* mutant genes [97] were also cloned into pYES2-GST. *RPA190-GFP* and *DBF4-TAP* sequences, along with their respective promoters, were amplified from genomic DNA from GFP [137] and TAP-tag strains respectively and cloned into pRS426. A complete list of plasmids is in Supplemental Table S3 [112].

DUB overexpression screen

GST-DUB overexpression plasmids were transformed into 37 TAP-tag strains expressing the tagged target proteins of interest. For the screen, strains were grown to mid-log phase in C medium lacking uracil (C-Ura) containing 2% raffinose in deep-well 96-well plates. To induce overexpression of DUBs, galactose was added

to the medium at a final concentration of 2% and cells were incubated for four hours at 30°C. Cells were pelleted in 96-well plates, lysed by TCA lysis, and Western blots performed (as described below). For each test DUB, the control (Ubp2) was induced in a matched set of strains and lysed side by side. All DUBs were screened twice. Multiple exposures of all Western blots were collected. Quantification was performed using ImageStudioLite software (Li-Cor Biosciences) on the lightest exposure in which a given protein was detected in both control and DUB samples. All TAP-signals were normalized to the loading control G6PDH and log2 fold change values were calculated. Any protein that could not be detected in one or both samples in a given experiment was not included in the dataset, since it was not possible to calculate an accurate fold change value. Proteins were considered up- or downregulated if levels changed at least 2-fold in both replicates of the screen. All fold change values are reported in Supplemental Data S2 [112].

Western blotting

For the DUB screen and all experiments except for those in Figure 4, equivalent optical densities of cells were collected and lysed using a previously described TCA lysis protocol [138]. For experiments in Figure 4, cells were lysed by bead beating in sample buffer [73]. Western blotting was performed with antibodies against TAP (CAB1001, ThermoFisher), GST (clone 4C10, BioLegend), ubiquitin (clone P4D1), GFP (clone JL8, Clontech), Cdc28 (sc-6709, Santa Cruz Biotechnology), and G6PDH (A9521, Sigma). Where indicated, Western blots were normalized using ImageStudioLite software, as described above.

Flow cytometry

Cells were fixed in 70% ethanol and stained with Sytox green (Invitrogen) as previously described [73]. Data was collected on a Becton Dickinson FACS Calibur or a Millipore Guava easyCyte HT. Data was analyzed using Flow-Jo software (FlowJo, LLC). In arrest-release experiments, S-phase progression was calculated from the mean DNA content of the population, as previously described [139].

Cycloheximide-chase assays

Cells were grown to mid-log phase and $50\mu g/ml$ cycloheximide was added to inhibit protein synthesis. Samples were collected at the indicated time points and analyzed by Western blotting.

Doubling time assays

To calculate doubling times of DUB deletion strains, saturated overnight cultures were diluted to an optical density of 0.2 in rich medium containing 2% dextrose in 96-well plates. Population growth was monitored using a Tecan Infinite PRO microplate reader at $30°C$ with continuous shaking, measuring the optical densities every 20 minutes. Doubling times were calculated using GraphPad prism software. For each genotype the doubling times of 2-6 independently derived strains were measured and statistical significance calculated using one-way ANOVA. All data are included in Supplemental Table S1 [112].

Serial dilution assays

Five-fold dilutions of strains with the indicated genotypes were plated on C-Ura plates containing 2% dextrose. Plates were imaged after 24 to 72 hours of incubation.

Chapter III: Investigation of Hof1 regulation by

Ubp5 and Ubp7

Introduction

Once cells have successfully replicated and segregated their DNA they must undergo the process of cytokinesis, which is the division of cellular contents to create two separate daughter cells. In budding yeast and many other eukaryotes cytokinesis is coordinated with completion of mitosis through the formation of a contractile ring containing actin and myosin (actomyosin). This actomyosin ring forms perpendicular to and around the central spindle during anaphase [1]. It attaches to the inside of the cell membrane at the site of division and cinches closed, allowing for the deposition of new cell wall and membrane [1]. A group of about 20 proteins conserved from yeast to humans regulates this process, which when not completed properly can result in defective cell division, which can contribute to cellular transformation [1, 140].

One of the proteins involved in regulation of cytokinesis in yeast is Hof1, which accumulates at the division site, or mother-bud neck, during G2/M to stabilize the actomyocin ring. Between mitotic exit and G1, Hof1 levels are reduced to allow for ring contraction and cell separation [37, 141]. This is accomplished by SCF^{Grr1}, an E3 complex containing the F-box protein Grr1 that specifically recognizes and ubiquitinates substrates such as Hof1. In Chapter II we identified Hof1 as a protein stabilized by the overexpression of Ubp5, Ubp7, and Ubp10, suggesting it may be a substrate of these DUBs. Previous work shows Hof1 and its F-box protein Grr1 localize to the mother-bud neck [37]. Ubp5 also accumulates at this location [102], suggesting these proteins may exist in a complex. We hypothesized Ubp5 stabilizes Hof1 by interacting with it either directly or by forming a complex with SCF^{Grr1} (Figure

3.1). To test this hypothesis, I performed assays to determine if Ubp5 could interact with Hof1 and Grr1 individually.

One challenge facing the identification of DUB-substrate pairs is the weak or transient nature of these interactions. BiFC allows visualization of interactions in living cells with greater success than with traditional methods such as yeast-2-hybrid or co-immunoprecipitation [35, 36]. Constructs containing proteins of interest fused to two halves of a fluorescent protein (which individually are non-fluorescent) are expressed in cells. When proteins of interest interact directly or are in close proximity in a complex the fluorescent protein is reconstituted and irreversibly stabilizes the protein-protein interaction (PPI), allowing PPIs to be easily visualized and quantified. This technique has recently been used in the systematic analysis of protein interactomes [36] and more relevantly in the validation of the cytokinesis regulator Hof1 as an SCF^{Grr1} substrate [37]. In this study we used bimolecular fluorescence complementation (BiFC) to try and capture a potentially weak DUB-substrate interaction between Ubp5 and Hof1.

Interestingly, Ubp5 and Ubp7 are among three budding yeast DUBs (Ubp4/Doa4, Ubp5, and Ubp7) that contain a rhodanese homology domain (Rhod) (Table 2.1). Rhodanese is a mitochondrial enzyme that converts cyanide to thiocyanate, but the Rhod in these DUBs has no catalytic activity and no known function in yeast [142]. It is also worth noting that neither of the Ubp5 or Ubp7 paralogs, Ubp4/Doa4 and Ubp11, have shown any regulation of Hof1. Although Ubp4/Doa4 and Ubp5 are paralogs, the former is localized to late endosomes/MVB (multivesicular body), they interact with distinct sets of proteins, and their Rhod differ

in sequence [143]. In addition, fusion of the Ubp4/Doa4 late endosomal localization sequence to Ubp5 redirects Ubp5 to endosomes, but it is not sufficient to rescue a *ubp4Δ* phenotype [143], suggesting each DUB's Rhod or other domains may be important for substrate recognition. It is possible that Ubp5 and Ubp7 could have redundant functions because they are both cytoplasmic DUBs and contain similar Rhod, so I tested for redundant regulation of Hof1 in a *ubp5Δ ubp7Δ* mutant.
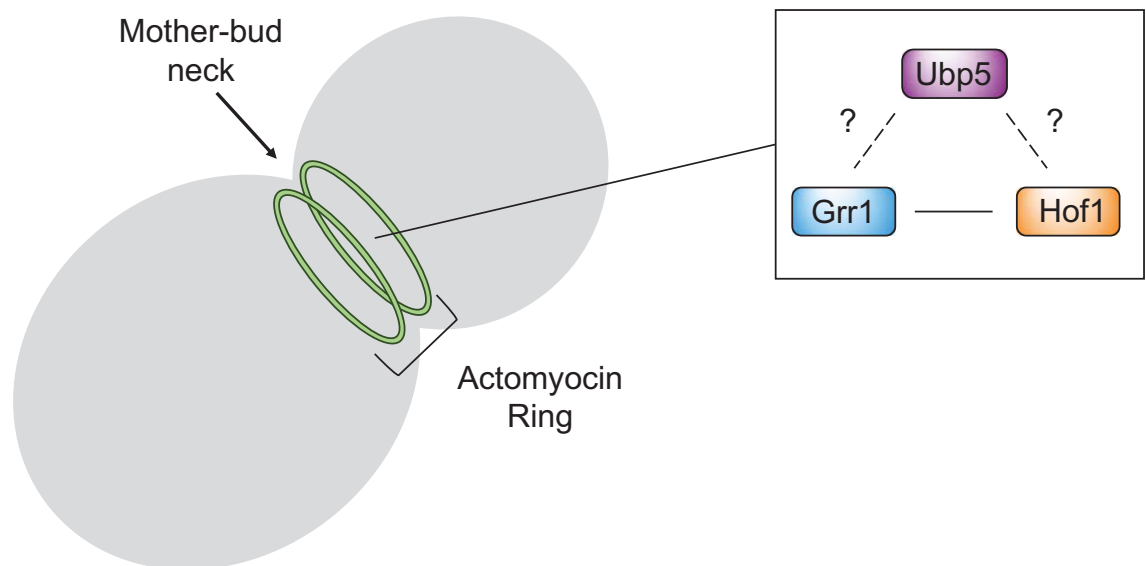
Figure 3.1. A model for Ubp5-Hof1 interaction. During mitosis an actomyosin ring forms at the mother-bud neck site to facilitate cytokinesis. Hof1 localizes to the ring to stabilize this structure until mitotic exit. Grr1 has been found to co-localize with Hof1 at the mother-bud neck but it is not known if these three proteins interact in a complex.

Results

We showed in Chapter II that Ubp5 overexpression stabilizes Hof1. To detect

and visualize an interaction between Ubp5 and Hof1 I employed a BiFC system in

which I fused N-terminal (VEN1) and C-terminal (VEN2) truncations of the Venus

fluorescent protein (VFP) to proteins of interest and expressed different pairs of

fusion proteins to detect PPIs within the putative DUB-substrate or DUB-F-box

interactions [144]. I treated cells with the microtubule depolymerizing drug

nocodazole for three hours to arrest cells in mitosis when Hof1 and Grr1 are

localized at the mother-bud neck, and I collected microscopy images (Figure 3.2). I

measured the interactions of Grr1 and Hof1, Ubp5 and Hof1, Ubp5 and Grr1, and

Ubp2 and Hof1 by quantifying the percentage of large budded cells with BiFC signal

at the bud neck – an indication that the two fusion proteins were interacting. The

established interaction between Grr1 and Hof1 served as a positive control, while a

strain expressing no fusions and a strain expressing Ubp2 and Hof1 fusions served

as negative controls. Because Ubp2 is a cytoplasmic DUB but it did not regulate

Hof1 in our screen we did not expect an interaction between Ubp2 and Hof1. In fact,

we did not observe an interaction between Ubp2 and Hof1, making it a useful control

for our experiments.
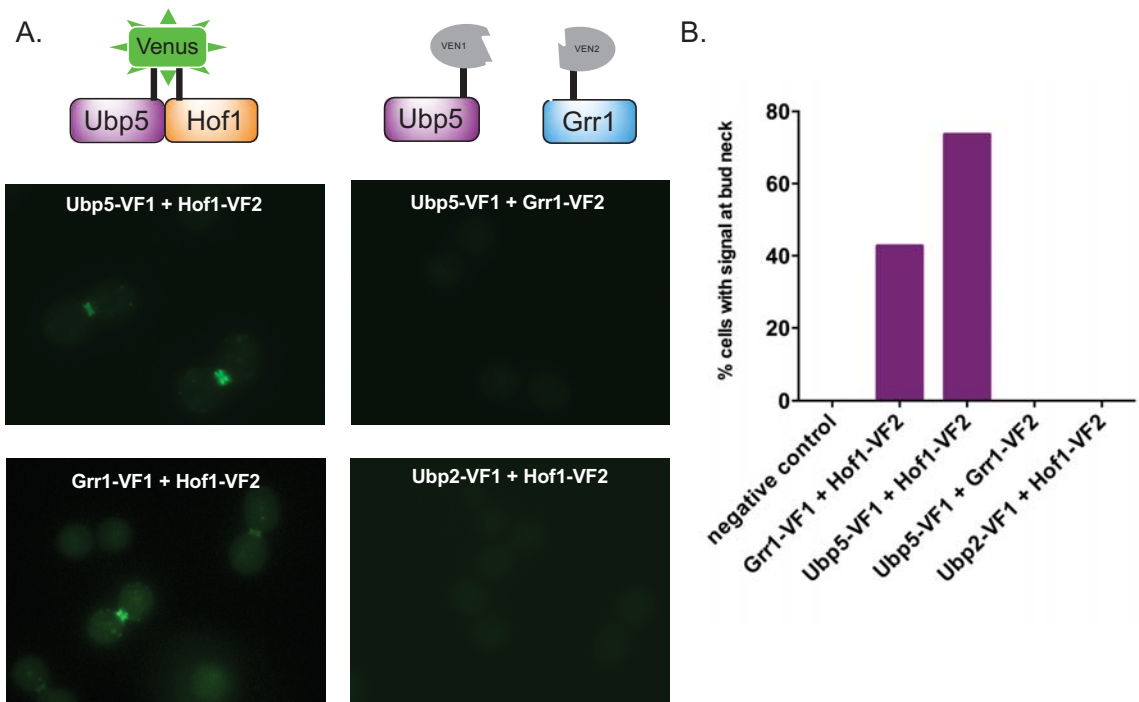
Figure 3.2. Ubp5 and Hof1 interact in vivo. Cells expressing each of the indicated pairs of fusion proteins were treated with nocodazole for 3 hours before being imaged. **(A)** Representative images of cells expressing combinations of fusion proteins as indicated. **(B)** A minimum of 100 cells were counted for each strain in one experiment and the percentage of cells with Venus signal at the bud neck was quantified.

As previously demonstrated, Grr1 and Hof1 interact at the bud neck [37]. Although this did not occur in 100% of cells, we did observe it in 40%. This positive interaction assured us that this system was working in our hands. I also detected an interaction between Ubp5 and Hof1 in approximately 70% of cells. While interaction of these two proteins with Hof1 supports our hypothesis for complex formation, it is not possible to determine if an interaction is direct or indirect by BiFC because fluorophore reconstitution occurs as long as fusion proteins are within 10nm of one another. While this work was ongoing another report was published that showed

Hof1 is required for Ubp5 localization to the bud neck [143], which lends more evidence for an interaction between Ubp5 and this Hof1.

Surprisingly, I found that Ubp5 and Grr1 do not interact, suggesting either the topology of the interaction does not allow BiFC to work or Ubp5 may interact with Grr1 indirectly (Figure 3.4, right). The negative BiFC result between Ubp5 and Grr1 cannot be interpreted as lack of complex formation, so I used a genetic approach to test whether Grr1 was required for this interaction. I performed the same BiFC analysis in *grr1Δ* cells and surprisingly the loss of *GRR1* inhibited the Ubp5-Hof1 interaction (Figure 3.3). These data suggest that either Grr1's physical presence or it's ubiquitination of Hof1 is required for Ubp5 to interact with Hof1.
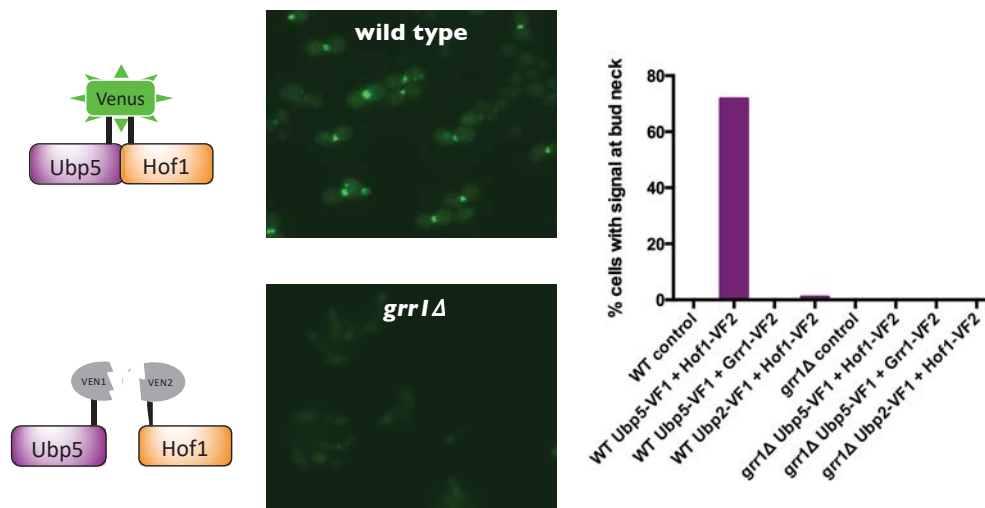
Figure 3.3. The Ubp5-Hof1 interaction is dependent on the F-box protein Grr1. Cells expressing each of the indicated pairs of fusion proteins were treated with nocodazole for 3 hours before being imaged. **(A)** Representative images of cells expressing Ubp5 and Hof1 fusion proteins in wild type (WT) and *grr1Δ* cells. **(B)** A minimum of 100 cells were counted for each strain in one experiment and the percentage of cells with Venus signal at the bud neck was quantified.

Indirect Interaction   Direct Interaction
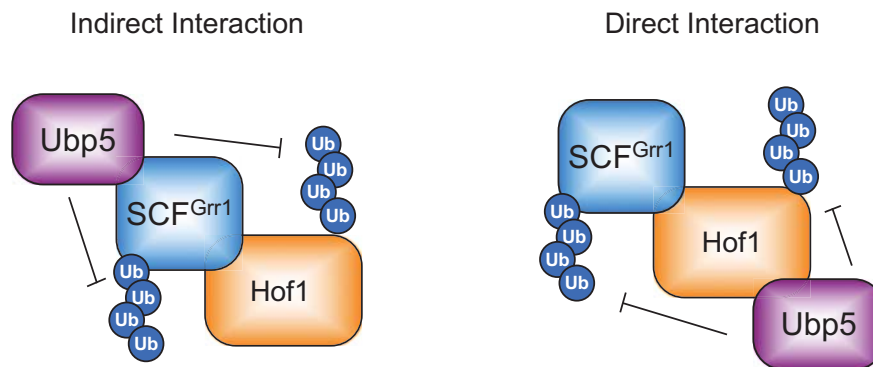
Figure 3.4. Models of Ubp5-Hof1 interaction. Some DUBs have been found to target substrates through interaction with, and/or regulation of, E3 components (left). Lack of a Ubp5-Grr1 interaction shown in Figure 3.2 suggests an alternative interaction model in which Hof1 is recognized by the Ubp5 independently of Grr1. However, data from Figure 3.3 in which the Ubp5-Hof1 interaction is disrupted in a Grr1 deletion strain suggests that for this interaction to occur in wild type cells Grr1's presence or ubiquitination function may be required.

Evidence shows Ubp5 and Hof1 interact at the mother-bud neck, so I wanted to determine if Hof1 is an endogenous substrate of Ubp5. I expressed Hof1-GFP and mCherry-TUB1 from their endogenous promoters in wild type and *ubp5Δ* cells. Using fluorescently-tagged tubulin as a marker for anaphase I was able to discern the difference between metaphase and anaphase cells, and I found the numbers of both Hof1-positive metaphase and anaphase cells to be 8-10% lower in *ubp5Δ* cells than in the wild type strain (Figure 3.5). However, this is not a convincing difference in Hof1 protein levels, so I next tested Ubp5 regulation of Hof1 by examining Hof1 stability in DUB deletion strains.
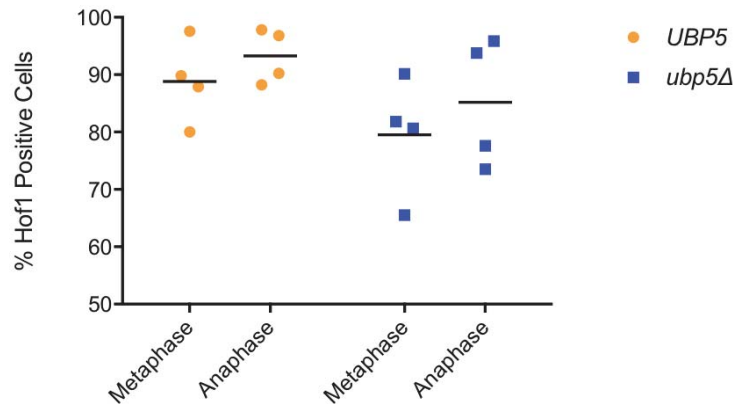
Figure 3.5. Hof1-GFP is less abundant at the bud neck in large-budded *ubp5Δ* cells than in wild type cells. Cells expressing endogenous HOF1-GFP and mCherry-TUB1 were grown to log phase in YM-1. Fluorescence images were collected and overlayed with bright field images. Fluorescently-tagged tubulin was used as a marker to distinguish metaphase (large budded with a short spindle) and anaphase (large budded with a long spindle) cells. For each experiment a minimum of 100 *UBP5* cells and 100 *ubp5Δ* cells were counted. The percentage of Hof1-positive cells four experiments are shown as data points and the median percentages from all four experiments are indicated.

Overexpression of both Ubp5 and Ubp7 stabilized Hof1, although to different degrees (Figure 2.6), so to determine if these DUBs regulate Hof1 we asked if Hof1 protein is less stable when these DUBs are deleted. I did not observe a significant difference in Hof1 stability in the single mutants (Figure 3.6). Because Ubp5 and Ubp7 contain similar Rhod it is possible that this domain plays a role in substrate specificity and they can compensate for one another, so I tested Hof1 half-life in a *ubp5Δ ubp7Δ* strain. The double DUB deletion strain also did not display a significant difference in Hof1 stability (Figure 3.6), and this could be due to other DUBs in yeast that can redundantly target Hof1.
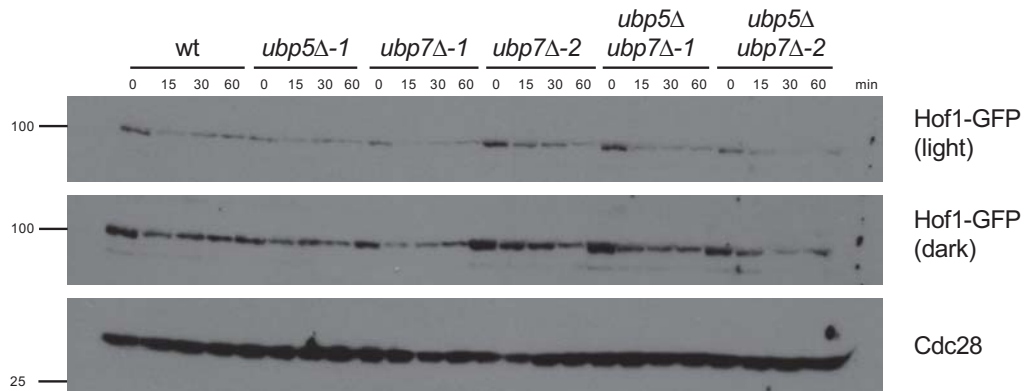
Figure 3.6. Deletion of *UBP5* and/or *UBP7* does not affect Hof1 stability. Cycloheximide-chase assays were conducted in asynchronous cells. Cells were grown to log phase, cycloheximide was added, and samples were collected as indicated. Western blots were performed for GFP-tagged Hof1 and Cdc28 (loading control). Light and dark exposures of the anti-GFP blot are shown. Strain numbers indicate different isolates. WT: wild type.

Because the Ubp5 and Hof1 appear to interact in mitotic cells I performed Western blots on nocodazole-treated cells to test if we could detect a difference in Hof1 steady-state protein levels. I expressed Hof1-GFP in the wild type, single DUB deletion strains, and a double DUB deletion strain in a set of asynchronous and nocodazole-treated cells and performed a Western blot for Hof1. I found no change in Hof1 protein among the different mutants in either nocodazole-treated cells, in which Hof1 is highly expressed, or wild type, in which Hof1 is degraded by SCF[Grr1] and not expected to be visible (Figure 3.7). Although our data show Hof1 interacts with Ubp5 at the mother-bud neck during mitosis it is possible the reason we do not observe regulation of Hof1 by Ubp5 is because another DUB can compensate for

loss of Ubp5 function. Because we could not find evidence that Hof1 is misregulated

in the *UBP5* deletion we decided not to pursue this interaction further.
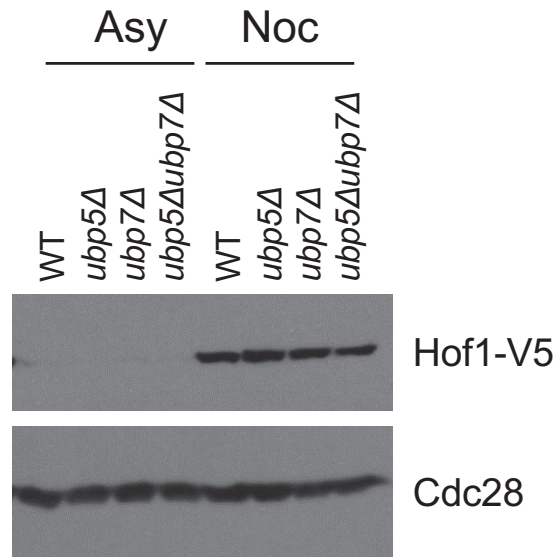
Figure 3.7. Deletion of *UBP5* and *UBP7* does not affect Hof1 levels during mitosis. Cells were grown to mid-log phase and either treated with no drug or treated with nocodazole for 3 hours before samples were collected. Western blots performed for Hof1 and Cdc28 (loading control).

Conclusions

From these data we confirmed previous reports that Hof1 accumulates at the mother-bud neck and that Grr1 and Hof1 interact in vivo by BiFC [37, 102]. Although this is an established interaction, we did not see it in 100% of mitotic cells. We found this was due to plasmid loss revealed by colony forming unit analysis. We also identified a novel interaction between Ubp5 and Hof1 – a UPS target that we show in a screen for DUB substrates is stabilized upon overexpression of Ubp5 (Figure 2.6). We measured the Ubp5-Hof1 interaction to be present in more cells than the Grr1-Hof1 interaction - 70% vs 40% of mitotic cells. This difference could be attributed to the timing of Hof1's interaction with each protein. It is likely that since the above microscopy was performed in cells during metaphase-anaphase – when Hof1 is required for actomyosin stabilization and when we posit Ubp5 could function to stabilize it, that we would see more of the Hof1-Ubp5 interaction. It is possible that if the same BiFC experiments were performed upon mitotic exit – when Grr1 marks Hof1 for degradation, we could detect more of the interaction between Grr1 and Hof1.

At the same time this work was conducted, another group reported that Ubp5's mother-bud neck localization is dependent upon Hof1's localization [143]. Their finding lends evidence to our conclusion that Ubp5 may regulate Hof1 in vivo. The cellular factors required for this interaction are still poorly understood, but my data demonstrate that the Ubp5-Hof1 interaction is dependent upon Grr1, as it is disrupted in grr1Δ cells. Even though we could not detect an interaction between

Grr1 and Ubp5 it is possible that Ubp5 recognizes Hof1 only when it has been ubiquitinated, which may or may not require Grr1 to be present.

Our observation that Grr1 (either its presence or E3 function) is required for Ubp5 and Hof1 to interact in vivo could be tested by using an F-box protein mutant of Grr1 that interrupts Grr1's interaction with the rest of the SCF complex. If this does not block the Ubp5-Hof1 interaction then it suggests it is simply Grr1's binding to Hof1 that is required and not Grr1's ubiquitination activity. If this is the case, Grr1 binding to Hof1 may induce a conformational shift that presents Hof1 as a better binding partner for Ubp5. However, if the F-box mutant inhibits the Ubp5 and Hof1 interaction, then it would not be possible to tell if either Grr1 binding or Grr1's ubiquitination of Hof1 is required. To test if Grr1's ubiquitination activity is responsible for promoting the Ubp5-Hof1 interaction, one could measure binding of Ubp5 to a lysineless Hof1 (lysines have been mutated so that it cannot be ubiquitinated). In this experiment Grr1 can still bind to its substrate but cannot transfer ubiquitin chains, so if this Hof1 mutant prevents interaction with Hof1 then it can be concluded that ubiquitination of Hof1 is necessary for Ubp5 binding.

From our interaction data and previously published work we can generate a model for the Ubp5-Hof1 interaction: Grr1 and Hof1 localize at the mother-bud neck where Grr1 can ubiquitinate Hof1 for degradation, but Ubp5 protects Hof1 from degradation by Grr1 until mitosis is complete, at which point Hof1 is degraded so that cytokinesis can proceed. However, more analysis was required to test if Hof1 was in fact regulated by Ubp5. I conducted experiments to quantify the abundance of Hof1 in ubp5Δ cells compared to the wild type, but found an insignificant change

in the number of mitotic cells in which Hof1 accumulated at the mother-bud neck

(Figure 3.5). I showed overexpression of Ubp5 and Ubp7 can stabilize Hof1, but I

was unable to show destabilization of Hof1 in cells deleted for UBP5 and/or UBP7

(Figure 3.6). These results, however, do not prove Ubp5 does not regulate Hof1;

other studies have reported individual DUB deletion strains display minor

phenotypes [22, 40, 41], so it is possible another DUB compensates for loss of Ubp5

by redundantly targeting Hof1.

Materials and Methods

Plasmid construction for Bimolecular Fluorescence Complementation

Proteins of interest were PCR-amplified from yeast genomic DNA and subcloned into multiple cloning sites of p413-L-VF[1] and p415-L-VF[2] [144].

Bimolecular Fluorescence Complementation

Wild type S288c yeast were transformed with pairs of plasmids depending on the interaction being tested. Cells were grown to log phase synthetic media lacking histidine and leucine, treated with nocodazole for 3 hours to capture cells in mitosis, and then imaged on a Nikon Eclipse E400 using a GFP filter cube. For each experiment, images were loaded into ImageJ, a minimum of 100 cells were counted from all images of a given strain, and a percentage of Venus-positive cells was calculated.

Hof1 microscopy in mitotic cells

Cells were grown to mid-log phase in YM-1 media containing dextrose (YPD) and nocodazole was added for 3 hours to capture cells in mitosis. Cells were then imaged on a Nikon Eclipse E400 using GFP, DAPI, and Texas Red filter cubes. mCherry-Tub1 was used to qualify the mitotic stage of each cell. For each experiment, images were loaded into ImageJ, a minimum of 100 cells were counted from all images of a given strain, and a percentage of Venus-positive cells was calculated.

Cycloheximide-chase assays

Cells were grown to mid-log phase and 50μg/ml cycloheximide was added to block protein synthesis. Equivalent ODs of cells were collected at 0, 15, 30, and 60 minutes after addition of cycloheximide and Western blots were performed.

Nocodazole arrest experiments

Cells were grown to mid-log phase in YPD and where indicated nocodazole (3 hours) was added to arrest cells. Cells were collected, washed with media, and released into YPD. Equivalent ODs of cells were collected and Western blots were performed.

Western blotting

Equivalent optical densities of cells were collected at the indicated time points, lysed as previously described [73], and Western blots were performed with antibodies for GFP (clone JL8, Clontech), V5 (Invitrogen), and Cdc28 (sc-6709, Santa Cruz Biotechnology).

Chapter IV: Temperature and drug sensitivity profiling of DUB deletion strains

Introduction

Many studies have reported little to no effect on viability or proliferation in DUB deletion strains [22, 145]. However, because 5 DUBs from our overexpression screen (Ubp5, Ubp6, Ubp7, Ubp10, and Yuh1) regulated so many cell cycle proteins (Figure 2.3), we thought that they might be redundant for essential cellular functions. Aside from strains containing both *ubp6Δ* and *ubp10Δ*, we observed *ubp10Δ* strains displayed significantly slower doubling time compared to wild type cells. However, no other DUB, alone or in combination, slowed proliferation, suggesting these DUBs are not redundant (Figure 2.12). We postulated that existing redundancies may not be evident under standard growth conditions but may be revealed under different stressors. To test for condition-specific genetic interactions among these DUBs I performed serial dilution assays with a panel of 32 strains that included all possible combinations of deletions in five DUBs (Table 4.1) under multiple conditions: elevated temperature, the microtubule destabilizing drug benomyl, and the replication inhibitor hydroxyurea (HU). The sensitivities of some of these individual DUB deletion strains have previously been evaluated. On benomyl plates, strains deleted for *UBP6* and *UBP10* are hyper-resistant while *ubp7Δ* displays sensitivity [146]. When grown on hydroxyurea plates, *ubp6Δ, ubp7Δ* strains are sensitive [147] [89]. However, the sensitivities of combinations of these DUBs to these stressors had not yet been tested.

Results

To determine if DUB deletions display temperature sensitivity I spotted cells onto rich media and incubated the plates at three temperatures: 23°C, 30°C, and 37°C (Figure 4.1). In Chapter II, I showed that unstressed DUB deletion strains do not display delayed doubling time with the exception of strains lacking *UBP10*, which are rescued by *ubp6Δ* (Figure 2.12). This was corroborated by slower growth and smaller colony size in the *ubp10Δ* mutant and wild type-like growth in *ubp6Δ ubp10Δ* mutant on YPD plates grown at 30°C (Figure 4.1, compare E1 to D2). I anticipated that loss of multiple cell cycle-regulatory DUBs might impair growth at non-optimal temperatures. On the contrary, no strains other than those containing *ubp10Δ UBP6* showed a growth defect at any temperature (Figure 4.1).

I next tested if DUB deletion strains were sensitive to the microtubule-destabilizing drug benomyl (Figure 4.2). Loss of *UBP7* has been shown to sensitize cells to benomyl while loss of *UBP6* or *UBP10* makes cells resistant [146]. I observed that *ubp6Δ* cells grew better than wild type in the presence of benomyl, confirming they are resistant (Figure 4.2, compare A1 to C1). Although *ubp10Δ* cells grew slower than wild type in the absence of benomyl, they grew as well as wild type on benomyl plates, confirming the previous finding that deletion of *UBP10* also confers resistance. In contrast, *ubp7Δ* cells grew as well as wild type both in the absence and presence of benomyl, suggesting they do not display the reported sensitivity (Figure 4.2, compare A1 to D1) [146]. Interestingly, *ubp6Δ* and *ubp10Δ* in any DUB deletion combination leads to enhanced growth on benomyl (Figure 4.2). This suggests misregulation of the proteasome or Ubp10-meditated processes

provides an advantage to cells that are challenged with microtubule depolymerizing drugs.

Lastly, I tested the panel of deletion strains for sensitivity to hydroxyurea, which inhibits replication by decreasing the dNTP pools in cells. Deletion of *UBP7* has also been reported to sensitize cells to hydroxyurea, which was suggested to be due to increased ubiquitination histone H2B [89]. However, I did not recapitulate this growth phenotype, perhaps due to the discrepancy in strain background between the two studies.

In contrast, I confirmed all mutants containing *ubp6Δ* display slower growth on hydroxyurea (Figure 4.3, examples: compare A1 to C1, C2, A3, and G4) [147]. The *ubp6Δ* sensitivity could not be rescued by deletion of any additional DUBs. In addition, no other DUB deletion strain combinations that express *UBP6* displayed significantly slower growth than wild type cells on hydroxyurea. Surprisingly, all quadruple and quintuple DUB deletion strains that lack *UBP6* were extremely sensitive to hydroxyurea compared to *ubp6Δ* alone (Figure 4.3, C4, D4, E4, G4, H4). These data suggest that negative interactions exist between *UBP6* and the other four DUBs in cells with slowed replication, and that there may be redundancies between these DUBs that are not evident under standard growth conditions.

	1	2	3	4
A	WT	ubp5 ubp10	ubp5 ubp6 ubp7	ubp6 ubp10 yuh1
B	ubp5	ubp5 yuh1	ubp5 ubp6 ubp10	ubp7 ubp10 yuh1
C	ubp6	ubp6 ubp7	ubp5 ubp6 yuh1	ubp5 ubp6 ubp7 ubp10
D	ubp7	ubp6 ubp10	ubp5 ubp7 ubp10	ubp5 ubp6 ubp7 yuh1
E	ubp10	ubp6 yuh1	ubp5 ubp7 yuh1	ubp5 ubp6 ubp10 yuh1
F	yuh1	ubp7 ubp10	ubp5 ubp10 yuh1	ubp5 ubp7 ubp10 yuh1
G	ubp5 ubp6	ubp7 yuh1	ubp6 ubp7 ubp10	ubp6 ubp7 ubp10 yuh1
H	ubp5 ubp7	ubp10 yuh1	ubp6 ubp7 yuh1	ubp5 ubp6 ubp7 ubp10 yuh1

Table 4.1. Layout of DUB deletion strains in serial dilution assays. Genotypes are as shown in Table 2.2.
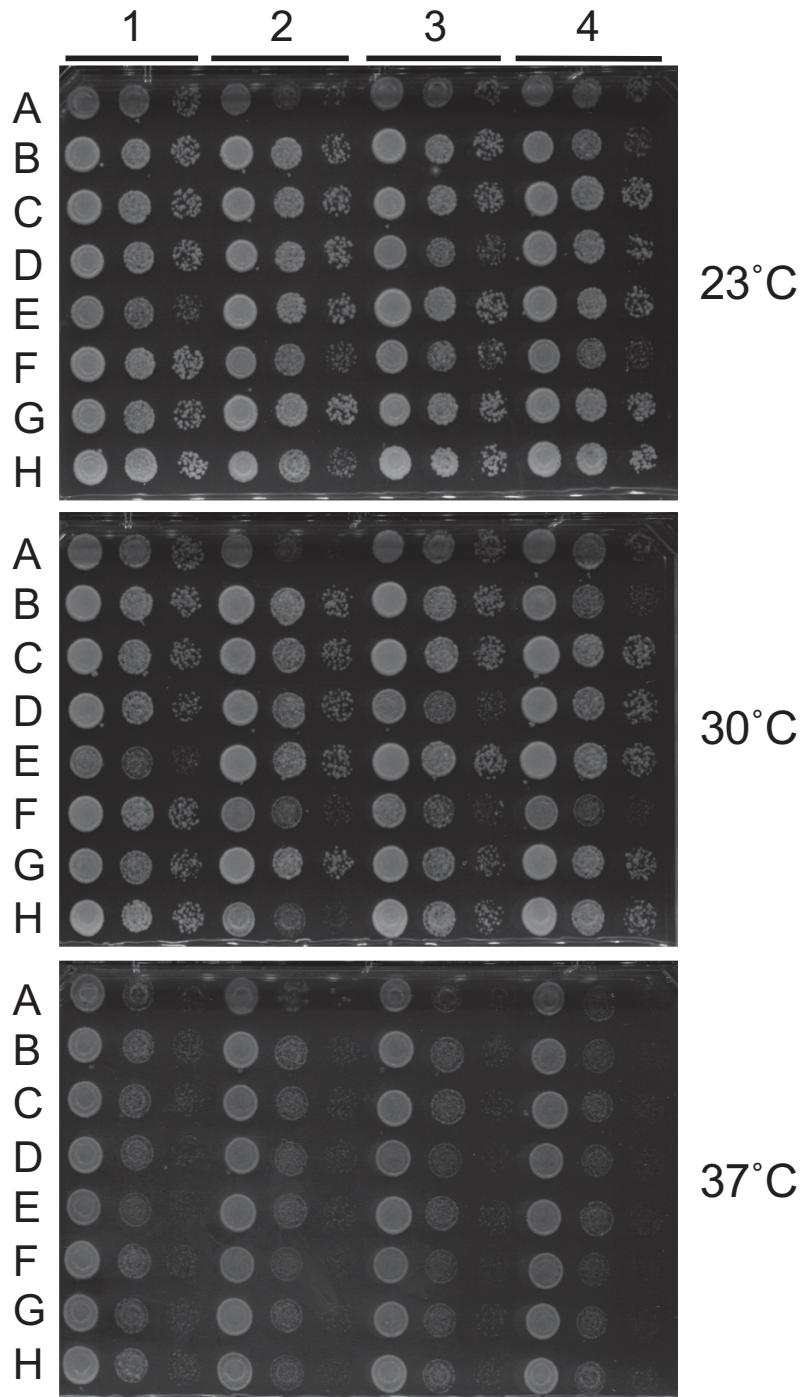
Figure 4.1. Temperature sensitivity assays. Cells were grown to log phase, and 10-fold serial dilutions were spotted (as in Table 4.1) onto YM-1 plates containing 2% dextrose and incubated at 23˚C, 30˚C, and 37˚C. Representative images are shown from 1 of 2 experiments. Plates were imaged between 24-48 hours.
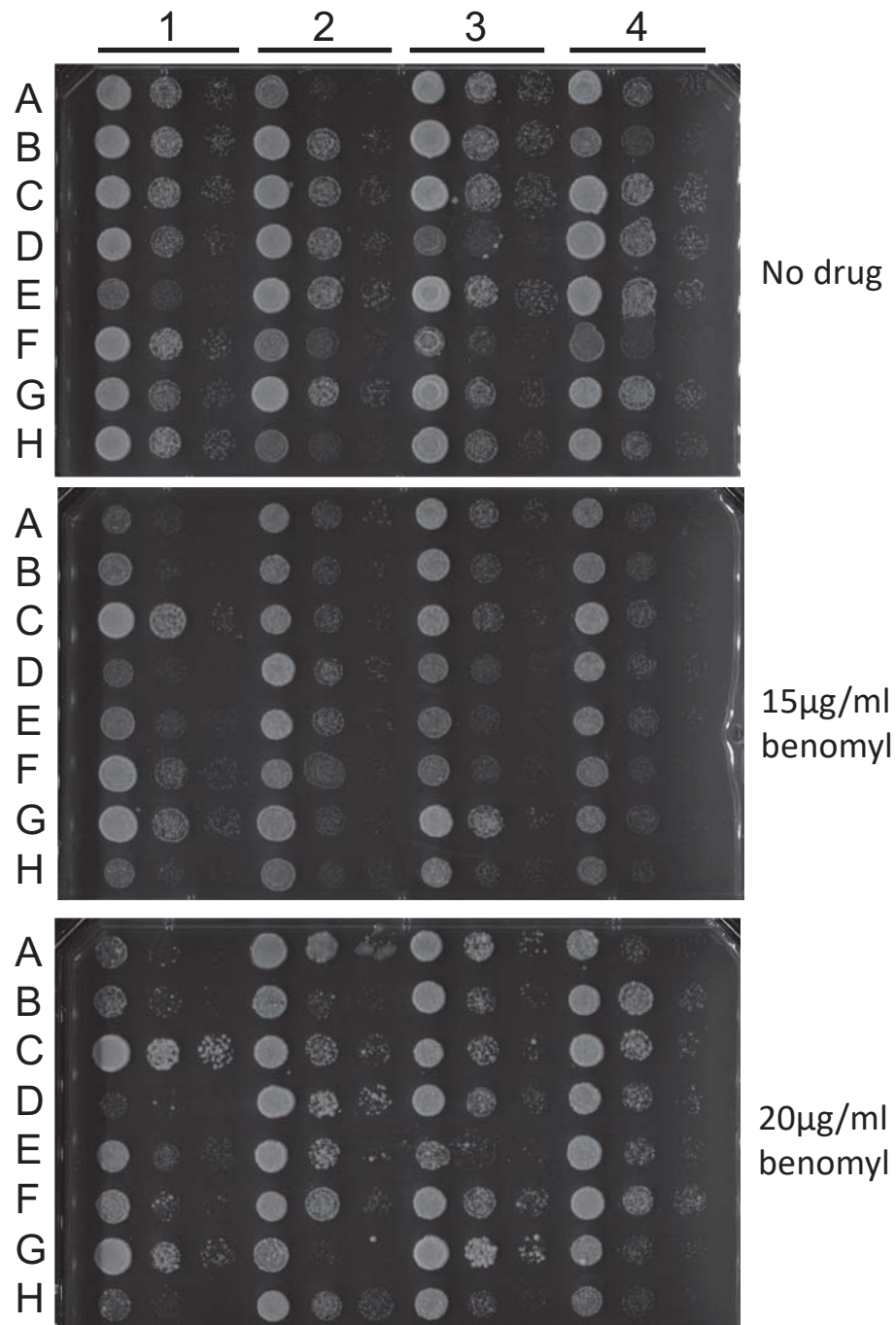
Figure 4.2. Benomyl sensitivity assays. Cells were grown to log phase, and 10-fold serial dilutions were spotted (as in Table 4.1) onto YM-1 plates containing 2% dextrose and 15g/ml benomyl. Plates were incubated 30°C. Representative images are shown from 1 of 2 experiments. Plates were imaged between 24-48 hours.
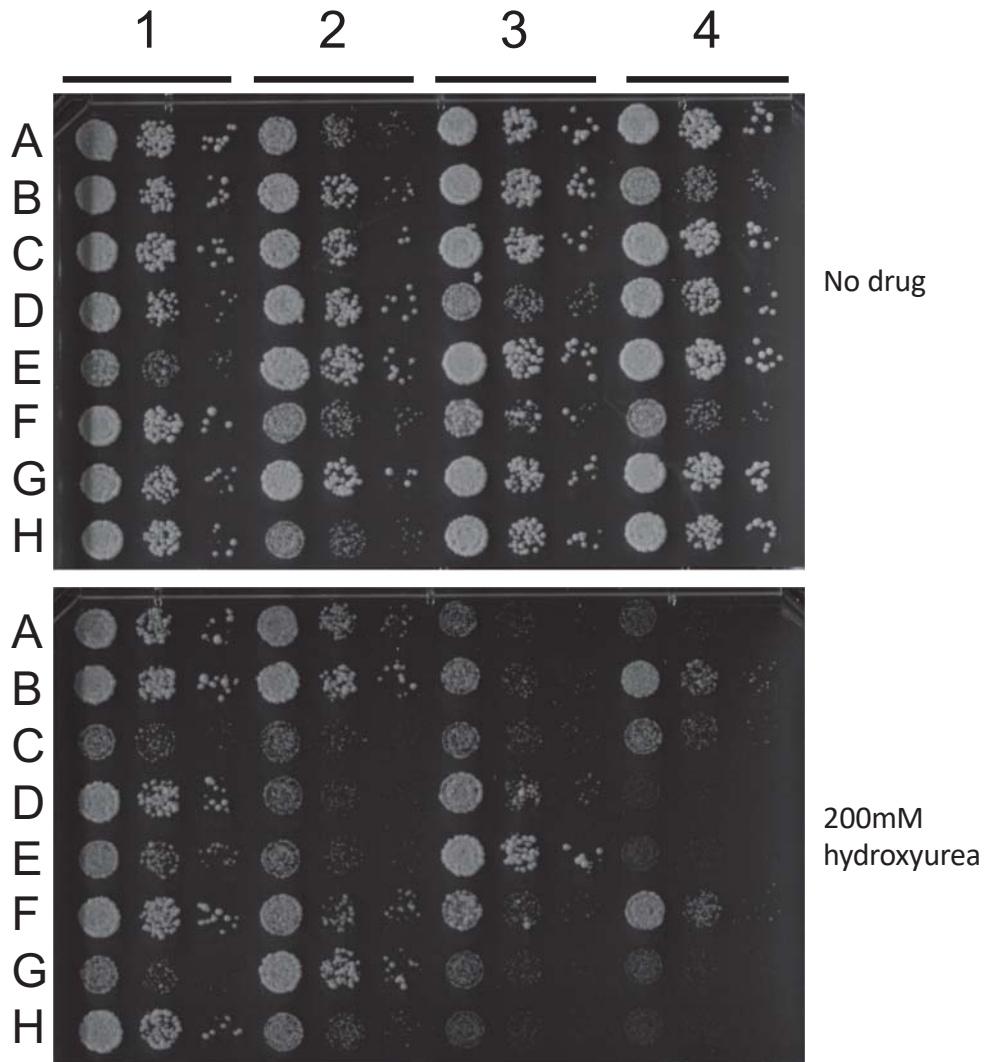
Figure 4.3. Hydroxyurea sensitivity assays. Cells were grown to log phase, and 10-fold serial dilutions were spotted (as in Table 4.1) onto YM-1 plates containing 2% dextrose and 15g/ml benomyl. Plates were incubated 30˚C. Representative images are shown from 1 of 2 experiments. Plates were imaged between 24-48 hours.

Conclusions

In this work I demonstrate that compound DUB deletion strains display a range of growth phenotypes based on the different stressors tested. Most striking are the phenotypes associated with *ubp6Δ* strains grown on benomyl and hydroxyurea. I show *ubp6Δ* (and less so *ubp10Δ*) single mutants are resistant to benomyl, and these deletions confer resistance to other DUB deletion combinations. In particular, *ubp6Δ* and *ubp10Δ* improve the growth of *ubp5Δ* and *ubp7Δ* single mutants (Figure 4.2; compare A1 to D1, C2, and F2; compare A1 to B1, G1, and A2), suggesting that loss of *UBP6* and *UBP10* provide a positive growth response when cells are challenged by mitotic spindle destabilization.

Ubp6 appears to modulate stress responses in different ways. When deletion strains were plated on hydroxyurea, I observed *ubp6Δ* displayed a slow growth phenotype both alone and in combination with other DUB deletions, and I could not identify a combination that rescued this defect. It was surprising to see that all *ubp6Δ* quadruple and quintuple deletions were hyper-sensitive compared to the single, double, and triple DUB combinations. These data suggest that loss of *UBP5, UBP7, UBP10,* and *YUH1* (either alone or in combination) does not significantly impair growth on hydroxyurea, but additional loss of *UBP6* in this condition is toxic to cells. It is possible that Ubp5, Ubp7, Ubp10 and Yuh1 function in a separate pathway from Ubp6, and that these pathways produce two different responses to DNA replication arrest that, when combined, result in a more severe growth phenotype than the individual responses. While we are unaware which pathway the other four DUBs may be involved in, Ubp6 has been implicated in modulating proteasome activity [95,

120, 124, 148, 149]. It is possible that a protein involved in pausing replication upon cells sensing hydroxyurea is rapidly degraded in *ubp6Δ* because of proteasome mis-regulation, resulting in continued replication at the cost of poor cell viability. To test this, I could analyze mass spectrometry data for replication or replication stress response proteins that are downregulated in *ubp6Δ* strains, and determine if upregulation of those proteins rescues sickness in cells challenged with hydroxyurea.

Beckley et al. reported a similar study in which they tried to identify redundancies among five fission yeast DUBs. These DUBs are implicated in membrane trafficking and are unrelated to the budding yeast DUBs examined in this work. For each possible *dubΔ* combination they evaluated growth phenotypes for genetic interactions and performed comparative proteomics to identify common substrates under various stressors. For most stressors they observed normal growth phenotypes from the 2, 3, and most 4 DUB deletion combinations, but more sickness or death in the quintuple DUB deletion strain. They also demonstrated that the DUBs they evaluated display substrate selectivity for different subsets of targets but share a small group of substrates. I observed a similar effect with our deletion strains grown on benomyl, on which the quintuple and all quadruple mutants containing *ubp6Δ* were the slowest growing (Figure 4.3). I also demonstrated that DUBs have specific but partially overlapping targets in budding yeast (Figure 2.3). Beckley et al. concluded that while their five fission yeast DUBs appear to have overlapping functions when grown in rich media, growth in different conditions prove they display degeneracy ("unique and overlapping functions by diverse structures").

Our data suggest the five DUBs from our screen may also be degenerate, but more

work is required to make this conclusion.

Materials and Methods

Serial dilution assays

Ten-fold serial dilutions of strains with the indicated genotypes were plated on YP plates containing 2% dextrose and where indicated, benomyl (15µg/ml, 20µg/ml), and hydroxyurea (200mM). Temperature sensitivity plates were grown at 23˚C, 30˚C, or 37˚C, while drug plates were grown at 30˚C. Plates were imaged after 24 to 72 hours of incubation.

Chapter V: Discussion

Since the discovery of ubiquitin-mediated protein degradation in the late 1970s and early 1980s, scientists have been working to better understand the details of this system. Much has been uncovered about the process of ubiquitin conjugation onto proteins, both for proteasomal degradation and other forms of protein regulation, but less is known about the proteins involved in the removal of this post-translational modification. The DUB field has largely been in pursuit of answers to the following questions: 1) Do DUBs have specificity for their protein or ubiquitin targets? 2) What are their roles in the cell? 3) How are they regulated? This thesis addresses the target specificity of yeast DUBs and their potential roles in cell cycle control. While this work does not directly interrogate DUB regulation, it explores physical and genetic requirements of a novel DUB-substrate interaction. Our work establishes an overexpression technique that can be used to screen DUBs for their specific targets in vivo. Data from this screen suggest that although some DUBs may redundantly target proteins (as had been previously reported by many groups using different approaches) DUBs do have specificity for distinct sets of targets, and some of these DUB-substrate interactions are important for accurate cell cycle progression. In particular, we demonstrated Ubp10 controls entry into the cell cycle, partially through its regulation of Dbf4, and that defective S-phase timing in *ubp10Δ* cells could be rescued with the deletion of DUBs that promote proteasome function. Furthermore, study in deletion strains of DUBs that regulated many cell cycle proteins in our screen revealed genetic interactions between some DUBs that may have evolved to maintain the cell cycle under stress.

An overexpression approach to determine DUB specificity

Previous approaches to studying DUBs were either performed in vitro or in DUB deletion strains, the conclusions from which strongly supported the model of redundancy [27, 30, 40, 41]. Our overexpression technique provided an advantage over previous approaches in that it allowed us to examine the effect of individual DUBs on the levels of a large number of physiological candidate substrates without the indirect effects associated with gene deletion. However, overexpression is not without its caveats. Excess protein synthesized can accumulate in its natural cellular compartment or become mislocalized if not properly degraded, and this accumulation can lead to forced interactions that can be interpreted as false positives in the screening process. However, follow-up experiments allow us to identify and eliminate these false positive interactions while confirming true interactions. In this work, we show that overexpression can be used as a broad screening method to identify DUB candidate targets from a subset of the proteome. Applying this screening method to other proteins or using DUB mutants to further test interactions will contribute to the field's knowledge of DUB substrate specificity.

Our DUB screen only looked at the 21 known DUBs in yeast, but it is possible that not all DUBs have been identified in eukaryotic cells [25]. In the past two years two new DUB families have been discovered in humans: MINDY and ZUFSP, suggesting there may be either other unknown cysteine proteases or known proteases with unknown ubiquitin binding or cleavage abilities. Our overexpression approach can be applied to other proteases as a first pass to determine if they regulate any UPS substrates.

Although there is no evidence for a ZUFSP member in budding yeast, there are two yeast homologs of MINDY, MIY1 and YGL082W [24]. We did not include YGL082W in our overexpression screen because it showed no deubiquitinating activity in the original study, suggesting it may function through non-catalytic mechanisms. We screened MIY1 against our panel of UPS substrates but did not find any targets. This is surprising given MIY1's high selectivity for K48 chains – the canonical signal for proteasomal degradation – which has been attributed to one of two MIU (motif interacting with ubiquitin) at its C-terminus [24, 150]. It is possible that MIY1 deubiquitinates K48-ubiquitinated proteins or functions under conditions that were not tested in our screen. To determine if MIY1 regulates UPS targets and the cell cycle, our screen can be expanded to include more proteins in asynchronous cells, cells synchronized at different stages of the cell cycle, and under different environmental stresses.

BiFC as a method to test DUB-substrate interactions

Many groups have attempted to classify pathways in which DUBs function by identifying their interacting partners. This technique was first applied in human cells by Sowa et al who immunoprecipitated DUBs and performed tandem mass spectrometry [32]. Their CompPASS software identified high-confidence interactions for 80% of human DUBs from proteomic datasets, but physical interactions could not be verified because of their transient nature and low steady-state levels of proteins involved [32]. In yeast, various mass spectrometry-based proteomics approaches in both wild type and deletion strains have been also been applied to identify DUB-

substrate pairs [22, 40, 41]. However, even global analysis of the fission yeast DUB interactome has not been able to identify DUB substrates because of low protein abundance [22]. In this work, we observed Ubp5 stabilizes Hof1 – a positive regulator of cytokinesis that localizes to the mother-bud neck, and we attempted to detect an interaction between these proteins. BiFC was an ideal method for following up on this interaction because it stabilizes weak or transient interactions and it was previously used to identify an interaction between Hof1 and its E3, Grr1 [37]. We successfully trapped and visualized the interaction between Ubp5 and Hof1, and using genetics I was able to determine that Grr1 is required for this interaction. I was unable to detect an interaction between Grr1 and Ubp5, potentially due to the topology of the BiFC fusions. In all experiments shown in Chapter III, the two halves of the Venus fluorophore were fused to the C-termini of the various proteins. It is possible that by making N-terminal fusions of Venus fused to one or both of these proteins we may be able to detect the Grr1-Ubp5 interaction for which we have genetic evidence, thus showing that these three proteins form a complex. Our results suggest BiFC can be a useful tool for testing other DUB-substrate pairs that are expected to physically interact.

However, BiFC also has its limitations: As we observed for cells expressing Ubp5 and Hof1 fusions, plasmid loss can occur, masking the frequency of interactions (Figure 3.2). Additionally, fusion proteins are overexpressed instead of expressed at their endogenous levels (potentially leading to false positive interactions) and interactions are limited by the orientation of fusion proteins (potentially leading to false negative interactions). For example, while we

demonstrated Ubp5 and Hof1 interact at the mother-bud neck in mitotic cells using BiFC, we were unable to show that Grr1 and Ubp5 interact. This does not rule out the possibility that Ubp5, Hof1, and Grr1 interact in a complex. In fact, our data in *grr1Δ* cells suggest that Grr1 is required for the DUB-substrate interaction although we have not identified if it is simply Grr1 binding to Hof1 or its ubiquitination of Hof1 that is a prerequisite for Ubp5 to recognize its substrate. From these data it is possible that these three proteins do form a complex, but because of the conformational constraints of BiFC we were unable to detect this interaction. Additional BiFC experiments need to be conducted with mutants that challenge either Grr1-Hof1 binding or Hof1 ubiquitination to further test Grr1's role in the Ubp5-Hof1 interaction and to determine if Ubp5 plays a role in regulating cytokinesis. BiFC could also be used to test remaining putative DUB-substrate interactions from our screen or from other DUB profiling studies.

BiFC can also be useful tool for determining the domains required for specific DUB-substrate interactions. The roles of some domains such as the Rhod in Ubp4, Ubp5, and Ubp7 are poorly understood. BiFC can be used to validate DUB-substrate interactions in domain mutants to determine if these domains play roles in substrate recognition. We can pair BiFC with our overexpression screening method to test DUBs mutated for putative interaction sites; these experiments would provide insight into both how DUBs regulate their substrates.

Ubp10 DUB functions and roles in the cell cycle

By screening for DUB substrates from a collection of UPS-targeted cell cycle proteins, we were able to determine if any of the 21 yeast DUBs have potential cell-cycle regulatory roles. Our data indicate Ubp10 had the largest effect on the proteins we tested. Ubp10 has established roles deubiquitinating PCNA to control its recruitment to sites of DNA repair, regulating telomere silencing through deubiquitination of H2B, and stabilizing Rpa190 for ribosome biogenesis [87, 97, 131]. Our data provide evidence of additional roles for Ubp10 in the stability of several cell cycle proteins and in cell cycle entry (Figures 2.7, 2.9). While our screen only examined a subset of cell cycle regulators, it can be expanded to screen other proteins to determine if Ubp10 is a broad regulator of the G1-S transition.

It is interesting that Ubp10 regulates so many proteins from our screen (40%) and essentially all of the APC substrates we tested. Of the 37 targets in the screen, 12 are ubiquitinated by the APC – 10 proteins were upregulated by Ubp10 in two replicates of the screen, one was regulated in one of two replicates, and the final target is degraded only in meiosis [151], a condition our screen did not cover (Figure 2.6). These data suggest Ubp10 employs a mechanism for regulating many different proteins, most of which are ubiquitinated by the APC, but it is unclear how Ubp10 accomplishes this. Several DUB-E3 interactions have been detected and these opposing functions appear to regulate the E3, fine-tune the ubiquitination status of common substrates, and edit ubiquitin chains [20]. One possibility for Ubp10's preference for APC substrates in our screen is that it recognizes its targets because of an association with the APC. BiFC could be used to test for interactions between

Ubp10, APC activators Cdc20 and Cdh1, and their shared substrates. Such interactions may reveal both an added layer of regulation to the vital processes the APC drives during the cell cycle and the mechanisms through which Ubp10 is regulated.

Ubp10 contains an N-terminal intrinsically disordered region (IDR) – a flexible region that allows a protein to adopt multiple conformations and interact with different protein partners. This characteristic of IDRs is supported by studies characterizing IDRs on other proteins, in particular on the nuclear-localized E3 San1 [152, 153]. Yeast two-hybrid analysis revealed San1 directly interacts with at least 25 aggregation-prone proteins through its IDR to promote their degradation and presumably prevent toxicity [153]. Cycloheximide-chase assays also indicate San1 regulation of a subset of misfolded proteins relies on the nuclear localization signal (NLS) of these substrates [153]. Similarly, all of the proteins regulated by Ubp10 in our screen display some level of nuclear localization (or have presumed nuclear function) and Ubp10 has been shown to deubiquitinate histones at defined sites [131, 154]. Additionally, Ubp10's IDR has been shown to contain sites for several established binding partners and contribute to the stability of candidate substrates [116] (Figure 2.7). These data suggest it is feasible for Ubp10 to be able to regulate many candidate targets from our screen with specificity for nuclear proteins. However, it is unknown if Ubp10 can regulate all chromatin-associated proteins and how it accomplishes substrate specificity. To determine if Ubp10 is a general deubiquitinase for chromatin-bound proteins, we can use our screen to identify chromatin-bound proteins that are stabilized upon Ubp10 overexpression (and

destabilized when *UBP10* is deleted or the protein is mis-localized), and perform

binding, stability, and deubiquitination assays to confirm Ubp10 regulation in vivo. If

Ubp10 is found to specifically regulate chromatin proteins it will be of interest to

investigate methods of substrate specificity. The plasticity of Ubp10's N-terminal IDR

and evidence that it confers specificity for some Ubp10 substrates suggests it may

contain binding sites for more proteins discovered from the proposed screen. Two-

hybrid assays with candidate Ubp10 targets can be used to determine the locations

of these sites within the IDR [116]. Further, analysis of conformational changes in

Ubp10 upon substrate binding may reveal mechanisms for how Ubp10 is regulated

and how interactions with so many different proteins are orchestrated. I suspect

Ubp10 may have evolved to play a role in many important processes through the

ability to interact with a number of proteins in its IDR and cleave different ubiquitin

signals.

We demonstrate loss of Ubp10 resulted in S-phase slowing and accelerated

degradation of the Ubp10 target Dbf4 (Figure 2.9). Because Dbf4 is the activating

subunit of the kinase Cdc7 and is essential for DNA replication initiation [117], we

hypothesized the cell cycle delay in *ubp10Δ* cells is caused by an insufficient amount

of Dbf4. To test this, we overexpressed *DBF4* in *ubp10Δ* cells and quantified S-

phase progression. Although overexpression of *DBF4* restored Dbf4 steady-state

protein levels, it only partially relieved S-phase slowing (Figure 2.11). These data

suggest that while Dbf4 levels are important for cell cycle entry there are other

factors misregulated in *ubp10Δ* strains. It is unclear if these proteins are substrates

of Ubp10 or if they are indirectly affected by loss of the DUB. The large number of

nuclear proteins upregulated by Ubp10 overexpression suggests loss of Ubp10 may

be misregulating additional S-phase regulators we have not yet examined (Figure

2.6), so we can apply our screen to identify more Ubp10 targets from a panel of S-

phase regulators. Isasa et al. reported that the levels of 216 proteins were

significantly altered in *ubp10Δ* cells; this was the second largest change to the

proteome observed in an individual DUB deletion strain. Of the top 20 proteins

affected in the *ubp10Δ* strain, 15 RNA processing proteins were significantly

upregulated [41]. To determine if misregulation of any of these RNA processing

proteins in the *ubp10Δ* is the cause of S-phase slowing, we could examine their

stability, ubiquitination status, and if upregulation of these proteins rescues the

ubp10Δ cell cycle defect.

Coordinated DUB functions in cell cycle control

The proteasome contains 2 of the 21 yeast DUBs: Ubp6 associates with the

proteasome base and Rpn11 is a core structural component of the lid. When

proteasome-bound, Ubp6 non-catalytically slows the rate of proteasome activity by

progressively cleaving ubiquitin in addition to Rpn11's en bloc deubiquitination of

proteasomal substrates [120]. Interestingly, I found deletion of Ubp6 rescued the

ubp10Δ cell cycle defect and restored the stabilities of several Ubp10 targets (Figure

2.12). To test if this genetic result was due to misregulation of proteasome activity

we deleted Ubp14 in the *ubp10Δ* strain. Ubp14 clears free ubiquitin chains in the

cell; when Ubp14 is lost, ubiquitin chains accumulate on the proteasome and inhibit

its activity [125]. I found loss of Ubp14 also restored the *ubp10Δ* doubling time defect

(Figure 2.13), confirming that proteasome inhibition reverses *ubp10Δ* phenotypes. Our data suggest that loss of proteasome regulation by DUBs stabilizes Ubp10 substrates and provides an advantage for *ubp10Δ* strains to maintain cell cycle progression.

This raises the question: do proteasome-associated DUBs regulate the cell cycle by stabilizing Ubp10 substrates? To answer this, it must be determined if Ubp6 can deubiquitinate Ubp10 substrates, if this regulation is dependent on Ubp6 association with the proteasome, and if loss of this regulation is sufficient to restore a perturbed cell cycle. Although our work does not address ubiquitin shuttle factors (proteins that escort ubiquitinated proteins to the proteasome [155]), it would be informative to test if these proteins facilitate binding of Ubp10 substrates to Ubp6 and if shuttle factors are regulated by either of these DUBs. For example, if loss of *UBP6* accelerates proteasomal degradation [95, 120], perhaps this accelerates the degradation of shuttle factors involved in recruiting Ubp10 substrates to the proteasome, inhibits recruitment of Ubp10 substrates, and thus restores Ubp10 target levels.

It is interesting that loss of Ubp6 stabilizes Ubp10 substrates that appear to be rapidly degraded in *ubp10Δ* strains. Many studies report mutants of Ubp6 and its human ortholog, Usp14, display increased degradation of proteasomal substrates due to the loss of suppression on the proteasome [95, 120, 124, 148, 149]. Another study presented a conflicting result that Ubp6 association with the proteasome stimulates proteasome activity, dependent on binding by ubiquitin conjugates with a loosely folded domain that can be easily entered into the gate of the 20S

proteasome [122]. The latter work provides evidence to support our hypothesis that loss of Ubp6 can slow degradation of Ubp10 substrates to rescue their accelerated degradation in *ubp10Δ* mutants. I suspect Ubp6 differentially regulates the proteasome and this ability may be controlled by substrate specificity. It is possible that proteins with flexible domains have evolved to be ideal candidates for tightly and quickly controlled degradation. Because these domains may contain sites that stably bind Ubp6, and unstructured regions enter the 20S proteasome more easily, it is possible such proteins experience quicker degradation than proteins that have weaker affinity for Ubp6. I imagine a reason most studies have reported solely on Ubp6/USP14's proteasome inhibition, and not its potential dual functions, is because the proteins used to study these DUBs have not been strong substrates and have not elicited the increased degradation response. It will be informative to identify ubiquitinated proteins that strongly bind Ubp6/USP14 and examine their structures for shared domains, unstructured regions, and how their interaction with these DUBs affects proteasome activity.

Redundancies in the DUB network

Several studies have investigated the effects of multiple DUB deletions in an attempt to find phenotypes within the DUB network [22, 98, 118]. Deletion combinations have not displayed lethality or severely defective growth, suggesting DUBs are highly redundant. This work demonstrates that budding yeast DUBs target specific subsets of cell-cycle regulatory proteins (Figure 2.3), suggesting yeast DUBs may not be as redundant for substrates as previously thought. Because Ubp5,

Ubp6, Ubp7, Ubp10, and Yuh1 regulated a large number of cell cycle proteins, we anticipated combined deletions of these DUBs might negatively impact proliferation rate. Surprisingly, all combinations (except for *ubp10Δ UBP6* strains) displayed doubling times that were not much different from wild type suggesting these five DUBs are not redundant for processes that promote proliferation (Figure 2.12A). However, it is possible that knockout of additional DUBs may reveal redundancies in the DUB network. To test this, I would first test deletion combinations that include paralogs of the five DUBs, as I anticipate paralogs that have common targets and functions are likely to display negative interactions. Ubp7's paralog Ubp11 has no known targets but together with Ubp5 confers growth resistance to an immunosuppressive drug [156]. While little is known about Ubp11 compared to its paralog Ubp7, its combined deletion with Ubp5 and Ubp7 may reveal interesting genetic interactions. I would then make combination deletion strains of the remaining DUBs that have established cell-cycle regulatory targets and share similar cellular localizations. I expect negative interactions will be observed upon deletion of DUBs that are involved in regulating the stabilities of cell cycle proteins rather than DUBs that play roles in other processes (such as membrane trafficking) or compartments (e.g. tethered to the membrane, vacuole).

This work reveals the five DUBs that regulated the largest number of targets from our screen are not redundant for essential functions in standard conditions. However, our preliminary experiments in Chapter IV identify genetic interactions between *UBP6* and other DUBs that may have evolved for cells to cope with different stresses. When grown on benomyl, *ubp6Δ* confers resistance to all other

deletion combinations. Meanwhile, additional loss of *UBP6* in deletion strains grown on hydroxyurea makes cells sicker, suggesting Ubp6 may differentially regulate stress responses. I suspect Ubp6 functions in a separate pathway than the remaining four DUBs, as deletion of all five DUBs on hydroxyurea was more detrimental than *ubp6Δ* alone or any combination of four deletions. It is possible that dual disruption of these pathways in the presence of hydroxyurea promotes a more severe growth defect. To further map redundancies among yeast DUBs it will be necessary to test proliferation of different combinations of deletion strains under a variety of conditions or stresses. It will also be informative to determine if Ubp6 is a broad regulator of stress responses and the mechanisms by which Ubp6 differentially regulates stress responses. Understanding when and why these interactions occur will improve our comprehension of the highly complex DUB network.

Ubp6, Ubp10, and Ubp14 functions in higher eukaryotes

While we have obtained a basic understanding of Ubp6, Ubp10, and Ubp14 functions in yeast, understanding their counterparts' functions in higher eukaryotes will provide insight into their importance in human disease.

In this thesis we demonstrate that Ubp10 is important for maintaining proper G1-S timing, likely through stabilization of specific targets including Dbf4. Similarly, its mammalian ortholog, USP36, has also been found to play important roles in cell growth and proliferation [114]. Like Ubp10 [97], USP36 also localizes to the nucleolus and positively regulates ribosome biogenesis – for example, USP36

stabilizes c-MYC (a transcription factor that induces expression of ribosomal proteins and RNA) in a feed-forward loop that promotes its own expression [114]. As c-MYC overexpression is found in most human cancers it is unsurprising that USP36 is upregulated in many primary breast cancer tissues that have been examined [114, 157]. In support of this conclusion that USP36 promotes cell growth and proliferation, knockdown of USP36 in human cell lines suppressed proliferation, induced apoptosis, and led to cell cycle arrest [158-160]. Similarly, impairment of development is seen in Drosophila where *Usp36* null mutants undergo increased apoptosis and are lethal in larval stages [161, 162], and in a Usp36-deficient mouse model where embryos are lethal prior to the blastocyst stage [160].

These deleterious effects of *USP36* loss or misregulation highlight the importance of understanding Ubp10/USP36 functions in vivo. Since USP36 and Ubp10 have well-conserved functions and protein domains, studies in less complex models – such as this study of Ubp10 in budding yeast, aid in this effort. As our study and other studies have identified that Ubp10/USP36 can specifically deubiquitinate several different substrates that play important roles in maintaining the cell cycle [87, 97, 112, 116, 154], it will be of interest to identify its additional targets. Using budding yeast to determine the mechanisms of Ubp10-substrate recognition and how Ubp10's regulation of these proteins impact cellular functions will better equip us to design mammalian disease models.

The yeast DUB Ubp14 and it human ortholog USP5 have been implicated in promoting proteasome function by removing unanchored K48 ubiquitin chains that competitively bind to the proteasome [125, 163]. While Ubp14 is non-essential,

increased ubiquitin conjugates are observed in *ubp14Δ* cells [125]. In Ubp14/USP5

mutants, this competitive inhibition has been shown to impair the degradation of

some UPS proteins [164, 165], although the mechanism determining which proteins

are affected is not clear. In human cells, USP5 expression has been linked to

increased tumorigenesis observed in melanoma, hepatocellular carcinoma, and

pancreatic cancer cell lines, suggesting USP5 is an oncogene [165-168]. USP5

knockdown has been shown to reduce tumorigenesis in human pancreatic cells and

in a pancreatic xenograft mouse model [165, 167]: In pancreatic cells lacking USP5,

ubiquitin chains out-compete ubiquitinated p53 at the proteasome, leading to p53

stabilization, increased apoptosis, and reduced cell proliferation [165]. In a mouse

model, the absence of USP5-mediated deubiquitination leads to rapid FOXM1

turnover, resulting in reduced tumor growth [167]. These data suggest USP5

controls proteasomal degradation in multiple ways – by directly targeting substrates

and by regulating proteasome activity. We demonstrated the latter when we deleted

UBP14 and rescued the slow growth phenotype in *ubp10Δ* cells that is associated

with increased protein degradation (Figure 12.13e). By allowing ubiquitin chains to

inhibit the proteasome in *ubp14Δ* cells we were able to reverse the rapid degradation

of Dbf4 and other Ubp10 substrates and restore G1-S timing.

In yeast, Ubp6 has been shown to reversibly associate with the proteasome

and inhibit its activity by slowing deubiquitination of substrates [95, 120, 124, 148,

149]. Deletion of *UBP6* resulted in decreased ubiquitin conjugates, but no growth

phenotype was seen in unstressed cells (Chapter II). In mammals, USP14 has been

studied in non-neuronal human cells, rat cerebral cortical neurons, and an *ataxia*

mouse model (ax^J) [169]. The hypomorphic USP14 allele in the ax^J model has reduced expression and ubiquitin levels in the brain, livers, hearts, and spleens of mice [170]. ax^J mice also display poor synaptic transmission and progressive motor function degeneration that leads to paralysis and death between 6 to 8 weeks – some physiological changes similar to those observed in neurodegenerative diseases such as Parkinson [171]. Together, these data indicate that USP14 may play a more important role in cell function than Ubp6 has revealed in yeast, and they highlight USP14 as a potential target for neurodegenerative disease therapies. In HeLa, MEF, and HEK293 cells, knockdown of USP14 accelerated degradation of ubiquitinated conjugates and the reporter substrate Ub-R-GFP [121, 172]. These data suggest that USP14 may slow proteasomal activity in human cells as some reports have shown for Ubp6 in yeast. Consistent with this conclusion, inhibition of USP14 with the small molecule IU1 exhibited decreased chain trimming and increased degradation of neurodegenerative disease-associated proteins (including tau, TDP-43, and ataxin-3) [121, 173].

However, data exist in support of a different model in which Ubp6/USP14 can promote, rather than inhibit, proteasomal degradation. Proteasomes purified from ax^J mice did not display reduced proteolytic activity compared to wild type proteasomes, suggesting loss of USP14 activity does not impair proteasomal function [170]. Data from rat and mouse (ax^J) neuronal cultures also demonstrate that inhibition of USP14 protease activity with IU1 does not reduce protein degradation [174]. Additional studies report increased stability of some ubiquitinated proteins when Ubp6/USP14 is deleted or inhibited [122, 175], including our finding

that Dbf4 is stabilized in *ubp6Δ* cells [112]. These data support the possibility that Ubp6/USP14 may promote the degradation of a subset of proteasomal substrates.

These contrasting data may be explained by the following: When Ubp6/USP14 DUB activity is inhibited (either in a catalytic mutant or by treatment with IU1) the DUB would no longer bind to its specific substrates and facilitate entry into the 20S core particle, leading to stabilization of this subset of UPS proteins. The increase in ubiquitin conjugates or specific proteins observed by several labs [121, 172, 173] may represent the stabilization of Ubp6/USP14 substrates. This may also account for the increased stability of Dbf4 in *ubp6Δ* cells (Figure 2.12d). However, if Ubp6/USP14 non-catalytic function is preserved (as with inhibited or catalytically inactive protein), then the Ubp6/USP14 mutants may still be able to allosterically stimulate the opening of the 20S core particle to promote the degradation of ubiquitinated substrates. Similarly, in the case of deletion of *UBP6/USP14*, another protein may possibly compensate for Ubp6/USP14 activation of the proteasome, resulting in normal proteolysis rates observed by some groups [170, 174].

In all, these contrasting reports about Ubp6/USP14 function indicate that there is still much about Ubp6/USP14 that we do not understand. Only about 40% of Ubp6/USP14 is associated with the proteasome in MEF cells [149], which suggests Ubp6/USP14 has other functions aside from regulating ubiquitin homeostasis and proteasomal activity. Interrogating the regulation, function, and substrate specificity of free DUBs may provide additional insight into the different phenotypes that have been observed in Ubp6/USP14 mutants.

Protein redundancy and specificity

Many studies that have analyzed DUBs in loss-of-function or in vitro systems suggest that many DUBs are highly redundant for the ability to deubiquitinate the same substrate or are redundant for cell growth under normal conditions [27, 30, 40, 41]. This is supported by the knowledge that yeast and human DUB paralogs arose from whole genome duplications and may have similar biochemical functions [176, 177]. However, the idea that all non-essential yeast or human DUBs are genetically redundant does not align with natural selection, so there must be a different explanation for why large subsets of DUBs display apparent redundancy.

Different levels of redundancy exist in the cell [178] and may be able to describe some of the apparent redundancies among UPS proteins. Genetic redundancy takes the form of multiple copies of genes that exist to meet the cell's high demands, such as ubiquitin, which is expressed from five repeats of the ubiquitin gene. Molecular redundancy occurs when two or more proteins modify the same target using the same mechanism, most similar to how Ubp8 and Ubp10 both deubiquitinate H2B [154]. Target redundancy occurs when two or more proteins modify the same target through distinct mechanisms; for example, APC[Cdh1] ubiquitinates Dbf4 [179] and our data show Dbf4 is likely to be deubiquitinated by Ubp10, suggesting SCF[Grr1] and Ubp5 are an example of proteins redundant for a target. On a higher level, proteins that display pathway redundancy promote a single pathway by targeting different pathway components, such as those involved in ubiquitin homeostasis – DUBs cleave ubiquitin precursors into monoubiquitin, associate with the proteasome to remove ubiquitin chains from substrates, and

break down free ubiquitin chains back into monoubiquitin. These forms of redundancy may explain why some DUBs deubiquitinate the same target in vitro or appear to have redundant roles in some cellular processes [22, 27].

Distinct functions allow DUBs to display target or pathway redundancy. Distinct functions of DUBs may have originated from the gain or loss of ubiquitin binding or specific protein binding domains over time, for example, members of the yeast UBP family of DUBs have a highly conserved catalytic core but variable additional domains that contribute to their different functions and protein specificity [180]. Protein specificity contributes to the condition-dependent nature of some redundant DUBs, just as the human DUB USP7 gains increased affinity for p53 only upon genotoxic stress, whereas in unstressed conditions USP7 has specificity for MDM2 [57]. In addition, this thesis and other work have shown that while some subsets of DUBs do not display redundancy under normal growth conditions, when cells deleted for these DUBs are challenged with different drugs cell viability is impaired (Figure 4.3)[98]. These data suggest a paradoxical model in which redundancy and specificity are incorporated into the different levels of protein function (e.g. molecular, target, pathway) under normal conditions, with redundancy or specificity only detectable under stress conditions as determined by evolutionary pressures.

The intertwining of redundancy and specificity creates a challenge when developing inhibitors for DUBs to treat human diseases. This and other studies have demonstrated that individual DUB deletions were not sufficient to kill cells, suggesting that inhibition of individual DUBs may not have a phenotype (Chapter II).

117

Additionally, analysis of DUB deletion strain sensitivities revealed that deletion strains can display different phenotypes under normal growth conditions than they do when combined with different stressors (Chapter IV), suggesting redundancy can be conditional. In order to prevent a DUB from promoting a disease-associated pathway, it is important to identify its specificity and any potential redundancies or genetic interactions. Inhibiting a DUB that targets a specific protein in a disease-causing pathway may not effectively inhibit this pathway if other DUBs are capable of compensating for its loss at a molecular or pathway level. However, administering inhibitors of a group of DUBs – in which only a single DUB is disease-associated – may result in unfavorable off target effects or positive genetic interactions that promote the disease state. Because we do not understand the mechanisms by which most DUBs function, we may be able to improve the potency and specificity of therapies by testing for advantageous combinations of DUB inhibitors and current standards-of-care.

Appendix: Regulation of a transcription factor network by Cdk1 regulates late cell cycle gene expression

Preface

Appendix Figures 1-3, their corresponding figure legends, and Materials and Methods are taken from Landry, et al and Appendix Figure 4 and its figure legend was taken from Arsenault, et al. Experiments in Appendix Figure 1 were performed by Benjamin Landry. All other experiments were performed by Claudine Mapa.

Landry, B. D., **C. E. Mapa**, H. E. Arsenault, K. E. Poti and J. A. Benanti (2014). "Regulation of a transcription factor network by Cdk1 coordinates late cell cycle gene expression." <u>EMBO J</u> **33**(9): 1044-1060.

Arsenault, H. E., J. Roy, **C. E. Mapa**, M. S. Cyert and J. A. Benanti (2015). "Hcm1 integrates signals from Cdk1 and calcineurin to control cell proliferation." <u>Mol Biol Cell</u> 26(20): 3570-3577.

Introduction

In all eukaryotes, cyclin-dependent kinases (CDKs) modulate the activities of networks of transcription factors (TFs) that control the expression of cell cycle genes [1]. This cell-cycle regulated transcription ensures the unidirectional progression of cell cycle events. Almost all cell cycle-regulatory TFs of one network are directly phosphorylated by Cdk1, but the details of this phosphoregulation are not known for many members of this network. In particular, it is unknown how exactly Cdk1 phosphorylation affects a group of four S-phase TFs (Hcm1, Tos4, Yox1, and Yhp1) that promotes the expression of late cell cycle genes [128, 181-183]. Hcm1 is a forkhead family transcriptional activator that regulates mitotic spindle regulators and downstream TFs, while Yox1 and Yhp1 serve as transcriptional repressors during S-phase [184]. Overexpression of Tos4 was reported to slow cell cycle progression and it was identified as a putative transcriptional repressor [185]. In this appendix I describe experiments to characterize Cdk1 regulation of these four TFs and the implications on the yeast cell cycle.

Results

To test the effect of Cdk1 on Tos4, Hcm1, Yox1, and Yhp1, we mutated all Cdk1 phosphorylation consensus sites from S/T-P to alanines to inhibit Cdk1 phosphorylation ("Cdk-" strains) and measured TF protein levels and cell cycle progression from a G1 arrest. We discovered protein levels of mutants are partially stabilized throughout the cell cycle relative to wild type proteins (Appendix Figure 1) and cell cycle progression was slowed [138]. This indicates Cdk1 phosphorylation

promotes both cyclic expression of these TFs and, as a result, progression of cells through the cell cycle. However, half-life assays in strains expressing Cdk1 or SCF mutants show these TFs are still degraded [138], suggesting that Cdk1-independent regulation of these TFs also exist.

After establishing Cdk1 regulates TF protein levels we asked how phosphorylation modulated their activities. Because we could not substantiate reports that Tos4 acts as a transcriptional repressor we did not pursue Tos4 phosphorylation regulation and instead focused on Yox1, Yhp1, and Hcm1. To determine how Cdk1 phosphorylation regulates the activities of Yox1 and its paralog Yhp1, I analyzed regulation of a subset of their target genes upon expression of phosphomutants integrated at their genomic loci (Appendix Figure 2A). Yox1 and Yhp1 both repress expression of genes that peak in M/G1, such as *DBF4, HST4, KIN3,* and *MCM3*, and Yox1 additionally targets *CDC20* and *SPO12*, which peak in G2/M [138, 184]. Expression of Yox1 and Yhp1 M/G1 target genes, but not G2/M genes, was downregulated upon individual and dual expression of phosphomutants. In addition, overexpression of *yox1-13A* led to mitotic arrest [138]. This is consistent with Yox1 and Yhp1's roles in repressing the expression of late cell cycle genes and suggests that Cdk1 phosphorylation relieves Yox1 and Yhp1 repressive activity to promote cell cycle progression. When I tested if this increased repression could be due to increased binding at G2/M gene promoters, I found that Yhp1-13A and particularly Yox1-9A were more abundant at promoters of these target genes (Appendix Figure 2B). These data support the model that Cdk1 phosphorylates Yox1

and Yhp1 to promote their degradation and limit their repressive activities to S-phase.
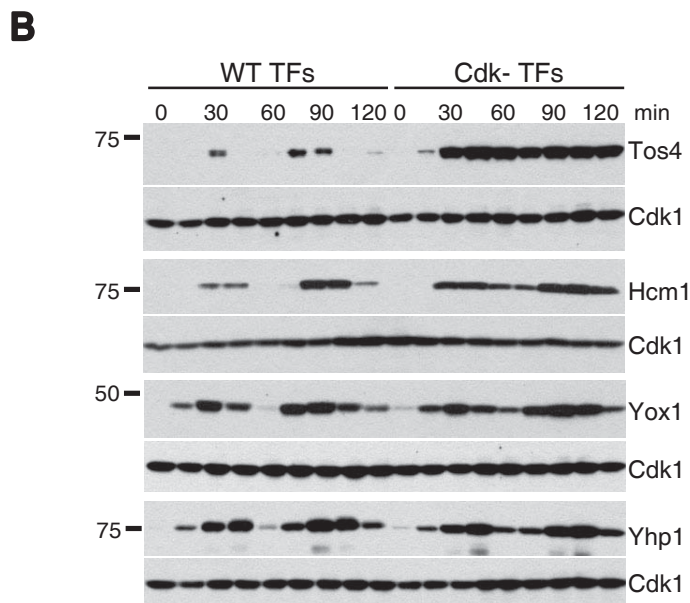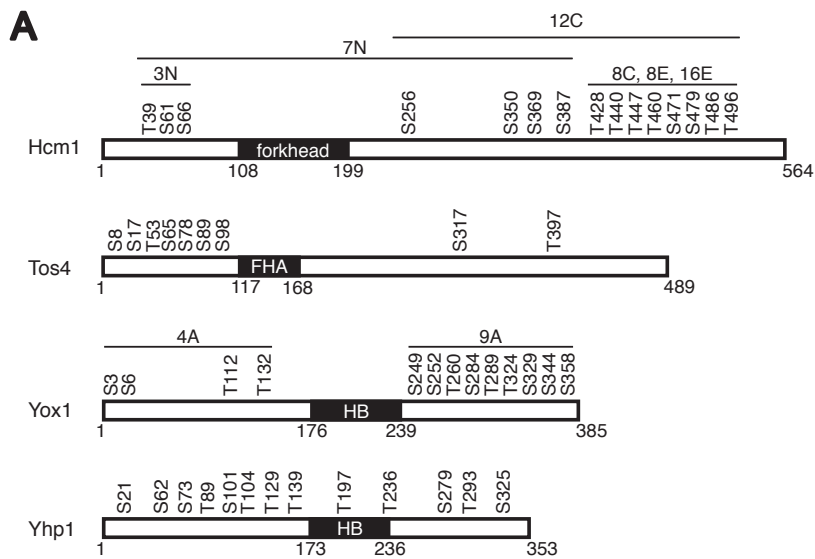
Appendix Figure 1. Cdk1 phosphorylation regulates cyclic TF protein expression. (A) Diagram of each S-phase TF with Cdk1 consensus sites (S/T-P) indicated. For all Cdk- alleles, each S or T was changed to an A, with the exception of the phosphomimetic mutants of Hcm1 (Hcm1-8E or 16E) where the same residues were changed to E (S/T-P to E-P in the 8E mutant, S/T-P to E-E in the 16E mutant). **(B)** Cells expressing Tos4-3FLAG, Tos4-9A-3FLAG, Hcm1-3HA, Hcm1-15A-3HA, Yox1-3V5, Yox1-9A-3V5, Yhp1-13MYC, or Yhp1-13A-13MYC were arrested in G1, released into the cell cycle, and samples taken for Western blot and flow cytometry at 15-min time points. Western blots against epitope tags on WT and Cdk- TFs are shown.
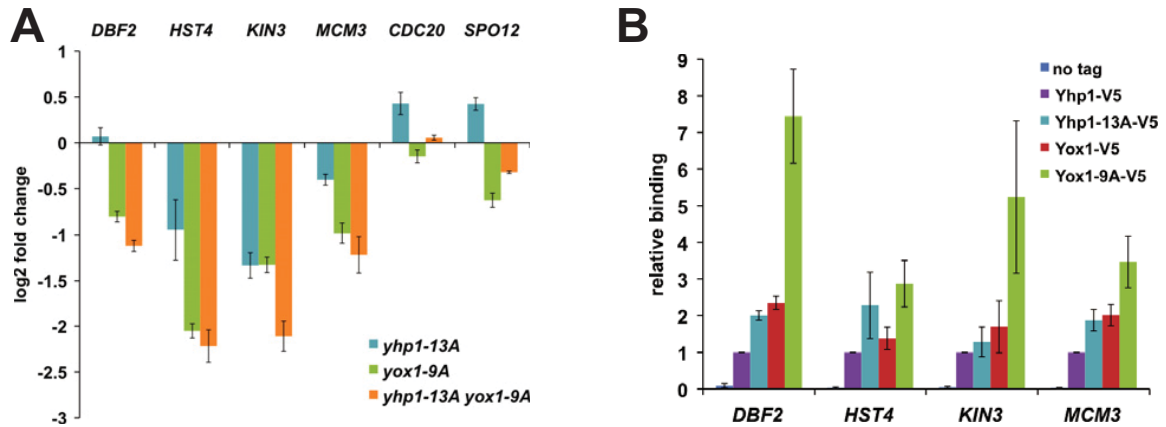
Appendix Figure 2. Phosphorylation inactivates Yox1 and Yhp1. (A) Expression of Yox1/Yhp1 target genes in asynchronous *yhp1-13A, yox1-9A, or yhp1-13A yox1-9A* cells compare to wild type. All values were normalized to *ACT1*. Mean and standard deviations from technical replicates of representative experiment are shown. **(B)** ChIP-qPCR of 3V5-tagged Yhp1, yhp1-13A, Yox1, and yox1-9A compared to an untagged control. Mean and standard deviations for three biological replicates are shown. For each primer set, binding is shown relative to Yhp1.

I also examined the effect of Cdk1 phosphorylation on the activity of the transcriptional activator Hcm1. There are 15 sites in Hcm1, including 2 clusters in the N and C termini; sites at the N terminus regulate degradation [138]. I investigated the function of the C-terminal sites and found mutation of the eight sites to alanine (Hcm1-8C) greatly reduces expression of Hcm1 target genes (Appendix Figure 3A), suggesting this mutant has reduced Hcm1 transcriptional activator function. As another assay to test Hcm1 function, I tested the growth of these mutants on the microtubule depolymerizing drug benomyl. Since Hcm1 regulates several genes that are important for mitotic spindle function, cells lacking Hcm1 activity are sensitive to benomyl. In agreement with my gene expression data, strains expressing Hcm1-15A and Hcm1-8C were both sensitive to the spindle poison benomyl, which indicate that both are loss of function alleles (Appendix Figure 3B). I next generated a phosphomimetic mutant for the 8C sites, Hcm1-16E (in which I mutated each S/T-P to an E-E), which displayed increased abundance at target promoters relative to the 8C mutant and rescued target gene expression and benomyl sensitivity (Appendix 3A-C). This suggests phosphorylation at the C-terminus regulates binding to promoters of its target genes. Together with data that suggests phosphorylation regulates protein stability at the N-terminus [138], these data indicate Cdk1 has opposing effects on Hcm1.
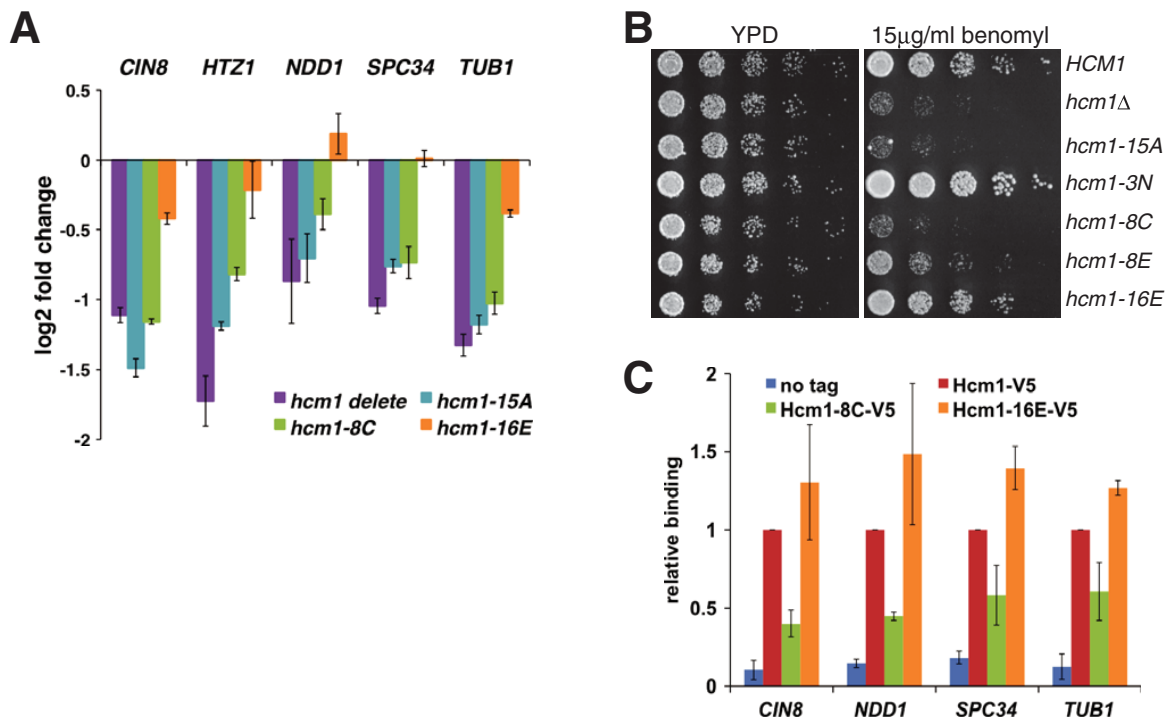
Appendix Figure 3. Phosphorylation of the C-terminus of Hcm1 is required for activity. (A) Cells with the indicated genotypes were synchronized in late S-phase by arresting in G1 and collected 45 min after release. Expression of target genes was compared by RT-qPCR. All values are normalized to *ACT1* and shown relative to Hcm1 WT cells. Mean and standard deviations from technical replicates of a representative experiment are shown. **(B)** Five-fold dilutions of cells with the indicated genotypes were spotted onto rich medium plates (YPD) or plates containing 15 µg/ml benomyl. **(C)** ChIP-qPCR of V5-tagged Hcm1, Hcm1-8C, Hcm1-16E, and an untagged control from cells that were arrested in G1 and collected 37 min after release. Mean and standard deviations from three biological replicates are shown. For each primer set, binding is shown relative to Hcm1 wild type.

While we understand that phosphorylation of different clusters of sites on the transcriptional activator Hcm1 by Cdk1 is important for the progression through the cell cycle, it is unknown if these two clusters are phosphorylated at different times or if they are phosphorylated simultaneously with one cluster being repressed by a phosphatase. In a two-hybrid screen, our collaborators in the Cyert lab identified Hcm1 as a candidate substrate of Calcineurin (CN), a Ca^{2+}-activated phosphatase, which interacts with the CN docking site (PSIEIQ) found on Hcm1 [186]. To characterize this docking site on Hcm1, I deleted the docking site in Hcm1 and generated the mutant *hcm1-ΔPSIEIQ*. I found that this mutant displays similar S-phase protein expression, cell cycle progression, and resistance to benomyl as wild type Hcm1 (Appendix Figure 4A and B), indicating Hcm1-ΔPSIEIQ is a functional protein. Further study of Hcm1 identified CN as the phosphatase that removes activating phosphosites to inhibit Hcm1 in response to environmental stress [186].
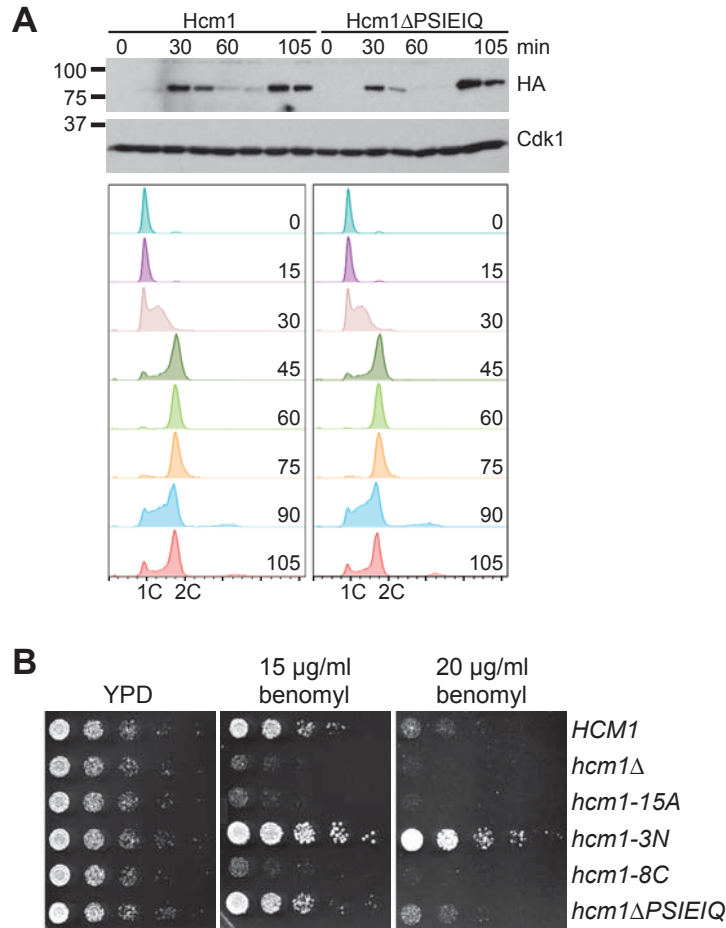
Appendix Figure 4. Characterization of the Hcm1 PSIEIQ mutant. (A) Cells expressing HA-tagged wild type Hcm1 or Hcm1ΔPSIEIQ were arrested in G1 with alpha-factor and released into the cell cycle. Samples were collected for standard Western blotting and flow cytometry at 15 minute intervals. **(B)** Five-fold dilutions of cells with the indicated genotypes were spotted onto rich medium plates (YPD) or plates containing the indicated concentrations of benomyl.

Conclusions

From these data we have a deeper understanding of how Cdk1 regulates late cell cycle events. Cdk1 phosphorylation displays differing control over a network of TFs including transcriptional repressors Yox1 and Yhp1 and transcriptional activator Hcm1. We demonstrated Cdk1 targets Yox1 and Yhp1 for degradation, relieving repression of their target genes (Appendix Figure 2). We also showed that Cdk1 phosphorylates different clusters of sites on Hcm1 to regulate both its stability and activity ([138], Appendix Figure 3). Cdk1-mediated activation of Hcm1 promotes the expression of genes important for proper spindle formation, and a subset of these activation sites are negatively regulated by the Ca^{2+}-activated phosphatase calcineurin [186]. This coordinated regulation of Hcm1 by both Cdk1 and CN allows cells to quickly and precisely tune the processes that drive proliferation in response to changes in the environment. It will be informative to examine what other phosphatases may regulate these cell cycle-regulatory transcription factors, and thus proliferation, under different conditions.

Materials and Methods

Cell cycle analysis

In all experiments, cell cycle positions were confirmed by flow cytometry. Cells were fixed and labeled with Sytox Green (Invitrogen) as previously described (Landry *et al*, 2012). Samples were analyzed using a FACScan (Becton Dickinson) and data analyzed with FlowJo (Tree Star, Inc.) software.

Western blotting

Equivalent optical densities of cells were collected and lysed as previously described (Landry *et al*, 2012). In these experiments, cell pellets were lysed in cold TCA buffer (10 mM Tris pH 8.0, 10% trichloroacetic acid, 25 mM ammonium acetate, 1 mM EDTA). After incubation on ice, lysates were then centrifuged and the pellets resuspended in Resuspension Solution (0.1 M Tris pH 11.0, 3% SDS). Samples were heated to 95°C for 5 minutes, allowed to cool to room temperature, and clarified by centrifugation. Supernatants were added to 4X SDS-PAGE Sample Buffer (0.25 M Tris pH 6.8, 8% SDS, 40% glycerol, 20% β-mercaptoethanol) and heated to 95°C for 5 minutes. Western blotting was performed as previously described (Landry *et al*, 2012) with antibodies against Cdc28 (Cdk1) (sc-6709, Santa Cruz Biotechnology), Flag (Clone M2, Sigma), HA (Clone 16B12, Covance), V5 (Invitrogen), Myc (Clone 9E10, Covance).

RT-qPCR

RNA was digested with DNaseI (New England Biolabs) and precipitated. 1-2 µg of RNA was then reverse transcribed using Random Primers (Invitrogen), followed by digestion with RNaseH (New England Biolabs). For qPCR, RT samples were mixed with 2X SYBR Fast Master Mix Universal (Kapa Biosystems) and indicated primers (Landry *et al* 2014) and reactions were carried out on a Mastercycler ep realplex (Eppendorf) or a Roche LightCycler 96. mRNA levels for each sample were calculated by first subtracting any signal from the no reverse transcriptase control reactions and then normalizing each value to corresponding value for *ACT1*. Fold change was calculated by comparing to mRNA levels in wild type cells.

Serial dilution assays

Cells were grown to mid-log phase and 5-fold dilutions were plated on rich media plates with 2% dextrose, rich media plates with 2% dextrose and benomyl, synthetic complete plates lacking histidine with 2% dextrose, or synthetic complete plates lacking histidine with 2% galactose and incubated at 30°C. Plates were removed from the incubator when colony sizes of control strains were comparable.

Chromatin immunoprecipitation

Equivalent optical densities of cells were fixed using 1/10th volume of Fix Solution (11% formaldehyde, 0.1 M NaCl, 1 mM EDTA, 50 mM HEPES-KOH pH7.6) for 10 minutes and the reaction was then quenched by the addition of 1/5th volume 2.5 M glycine for 5 minutes. Cells were pelleted, washed twice with cold TBS and lysed in

1X Lysis Buffer (25mM HEPES-KOH pH7.6, 400mM NaCl, 0.2% Triton X-100, 1mM EDTA, 10% glycerol, 1 μg/ml leupeptin, 1 μg/ml bestatin, 1 mM benzamidine, 1 μg/ml pepstatin A, 17 μg/ml PMSF, 5 mM sodium fluoride, 80 mM β-glycerophosphate and 1 mM sodium orthovanadate) by bead beating cold for 5 minutes. Cell lysates were washed 3 times with FA Buffer + PIC (50 mM HEPES-KOH pH 7.6, 150 mM NaCl, 1 mM EDTA, 1% Triton X-100, 0.1% Na deoxycholate, 1 μg/ml leupeptin, 1 μg/ml bestatin, 1 mM benzamidine, 1 μg/ml pepstatin A, 17 μg/ml PMSF, 5 mM sodium fluoride, 80 mM β-glycerophosphate and 1 mM sodium orthovanadate), resuspended in 1mL FA Buffer + PIC and sonicated in a Bioruptor (UCD-200) for 30 minutes. Cell lysates were centrifuged and supernatant was transferred to a new tube, a fraction of the lysate was aliquotted into 2X Stop Buffer (20 mM Tris-HCl pH8.0, 100 mM NaCl, 20 mM EDTA, 1% SDS) and the remainder incubated overnight with magnetic beads pre-coupled to the specified antibody. Lysates were then washed 2X with ChIP Buffer + PIC (20 mM Tris-HCl pH 8.0, 150 mM NaCl, 2 mM EDTA, 1% Triton X-100, 1 μg/ml leupeptin, 1 μg/ml bestatin, 1 mM benzamidine), 2X with High Salt ChIP Buffer + PIC (20 mM Tris-HCl pH 8.0, 650 mM NaCl, 2 mM EDTA, 1% Triton X-100, 1 μg/ml leupeptin, 1 μg/ml bestatin, 1 mM benzamidine) and 4X with RIPA Buffer (10 mM Tris-HCl pH 8.0, 0.25 M LiCl, 1 mM EDTA, 0.5% NP-40, 0.5% Na deoxycholate). Crosslinking was reversed by mixing at 65°C for 30 minutes in 2X Stop Buffer. 200 μL TE was added to lysates and samples were treated with Proteinase K for 4 hours at 65°C. Samples were then phenol:chloroform:isoamyl alcohol extracted using phase-lock tubes. Chromatin was

resuspended in 10 mM Tris-HCl pH 8.0 + 1μg/mL RNase A and incubated at 37°C

for 20 minutes. qPCR was then performed as described above compared to a

dilution series made from the input DNA as the standard curve.

Bibliography

1.   Morgan, D. and D.O. Morgan, *The Cell Cycle: Principles of Control*. 2007: OUP/New Science Press.
2.   Hartwell, L., *Defects in a cell cycle checkpoint may be responsible for the genomic instability of cancer cells.* Cell, 1992. **71**(4): p. 543-6.
3.   Hartwell, L.H. and M.B. Kastan, *Cell cycle control and cancer.* Science, 1994. **266**(5192): p. 1821-8.
4.   Price, C., K. Nasmyth, and T. Schuster, *A general approach to the isolation of cell cycle-regulated genes in the budding yeast, Saccharomyces cerevisiae.* J Mol Biol, 1991. **218**(3): p. 543-56.
5.   Hereford, L.M., et al., *Cell-cycle regulation of yeast histone mRNA.* Cell, 1981. **24**(2): p. 367-75.
6.   Cho, R.J., et al., *A genome-wide transcriptional analysis of the mitotic cell cycle.* Mol Cell, 1998. **2**(1): p. 65-73.
7.   Spellman, P.T., et al., *Comprehensive identification of cell cycle-regulated genes of the yeast Saccharomyces cerevisiae by microarray hybridization.* Mol Biol Cell, 1998. **9**(12): p. 3273-97.
8.   Grant, G.D., et al., *Identification of cell cycle-regulated genes periodically expressed in U2OS cells and their regulation by FOXM1 and E2F transcription factors.* Mol Biol Cell, 2013. **24**(23): p. 3634-50.
9.   Gancedo, J.M., S. Lopez, and F. Ballesteros, *Calculation of half-lives of proteins in vivo. Heterogeneity in the rate of degradation of yeast proteins.* Mol Cell Biochem, 1982. **43**(2): p. 89-95.
10.   Belle, A., et al., *Quantification of protein half-lives in the budding yeast proteome.* Proc Natl Acad Sci U S A, 2006. **103**(35): p. 13004-9.
11.   Christiano, R., et al., *Global proteome turnover analyses of the Yeasts S. cerevisiae and S. pombe.* Cell Rep, 2014. **9**(5): p. 1959-1965.
12.   Chau, V., et al., *A multiubiquitin chain is confined to specific lysine in a targeted short-lived protein.* Science, 1989. **243**(4898): p. 1576-83.
13.   Peng, J., et al., *A proteomics approach to understanding protein ubiquitination.* Nat Biotechnol, 2003. **21**(8): p. 921-6.
14.   Spence, J., et al., *A ubiquitin mutant with specific defects in DNA repair and multiubiquitination.* Mol Cell Biol, 1995. **15**(3): p. 1265-73.
15.   Lauwers, E., C. Jacob, and B. Andre, *K63-linked ubiquitin chains as a specific signal for protein sorting into the multivesicular body pathway.* J Cell Biol, 2009. **185**(3): p. 493-502.
16.   Zheng, N. and N. Shabek, *Ubiquitin Ligases: Structure, Function, and Regulation.* Annu Rev Biochem, 2017. **86**: p. 129-157.
17.   Metzger, M.B., V.A. Hristova, and A.M. Weissman, *HECT and RING finger families of E3 ubiquitin ligases at a glance.* J Cell Sci, 2012. **125**(Pt 3): p. 531-7.

18.   Willems, A.R., M. Schwab, and M. Tyers, *A hitchhiker's guide to the cullin ubiquitin ligases: SCF and its kin.* Biochim Biophys Acta, 2004. **1695**(1-3): p. 133-70.

19.   Davey, N.E. and D.O. Morgan, *Building a Regulatory Network with Short Linear Sequence Motifs: Lessons from the Degrons of the Anaphase-Promoting Complex.* Mol Cell, 2016. **64**(1): p. 12-23.

20.   Komander, D., M.J. Clague, and S. Urbe, *Breaking the chains: structure and function of the deubiquitinases.* Nat Rev Mol Cell Biol, 2009. **10**(8): p. 550-63.

21.   Leznicki, P. and Y. Kulathu, *Mechanisms of regulation and diversification of deubiquitylating enzyme function.* J Cell Sci, 2017. **130**(12): p. 1997-2006.

22.   Kouranti, I., et al., *A global census of fission yeast deubiquitinating enzyme localization and interaction networks reveals distinct compartmentalization profiles and overlapping functions in endocytosis and polarity.* PLoS Biol, 2010. **8**(9).

23.   Amerik, A.Y. and M. Hochstrasser, *Mechanism and function of deubiquitinating enzymes.* Biochim Biophys Acta, 2004. **1695**(1-3): p. 189-207.

24.   Abdul Rehman, S.A., et al., *MINDY-1 Is a Member of an Evolutionarily Conserved and Structurally Distinct New Family of Deubiquitinating Enzymes.* Mol Cell, 2016. **63**(1): p. 146-55.

25.   Mevissen, T.E.T. and D. Komander, *Mechanisms of Deubiquitinase Specificity and Regulation.* Annu Rev Biochem, 2017. **86**: p. 159-192.

26.   Mevissen, T.E., et al., *OTU deubiquitinases reveal mechanisms of linkage specificity and enable ubiquitin chain restriction analysis.* Cell, 2013. **154**(1): p. 169-84.

27.   Schaefer, J.B. and D.O. Morgan, *Protein-linked ubiquitin chain structure restricts activity of deubiquitinating enzymes.* J Biol Chem, 2011. **286**(52): p. 45186-96.

28.   Worden, E.J., C. Padovani, and A. Martin, *Structure of the Rpn11-Rpn8 dimer reveals mechanisms of substrate deubiquitination during proteasomal degradation.* Nat Struct Mol Biol, 2014. **21**(3): p. 220-7.

29.   Mansour, W., et al., *Disassembly of Lys11 and mixed linkage polyubiquitin conjugates provides insights into function of proteasomal deubiquitinases Rpn11 and Ubp6.* J Biol Chem, 2015. **290**(8): p. 4688-704.

30.   Ritorto, M.S., et al., *Screening of DUB activity and specificity by MALDI-TOF mass spectrometry.* Nat Commun, 2014. **5**: p. 4763.

31.   Ventii, K.H. and K.D. Wilkinson, *Protein partners of deubiquitinating enzymes.* Biochem J, 2008. **414**(2): p. 161-75.

32.   Sowa, M.E., et al., *Defining the human deubiquitinating enzyme interaction landscape.* Cell, 2009. **138**(2): p. 389-403.

33.   Bachmair, A., D. Finley, and A. Varshavsky, *In vivo half-life of a protein is a function of its amino-terminal residue.* Science, 1986. **234**(4773): p. 179-86.

34.   Nicassio, F., et al., *Human USP3 is a chromatin modifier required for S phase progression and genome stability.* Curr Biol, 2007. **17**(22): p. 1972-7.

35.   Kerppola, T.K., *Bimolecular fluorescence complementation (BiFC) analysis as a probe of protein interactions in living cells.* Annu Rev Biophys, 2008. **37**: p. 465-87.

36. Miller, K.E., et al., *Bimolecular Fluorescence Complementation (BiFC) Analysis: Advances and Recent Applications for Genome-Wide Interaction Studies.* J Mol Biol, 2015. **427**(11): p. 2039-2055.

37. Blondel, M., et al., *Degradation of Hof1 by SCF(Grr1) is important for actomyosin contraction during cytokinesis in yeast.* EMBO J, 2005. **24**(7): p. 1440-52.

38. Nijman, S.M., et al., *A genomic and functional inventory of deubiquitinating enzymes.* Cell, 2005. **123**(5): p. 773-86.

39. Loch, C.M. and J.E. Strickler, *A microarray of ubiquitylated proteins for profiling deubiquitylase activity reveals the critical roles of both chain and substrate.* Biochim Biophys Acta, 2012. **1823**(11): p. 2069-78.

40. Poulsen, J.W., et al., *Comprehensive profiling of proteome changes upon sequential deletion of deubiquitylating enzymes.* J Proteomics, 2012. **75**(13): p. 3886-97.

41. Isasa, M., et al., *Multiplexed, Proteome-Wide Protein Expression Profiling: Yeast Deubiquitylating Enzyme Knockout Strains.* J Proteome Res, 2015. **14**(12): p. 5306-17.

42. D'Arcy, P. and S. Linder, *Proteasome deubiquitinases as novel targets for cancer therapy.* Int J Biochem Cell Biol, 2012. **44**(11): p. 1729-38.

43. Heideker, J. and I.E. Wertz, *DUBs, the regulation of cell identity and disease.* Biochem J, 2015. **467**(1): p. 191.

44. Stegmeier, F., et al., *Anaphase initiation is regulated by antagonistic ubiquitination and deubiquitination activities.* Nature, 2007. **446**(7138): p. 876-81.

45. Qiu, X.B. and A.L. Goldberg, *Nrdp1/FLRF is a ubiquitin ligase promoting ubiquitination and degradation of the epidermal growth factor receptor family member, ErbB3.* Proc Natl Acad Sci U S A, 2002. **99**(23): p. 14843-8.

46. Wu, X., et al., *Stabilization of the E3 ubiquitin ligase Nrdp1 by the deubiquitinating enzyme USP8.* Mol Cell Biol, 2004. **24**(17): p. 7748-57.

47. De Ceuninck, L., et al., *Reciprocal cross-regulation between RNF41 and USP8 controls cytokine receptor sorting and processing.* J Cell Sci, 2013. **126**(Pt 16): p. 3770-81.

48. Holbro, T., G. Civenni, and N.E. Hynes, *The ErbB receptors and their role in cancer progression.* Exp Cell Res, 2003. **284**(1): p. 99-110.

49. Shi, C.S. and J.H. Kehrl, *Tumor necrosis factor (TNF)-induced germinal center kinase-related (GCKR) and stress-activated protein kinase (SAPK) activation depends upon the E2/E3 complex Ubc13-Uev1A/TNF receptor-associated factor 2 (TRAF2).* J Biol Chem, 2003. **278**(17): p. 15429-34.

50. Jono, H., et al., *NF-kappaB is essential for induction of CYLD, the negative regulator of NF-kappaB: evidence for a novel inducible autoregulatory feedback pathway.* J Biol Chem, 2004. **279**(35): p. 36171-4.

51. Trompouki, E., et al., *CYLD is a deubiquitinating enzyme that negatively regulates NF-kappaB activation by TNFR family members.* Nature, 2003. **424**(6950): p. 793-6.

52. Brummelkamp, T.R., et al., *Loss of the cylindromatosis tumour suppressor inhibits apoptosis by activating NF-kappaB.* Nature, 2003. **424**(6950): p. 797-801.

53. Kovalenko, A., et al., *The tumour suppressor CYLD negatively regulates NF-kappaB signalling by deubiquitination.* Nature, 2003. **424**(6950): p. 801-5.

54.   Sheng, Y., et al., *Molecular recognition of p53 and MDM2 by USP7/HAUSP.* Nat Struct Mol Biol, 2006. **13**(3): p. 285-91.

55.   Haupt, Y., et al., *Mdm2 promotes the rapid degradation of p53.* Nature, 1997. **387**(6630): p. 296-9.

56.   Fang, S., et al., *Mdm2 is a RING finger-dependent ubiquitin protein ligase for itself and p53.* J Biol Chem, 2000. **275**(12): p. 8945-51.

57.   Vijayakumaran, R., et al., *Regulation of Mutant p53 Protein Expression.* Front Oncol, 2015. **5**: p. 284.

58.   Kee, Y., N. Lyon, and J.M. Huibregtse, *The Rsp5 ubiquitin ligase is coupled to and antagonized by the Ubp2 deubiquitinating enzyme.* EMBO J, 2005. **24**(13): p. 2414-24.

59.   Fang, N.N., et al., *Deubiquitinase activity is required for the proteasomal degradation of misfolded cytosolic proteins upon heat-stress.* Nat Commun, 2016. **7**: p. 12907.

60.   Kee, Y., et al., *The deubiquitinating enzyme Ubp2 modulates Rsp5-dependent Lys63-linked polyubiquitin conjugates in Saccharomyces cerevisiae.* J Biol Chem, 2006. **281**(48): p. 36724-31.

61.   Kimura, Y. and K. Tanaka, *Regulatory mechanisms involved in the control of ubiquitin homeostasis.* J Biochem, 2010. **147**(6): p. 793-8.

62.   Finley, D., E. Ozkaynak, and A. Varshavsky, *The yeast polyubiquitin gene is essential for resistance to high temperatures, starvation, and other stresses.* Cell, 1987. **48**(6): p. 1035-46.

63.   Ryu, K.Y., et al., *The mouse polyubiquitin gene UbC is essential for fetal liver development, cell-cycle progression and stress tolerance.* EMBO J, 2007. **26**(11): p. 2693-706.

64.   Ryu, K.Y., et al., *The mouse polyubiquitin gene Ubb is essential for meiotic progression.* Mol Cell Biol, 2008. **28**(3): p. 1136-46.

65.   Ryu, K.Y., et al., *Hypothalamic neurodegeneration and adult-onset obesity in mice lacking the Ubb polyubiquitin gene.* Proc Natl Acad Sci U S A, 2008. **105**(10): p. 4016-21.

66.   London, M.K., et al., *Regulatory mechanisms controlling biogenesis of ubiquitin and the proteasome.* FEBS Lett, 2004. **567**(2-3): p. 259-64.

67.   Zhou, J., et al., *Role and regulation of autophagy in heat stress responses of tomato plants.* Front Plant Sci, 2014. **5**: p. 174.

68.   Sun, C., et al., *Elevation of proteasomal substrate levels sensitizes cells to apoptosis induced by inhibition of proteasomal deubiquitinases.* PLoS One, 2014. **9**(10): p. e108839.

69.   Yau, R.G., et al., *Assembly and Function of Heterotypic Ubiquitin Chains in Cell-Cycle and Protein Quality Control.* Cell, 2017. **171**(4): p. 918-933 e20.

70.   Costanzo, M., et al., *CDK activity antagonizes Whi5, an inhibitor of G1/S transcription in yeast.* Cell, 2004. **117**(7): p. 899-913.

71.   de Bruin, R.A., et al., *Cln3 activates G1-specific transcription via phosphorylation of the SBF bound repressor Whi5.* Cell, 2004. **117**(7): p. 887-98.

72. Tyers, M., et al., *The Cln3-Cdc28 kinase complex of S. cerevisiae is regulated by proteolysis and phosphorylation.* EMBO J, 1992. **11**(5): p. 1773-84.

73. Landry, B.D., et al., *F-box protein specificity for g1 cyclins is dictated by subcellular localization.* PLoS Genet, 2012. **8**(7): p. e1002851.

74. Tyers, M., *The cyclin-dependent kinase inhibitor p40SIC1 imposes the requirement for Cln G1 cyclin function at Start.* Proc Natl Acad Sci U S A, 1996. **93**(15): p. 7772-6.

75. Schwob, E., et al., *The B-type cyclin kinase inhibitor p40SIC1 controls the G1 to S transition in S. cerevisiae.* Cell, 1994. **79**(2): p. 233-44.

76. Lanker, S., M.H. Valdivieso, and C. Wittenberg, *Rapid degradation of the G1 cyclin Cln2 induced by CDK-dependent phosphorylation.* Science, 1996. **271**(5255): p. 1597-601.

77. Willems, A.R., et al., *Cdc53 targets phosphorylated G1 cyclins for degradation by the ubiquitin proteolytic pathway.* Cell, 1996. **86**(3): p. 453-63.

78. Dirick, L. and K. Nasmyth, *Positive feedback in the activation of G1 cyclins in yeast.* Nature, 1991. **351**(6329): p. 754-7.

79. Clute, P. and J. Pines, *Temporal and spatial control of cyclin B1 destruction in metaphase.* Nat Cell Biol, 1999. **1**(2): p. 82-7.

80. Uhlmann, F., F. Lottspeich, and K. Nasmyth, *Sister-chromatid separation at anaphase onset is promoted by cleavage of the cohesin subunit Scc1.* Nature, 1999. **400**(6739): p. 37-42.

81. Charles, J.F., et al., *The Polo-related kinase Cdc5 activates and is destroyed by the mitotic cyclin destruction machinery in S. cerevisiae.* Curr Biol, 1998. **8**(9): p. 497-507.

82. Zachariae, W. and K. Nasmyth, *Whose end is destruction: cell division and the anaphase-promoting complex.* Genes Dev, 1999. **13**(16): p. 2039-58.

83. McGarry, T.J. and M.W. Kirschner, *Geminin, an inhibitor of DNA replication, is degraded during mitosis.* Cell, 1998. **93**(6): p. 1043-53.

84. Petersen, B.O., et al., *Cell cycle- and cell growth-regulated proteolysis of mammalian CDC6 is dependent on APC-CDH1.* Genes Dev, 2000. **14**(18): p. 2330-43.

85. Ferreira, M.F., et al., *Dbf4p, an essential S phase-promoting factor, is targeted for degradation by the anaphase-promoting complex.* Mol Cell Biol, 2000. **20**(1): p. 242-8.

86. Ostapenko, D., J.L. Burton, and M.J. Solomon, *The Ubp15 deubiquitinase promotes timely entry into S phase in Saccharomyces cerevisiae.* Mol Biol Cell, 2015. **26**(12): p. 2205-16.

87. Gallego-Sanchez, A., et al., *Reversal of PCNA ubiquitylation by Ubp10 in Saccharomyces cerevisiae.* PLoS Genet, 2012. **8**(7): p. e1002826.

88. Ren, J., et al., *Hse1, a component of the yeast Hrs-STAM ubiquitin-sorting complex, associates with ubiquitin peptidases and a ligase to control sorting efficiency into multivesicular bodies.* Mol Biol Cell, 2007. **18**(1): p. 324-35.

89. Bohm, S., et al., *The Budding Yeast Ubiquitin Protease Ubp7 Is a Novel Component Involved in S Phase Progression.* J Biol Chem, 2016. **291**(9): p. 4442-52.

90. Alcasabas, A.A., et al., *Mrc1 transduces signals of DNA replication stress to activate Rad53.* Nat Cell Biol, 2001. **3**(11): p. 958-65.

91.   Benanti, J.A., *Coordination of cell growth and division by the ubiquitin-proteasome system.* Semin Cell Dev Biol, 2012. **23**(5): p. 492-8.

92.   Mocciaro, A. and M. Rape, *Emerging regulatory mechanisms in ubiquitin-dependent cell cycle control.* J Cell Sci, 2012. **125**(Pt 2): p. 255-63.

93.   Elmore, Z.C., et al., *Histone H2B ubiquitination promotes the function of the anaphase-promoting complex/cyclosome in Schizosaccharomyces pombe.* G3 (Bethesda), 2014. **4**(8): p. 1529-38.

94.   Darling, S., et al., *Regulation of the cell cycle and centrosome biology by deubiquitylases.* Biochem Soc Trans, 2017. **45**(5): p. 1125-1136.

95.   Leggett, D.S., et al., *Multiple associated proteins regulate proteasome structure and function.* Mol Cell, 2002. **10**(3): p. 495-507.

96.   Krogan, N.J., et al., *Global landscape of protein complexes in the yeast Saccharomyces cerevisiae.* Nature, 2006. **440**(7084): p. 637-43.

97.   Richardson, L.A., et al., *A conserved deubiquitinating enzyme controls cell growth by regulating RNA polymerase I stability.* Cell Rep, 2012. **2**(2): p. 372-85.

98.   Beckley, J.R., et al., *A Degenerate Cohort of Yeast Membrane Trafficking DUBs Mediates Cell Polarity and Survival.* Mol Cell Proteomics, 2015. **14**(12): p. 3132-41.

99.   Sopko, R., et al., *Mapping pathways and phenotypes by systematic gene overexpression.* Mol Cell, 2006. **21**(3): p. 319-30.

100.   Chong, Y.T., et al., *Yeast Proteome Dynamics from Single Cell Imaging and Automated Analysis.* Cell, 2015. **161**(6): p. 1413-24.

101.   Cohen, M., et al., *Ubp3 requires a cofactor, Bre5, to specifically de-ubiquitinate the COPII protein, Sec23.* Nat Cell Biol, 2003. **5**(7): p. 661-7.

102.   Amerik, A., N. Sindhi, and M. Hochstrasser, *A conserved late endosome-targeting signal required for Doa4 deubiquitylating enzyme function.* J Cell Biol, 2006. **175**(5): p. 825-35.

103.   Luhtala, N. and G. Odorizzi, *Bro1 coordinates deubiquitination in the multivesicular body pathway by recruiting Doa4 to endosomes.* J Cell Biol, 2004. **166**(5): p. 717-29.

104.   Verma, R., et al., *Proteasomal proteomics: identification of nucleotide-sensitive proteasome-interacting proteins by mass spectrometric analysis of affinity-purified proteasomes.* Mol Biol Cell, 2000. **11**(10): p. 3425-39.

105.   Henry, K.W., et al., *Transcriptional activation via sequential histone H2B ubiquitylation and deubiquitylation, mediated by SAGA-associated Ubp8.* Genes Dev, 2003. **17**(21): p. 2648-63.

106.   Kahana, A. and D.E. Gottschling, *DOT4 links silencing and cell growth in Saccharomyces cerevisiae.* Mol Cell Biol, 1999. **19**(10): p. 6608-20.

107.   Godderz, D., et al., *The deubiquitylating enzyme Ubp12 regulates Rad23-dependent proteasomal degradation.* J Cell Sci, 2017. **130**(19): p. 3336-3346.

108.   Debelyy, M.O., et al., *Ubp15p, a ubiquitin hydrolase associated with the peroxisomal export machinery.* J Biol Chem, 2011. **286**(32): p. 28223-34.

109.   Kinner, A. and R. Kolling, *The yeast deubiquitinating enzyme Ubp16 is anchored to the outer mitochondrial membrane.* FEBS Lett, 2003. **549**(1-3): p. 135-40.

110. Rumpf, S. and S. Jentsch, *Functional division of substrate processing cofactors of the ubiquitin-selective Cdc48 chaperone.* Mol Cell, 2006. **21**(2): p. 261-9.

111. Ghaemmaghami, S., et al., *Global analysis of protein expression in yeast.* Nature, 2003. **425**(6959): p. 737-41.

112. Mapa, C.E., et al., *A balance of deubiquitinating enzymes controls cell cycle entry.* Mol Biol Cell, 2018: p. mbcE18070425.

113. Schulein-Volk, C., et al., *Dual regulation of Fbw7 function and oncogenic transformation by Usp28.* Cell Rep, 2014. **9**(3): p. 1099-109.

114. Sun, X.X., et al., *The nucleolar ubiquitin-specific protease USP36 deubiquitinates and stabilizes c-Myc.* Proc Natl Acad Sci U S A, 2015. **112**(12): p. 3734-9.

115. Singer, M.S., et al., *Identification of high-copy disruptors of telomeric silencing in Saccharomyces cerevisiae.* Genetics, 1998. **150**(2): p. 613-32.

116. Reed, B.J., M.N. Locke, and R.G. Gardner, *A Conserved Deubiquitinating Enzyme Uses Intrinsically Disordered Regions to Scaffold Multiple Protein Interaction Sites.* J Biol Chem, 2015. **290**(33): p. 20601-12.

117. Fragkos, M., et al., *DNA replication origin activation in space and time.* Nat Rev Mol Cell Biol, 2015. **16**(6): p. 360-74.

118. Costanzo, M., et al., *A global genetic interaction network maps a wiring diagram of cellular function.* Science, 2016. **353**(6306).

119. Hanna, J., D.S. Leggett, and D. Finley, *Ubiquitin depletion as a key mediator of toxicity by translational inhibitors.* Mol Cell Biol, 2003. **23**(24): p. 9251-61.

120. Hanna, J., et al., *Deubiquitinating enzyme Ubp6 functions noncatalytically to delay proteasomal degradation.* Cell, 2006. **127**(1): p. 99-111.

121. Lee, B.H., et al., *Enhancement of proteasome activity by a small-molecule inhibitor of USP14.* Nature, 2010. **467**(7312): p. 179-84.

122. Peth, A., H.C. Besche, and A.L. Goldberg, *Ubiquitinated proteins activate the proteasome by binding to Usp14/Ubp6, which causes 20S gate opening.* Mol Cell, 2009. **36**(5): p. 794-804.

123. Amerik, A.Y., S.J. Li, and M. Hochstrasser, *Analysis of the deubiquitinating enzymes of the yeast Saccharomyces cerevisiae.* Biol Chem, 2000. **381**(9-10): p. 981-92.

124. Chernova, T.A., et al., *Pleiotropic effects of Ubp6 loss on drug sensitivities and yeast prion are due to depletion of the free ubiquitin pool.* J Biol Chem, 2003. **278**(52): p. 52102-15.

125. Amerik, A., et al., *In vivo disassembly of free polyubiquitin chains by yeast Ubp14 modulates rates of protein degradation by the proteasome.* EMBO J, 1997. **16**(16): p. 4826-38.

126. Verma, R., et al., *Role of Rpn11 metalloprotease in deubiquitination and degradation by the 26S proteasome.* Science, 2002. **298**(5593): p. 611-5.

127. Ficarro, S.B., et al., *Phosphoproteome analysis by mass spectrometry and its application to Saccharomyces cerevisiae.* Nat Biotechnol, 2002. **20**(3): p. 301-5.

128. Holt, L.J., et al., *Global analysis of Cdk1 substrate phosphorylation sites provides insights into evolution.* Science, 2009. **325**(5948): p. 1682-6.

129. Wu, R., et al., *A large-scale method to measure absolute protein phosphorylation stoichiometries.* Nat Methods, 2011. **8**(8): p. 677-83.

130. Linghu, B., J. Callis, and M.G. Goebl, *Rub1p processing by Yuh1p is required for wild-type levels of Rub1p conjugation to Cdc53p.* Eukaryot Cell, 2002. **1**(3): p. 491-4.

131. Gardner, R.G., Z.W. Nelson, and D.E. Gottschling, *Ubp10/Dot4p regulates the persistence of ubiquitinated histone H2B: distinct roles in telomeric silencing and general chromatin.* Mol Cell Biol, 2005. **25**(14): p. 6123-39.

132. Shi, Y., et al., *Rpn1 provides adjacent receptor sites for substrate binding and deubiquitination by the proteasome.* Science, 2016. **351**(6275).

133. Lee, B.H., et al., *USP14 deubiquitinates proteasome-bound substrates that are ubiquitinated at multiple sites.* Nature, 2016. **532**(7599): p. 398-401.

134. Benanti, J.A., et al., *A proteomic screen reveals SCFGrr1 targets that regulate the glycolytic-gluconeogenic switch.* Nat Cell Biol, 2007. **9**(10): p. 1184-91.

135. Rothstein, R., *Targeting, disruption, replacement, and allele rescue: integrative DNA transformation in yeast.* Methods Enzymol, 1991. **194**: p. 281-301.

136. Kishi, T. and F. Yamao, *An essential function of Grr1 for the degradation of Cln2 is to act as a binding core that links Cln2 to Skp1.* J Cell Sci, 1998. **111 (Pt 24)**: p. 3655-61.

137. Huh, W.K., et al., *Global analysis of protein localization in budding yeast.* Nature, 2003. **425**(6959): p. 686-91.

138. Landry, B.D., et al., *Regulation of a transcription factor network by Cdk1 coordinates late cell cycle gene expression.* EMBO J, 2014. **33**(9): p. 1044-60.

139. Willis, N. and N. Rhind, *Mus81, Rhp51(Rad51), and Rqh1 form an epistatic pathway required for the S-phase DNA damage checkpoint.* Mol Biol Cell, 2009. **20**(3): p. 819-33.

140. Sagona, A.P. and H. Stenmark, *Cytokinesis and cancer.* FEBS Lett, 2010. **584**(12): p. 2652-61.

141. Vallen, E.A., J. Caviston, and E. Bi, *Roles of Hof1p, Bni1p, Bnr1p, and myo1p in cytokinesis in Saccharomyces cerevisiae.* Mol Biol Cell, 2000. **11**(2): p. 593-611.

142. Wang, S.F. and M. Volini, *Studies on the active site of rhodanese.* J Biol Chem, 1968. **243**(20): p. 5465-70.

143. Wolters, N. and A. Amerik, *The N-terminal domains determine cellular localization and functions of the Doa4 and Ubp5 deubiquitinating enzymes.* Biochem Biophys Res Commun, 2015. **467**(3): p. 570-6.

144. Malleshaiah, M.K., et al., *The scaffold protein Ste5 directly controls a switch-like mating decision in yeast.* Nature, 2010. **465**(7294): p. 101-5.

145. Baker, R.T., J.W. Tobias, and A. Varshavsky, *Ubiquitin-specific proteases of Saccharomyces cerevisiae. Cloning of UBP2 and UBP3, and functional analysis of the UBP gene family.* J Biol Chem, 1992. **267**(32): p. 23364-75.

146. Brew, C.T. and T.C. Huffaker, *The yeast ubiquitin protease, Ubp3p, promotes protein stability.* Genetics, 2002. **162**(3): p. 1079-89.

147. Kapitzky, L., et al., *Cross-species chemogenomic profiling reveals evolutionarily conserved drug mode of action.* Mol Syst Biol, 2010. **6**: p. 451.

148. Bashore, C., et al., *Ubp6 deubiquitinase controls conformational dynamics and substrate degradation of the 26S proteasome.* Nat Struct Mol Biol, 2015. **22**(9): p. 712-9.

149. Kim, H.T. and A.L. Goldberg, *The deubiquitinating enzyme Usp14 allosterically inhibits multiple proteasomal activities and ubiquitin-independent proteolysis.* J Biol Chem, 2017. **292**(23): p. 9830-9839.

150. Kristariyanto, Y.A., et al., *A single MIU motif of MINDY-1 recognizes K48-linked polyubiquitin chains.* EMBO Rep, 2017. **18**(3): p. 392-402.

151. Xu, M., et al., *Timing of transcriptional quiescence during gametogenesis is controlled by global histone H3K4 demethylation.* Dev Cell, 2012. **23**(5): p. 1059-71.

152. Wright, P.E. and H.J. Dyson, *Intrinsically disordered proteins in cellular signalling and regulation.* Nat Rev Mol Cell Biol, 2015. **16**(1): p. 18-29.

153. Rosenbaum, J.C., et al., *Disorder targets misorder in nuclear quality control degradation: a disordered ubiquitin ligase directly recognizes its misfolded substrates.* Mol Cell, 2011. **41**(1): p. 93-106.

154. Schulze, J.M., et al., *Splitting the task: Ubp8 and Ubp10 deubiquitinate different cellular pools of H2BK123.* Genes Dev, 2011. **25**(21): p. 2242-7.

155. Finley, D., *Recognition and processing of ubiquitin-protein conjugates by the proteasome.* Annu Rev Biochem, 2009. **78**: p. 477-513.

156. Welsch, C.A., et al., *Ubiquitin pathway proteins influence the mechanism of action of the novel immunosuppressive drug FTY720 in Saccharomyces cerevisiae.* J Biol Chem, 2003. **278**(29): p. 26976-82.

157. Meyer, N. and L.Z. Penn, *Reflecting on 25 years with MYC.* Nat Rev Cancer, 2008. **8**(12): p. 976-90.

158. DeVine, T., R.C. Sears, and M.S. Dai, *The ubiquitin-specific protease USP36 is a conserved histone H2B deubiquitinase.* Biochem Biophys Res Commun, 2018. **495**(3): p. 2363-2368.

159. Sun, X.X., R.C. Sears, and M.S. Dai, *Deubiquitinating c-Myc: USP36 steps up in the nucleolus.* Cell Cycle, 2015. **14**(24): p. 3786-93.

160. Fraile, J.M., et al., *Loss of the deubiquitinase USP36 destabilizes the RNA helicase DHX33 and causes preimplantation lethality in mice.* J Biol Chem, 2018. **293**(6): p. 2183-2194.

161. Thevenon, D., et al., *The Drosophila ubiquitin-specific protease dUSP36/Scny targets IMD to prevent constitutive immune signaling.* Cell Host Microbe, 2009. **6**(4): p. 309-20.

162. Taillebourg, E., et al., *The deubiquitinating enzyme USP36 controls selective autophagy activation by ubiquitinated proteins.* Autophagy, 2012. **8**(5): p. 767-79.

163. Hadari, T., et al., *A ubiquitin C-terminal isopeptidase that acts on polyubiquitin chains. Role in protein degradation.* J Biol Chem, 1992. **267**(2): p. 719-27.

164. Eisele, F., et al., *Mutants of the deubiquitinating enzyme Ubp14 decipher pathway diversity of ubiquitin-proteasome linked protein degradation.* Biochem Biophys Res Commun, 2006. **350**(2): p. 329-33.

165.   Dayal, S., et al., *Suppression of the deubiquitinating enzyme USP5 causes the accumulation of unanchored polyubiquitin and the activation of p53.* J Biol Chem, 2009. **284**(8): p. 5030-41.

166.   Liu, Y., et al., *Usp5 functions as an oncogene for stimulating tumorigenesis in hepatocellular carcinoma.* Oncotarget, 2017. **8**(31): p. 50655-50664.

167.   Li, X.Y., et al., *USP5 promotes tumorigenesis and progression of pancreatic cancer by stabilizing FoxM1 protein.* Biochem Biophys Res Commun, 2017. **492**(1): p. 48-54.

168.   Potu, H., et al., *Usp5 links suppression of p53 and FAS levels in melanoma to the BRAF pathway.* Oncotarget, 2014. **5**(14): p. 5559-69.

169.   D'Amato, C.J. and S.P. Hicks, *Neuropathologic alterations in the ataxia (paralytic) mouse.* Arch Pathol, 1965. **80**(6): p. 604-12.

170.   Anderson, C., et al., *Loss of Usp14 results in reduced levels of ubiquitin in ataxia mice.* J Neurochem, 2005. **95**(3): p. 724-31.

171.   Wilson, S.M., et al., *Synaptic defects in ataxia mice result from a mutation in Usp14, encoding a ubiquitin-specific protease.* Nat Genet, 2002. **32**(3): p. 420-5.

172.   Koulich, E., X. Li, and G.N. DeMartino, *Relative structural and functional roles of multiple deubiquitylating proteins associated with mammalian 26S proteasome.* Mol Biol Cell, 2008. **19**(3): p. 1072-82.

173.   Boselli, M., et al., *An inhibitor of the proteasomal deubiquitinating enzyme USP14 induces tau elimination in cultured neurons.* J Biol Chem, 2017. **292**(47): p. 19209-19225.

174.   Kiprowska, M.J., et al., *Neurotoxic mechanisms by which the USP14 inhibitor IU1 depletes ubiquitinated proteins and Tau in rat cerebral cortical neurons: Relevance to Alzheimer's disease.* Biochim Biophys Acta Mol Basis Dis, 2017. **1863**(6): p. 1157-1170.

175.   Liu, B., et al., *Proteome-wide analysis of USP14 substrates revealed its role in hepatosteatosis via stabilization of FASN.* Nat Commun, 2018. **9**(1): p. 4770.

176.   Kellis, M., B.W. Birren, and E.S. Lander, *Proof and evolutionary analysis of ancient genome duplication in the yeast Saccharomyces cerevisiae.* Nature, 2004. **428**(6983): p. 617-24.

177.   Dehal, P. and J.L. Boore, *Two rounds of whole genome duplication in the ancestral vertebrate.* PLoS Biol, 2005. **3**(10): p. e314.

178.   Ghosh, S. and T.J. O'Connor, *Beyond Paralogs: The Multiple Layers of Redundancy in Bacterial Pathogenesis.* Front Cell Infect Microbiol, 2017. **7**: p. 467.

179.   Yamada, M., et al., *ATR-Chk1-APC/CCdh1-dependent stabilization of Cdc7-ASK (Dbf4) kinase is required for DNA lesion bypass under replication stress.* Genes Dev, 2013. **27**(22): p. 2459-72.

180.   Reyes-Turcu, F.E., K.H. Ventii, and K.D. Wilkinson, *Regulation and cellular roles of ubiquitin-specific deubiquitinating enzymes.* Annu Rev Biochem, 2009. **78**: p. 363-97.

181.   Ubersax, J.A., et al., *Targets of the cyclin-dependent kinase Cdk1.* Nature, 2003. **425**(6960): p. 859-64.

182.   Loog, M. and D.O. Morgan, *Cyclin specificity in the phosphorylation of cyclin-dependent kinase substrates.* Nature, 2005. **434**(7029): p. 104-8.

183.   Koivomagi, M., et al., *Cascades of multisite phosphorylation control Sic1 destruction at the onset of S phase.* Nature, 2011. **480**(7375): p. 128-31.

184.   Pramila, T., et al., *Conserved homeodomain proteins interact with MADS box protein Mcm1 to restrict ECB-dependent transcription to the M/G1 phase of the cell cycle.* Genes Dev, 2002. **16**(23): p. 3034-45.

185.   Bastos de Oliveira, F.M., et al., *Linking DNA replication checkpoint to MBF cell-cycle transcription reveals a distinct class of G1/S genes.* EMBO J, 2012. **31**(7): p. 1798-810.

186.   Arsenault, H.E., et al., *Hcm1 integrates signals from Cdk1 and calcineurin to control cell proliferation.* Mol Biol Cell, 2015. **26**(20): p. 3570-7.